RHODES UNIVERSITY
Where leaders learn

Quinolone-Pyrazinamide Derivatives: Synthesis, characterisation, *in silico* ADME analysis and *in vitro* biological evaluation against *Mycobacterium tuberculosis*.

A dissertation submitted to Rhodes University

by

Kudakwashe Gerald Rukweza, BPHARM (RU)

In fulfilment of the requirements for the degree

of

Master of Science

in Chemistry

2023

Abstract

Tuberculosis is one of the leading causes of death worldwide caused by an infectious species, *Mycobacterium tuberculosis* (*Mtb*). Some of the factors that contribute to the prevalence of this disease include the complexity of diagnosis, prolonged period of therapy, side effects associated with current TB drugs, the prevalence of resistance against the current treatment options and a high incidence of co-infection with HIV/AIDS. Thus, there is a need for new alternative drugs to provide safer and shorter treatment therapy options that are not susceptible to the development of drug resistance.

In this project, we focus our attention on the quinolone pharmacophore. Quinolones are currently used as alternative options in the treatment of resistant strains of *Mtb*. Previous work pertaining to quinolone-isoniazid hybrid compounds showed promising *in vitro* activity against the $H_{37}Rv$ strain of *Mtb* and served as the inspiration to pursue this project. The journey commenced with the synthesis of quinolone-pyrazinamide hybrid compounds (**Figure 3.1**). These compounds were synthesised, through the attachment of the quinolone and the pyrazinamide entity through a hydrazine linker.
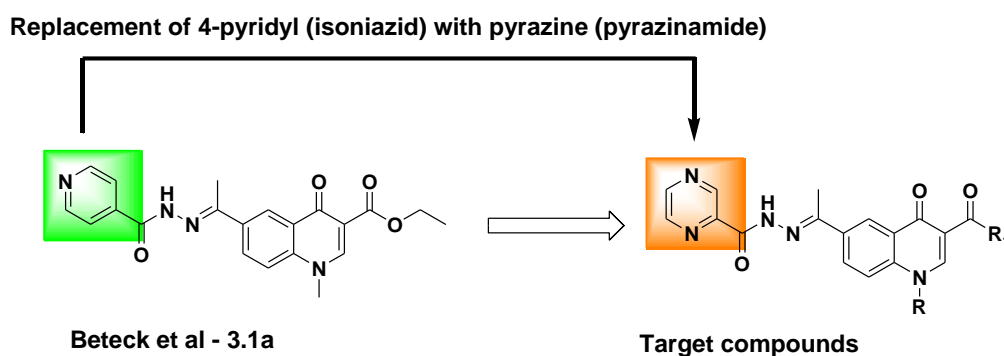
Figure 3.3: Design of target **quinolone-pyrazinamide** hybrid molecules.

The synthesised compounds were purified, and their structural identity confirmed using common spectroscopic techniques including ^1H and ^{13}C NMR, infra-red (IR) and mass spectrometry. *In vitro* biological assays were performed by testing for the activity against the $H_{37}RvMA$ strain of *Mtb*. The bioassays were performed in triplicates to ensure the accuracy of the results. Moxifloxacin and isoniazid were tested as control

compounds. Finally, the resultant compounds were profiled *in silico* for physicochemical and ADMET properties using open access software SwissADME.

All the synthesised compounds **3.8a-f** showed no activity against $H_{37}RvMA$. In most cases, the resulting compounds showed minimal to no activity (MICs ≥ 57.3 µM) in all three media. During the *in vitro* studies, the compounds showed significant precipitation in the media over time suggesting poor aqueous solubility. The SwissADME analysis of these compounds indicated poor solubility in aqueous media, which is likely linked to their molecular size and complexity. Despite poor aqueous solubility, compounds **3.8a-f** showed acceptable physicochemical properties and ADME parameters. No PAINs (Pan-assay interference compounds) were observed. Minimal to no interaction with CYP enzymes were predicted. Most of the compounds were compatible with the Lipinski's rules of five.

Dedication

Ecclesiastes 3:11 KJV

He hath made everything beautiful in his time: also, he hath set the world in their heart, so that no man can find out the work that God maketh from the beginning to the end.

Dedicated to my family, Albert Rukweza, Esther Rukweza, Aretha Mushimbo, Monica Makhaya, Princess Shiriyedenga, Daphne Mamhende and Tadiwanashe Rukweza

Acknowledgements

Thank you, Jesus Christ, for your Grace that has been, abounding in my life. If it weren't for his goodness… Psalm 27:13 I wouldn't be where I am today.

I want to present my utmost gratitude to my supervisor Prof. Setshaba D Khanye, for his belief in me when I did not believe in myself. For his steadfast presence that never wavered and his expertise that is written all over this thesis.

I want to thank all the staff in the Faculty of Pharmacy and the Division of Pharmaceutical Chemistry for laboratory space and supportive environment to conduct this research. I am grateful to all my laboratory colleagues, Dr. Ayanda Zulu, Mr. Thando Matshare, Ms. Mbali Mahlobo, Ms. Nonkululelo Zulu, Dr. Mokhitli Morake, Mr. Hugan West and Mr. Gervase Makoni who were my mentors throughout this journey. I thank you for your hand in improving me as a scientist and in my expertise. I am grateful to the support staff for working tirelessly in procuring and supplying all the equipment and chemicals we used. I would like to thank my fellow class of 2019 master's colleagues, Ms. Simise Sikhondze, Ms. Chiedza Kakono, Ms. Chiamaka Onyekwuluje, Mr. Charles Arinitwe and Mr. Sam Okeyo, for walking this journey with me.

I am greatly indebted to my support structure outside my academic circles, my spiritual guides; Mr. T. and Mrs. P. Chimombe, Pst. and Mama Matepo, Mr. and Mrs. Makoni, Mr. Burgess, Mr. Z Gumbo, Mr. T. Gudza, Mjr. C.Tenesi, Mjr. E. Mhukayesango, Pst. B. Musiiwa, Ms. Sotashe, Mrs. E. Rukweza … Friends of the journey; Ms. T. Mbira, Ms. M. Makoni, Ms P. Munemo, Mr. Bloem, Mr. Dhlamini, Dr N. Mushambi. Important mention goes to my Chi Alpha Family (Linathi, Rue, Olwethu), My River of Life family (Sis Andi, Magda), the Rhodes basketball Team and the SAC (Prep) Basketball Team.

I am thankful to Rhodes University for giving a young dreamer like me a chance to live his dream to play a role in changing the world, and I believe I am well on that path. Lastly, I want to thank my family for always being supportive. I want to thank my mom and dad for encouraging me and giving me the strength that I needed every single day. I believe that I have made them proud.

Table of Contents

List of symbols and abbreviations

AIDS	Acquired Immunodeficiency Syndrome
AcOH	Acetic acid
aq.	Aqueous
bs.	Broad singlet
°C	Degrees Celsius
Calcd	Calculated
conc.	Concentrated
^{13}C NMR	Carbon-13 Nuclear Magnetic Resonance
Δ	Chemical shift
DCM	Dichloromethane
DMSO	Dimethyl sulfoxide
Eq	Equivalent
EtOAc	Ethyl acetate
EtOH	Ethanol
g	Gram
h	Hour
HIV	Human Immunodeficiency Virus
^{1}H NMR	Hydrogen-1 (Proton) Nuclear Magnetic Resonance
HRMS	High-resolution mass spectrometry
MIC_{50}	50% Minimum Inhibitory Concentration
MIC_{90}	90% Minimum Inhibitory Concentration
IR	Infra-red spectroscopy
J	Coupling constant
K	Kelvin
lit	Literature
m	Multiplet
Me	Methyl
mg	Milligram
MHz	Megahertz
min	Minute

ml	Millilitre
mM	Millimolar
mol	Moles
M.p.	Melting point
Mtb	*Mycobacterium tuberculosis*
NMR	Nuclear Magnetic Resonance
r.t	Room temperature
s	Singlet
SAR	Structure-activity relationship
t	Triplet
TB	Tuberculosis
TLC	Thin Layer Chromatography
µg	Microgram
WHO	World Health Organization

Chapter One

Tuberculosis: The treatment and management of TB

1.1   Introduction

Since 2020, tuberculosis (TB) is the second leading cause of death from a single infection after COVID-19[1]. TB is a global health concern and has put millions of lives at risk. Approximately 1.4 million people died from TB in 2021 including HIV-negative people[2]. An estimated 187000 deaths recorded were of people co-infected with Human Immunodeficiency Virus (HIV)[2]. HIV increases one's susceptibility to reinfection from latent TB. Since the end of 2019, the world has been dominated by the prevalence of the coronavirus virus (COVID-19) which resulted in a decrease in the TB cases reported[2]. In 2021, approximately 10.6 million people were reported to have been infected by TB, an increase in the TB incidence rate by 3.6% between 2020 and 2021[2]. Thus, the World Health Organization (WHO) has made the eradication of TB a top priority. Although 2020 was plagued by the coronavirus pandemic, TB remains prevalent[1]. Disease-causing organisms are developing resistance against treatment options that are being used as both Mono- and combination therapy[3]. This chapter will provide an overview of TB and summarise recent relevant information about TB and its treatment. The chapter is structured in a way that it gives a historical background of TB infection and treatment, and it narrows down to the current literature reports on the treatment of TB. The emphasis of this study is on pyrazinamide and its role in the treatment of TB. This research is intended to explore the hybridization of pyrazinamide with quinolone scaffold to design novel antimycobacterial compounds as effective agents against *Mycobacterium tuberculosis* (*Mtb*), the main causative agent of TB in human beings.

1.2 History and epidemiology of TB

Although there is no concrete evidence and information recorded about the earliest cases of TB, most of the records surfaced the symptoms as early as times of the biblical events[4]. The origin of TB was hypothesised in 1720 by an English physician, Benjamin Marten[4]. He shed light on the epidemiology of TB. Subsequently, Robert Koch

contributed immensely by isolating *tubercle bacillus* using methylene blue staining previously recommended by Paul Ehrlich[4].

TB is a communicable disease that is highly prevalent and has been responsible for millions of deaths in the 21st century. In 2021, approximately 10.6 million people fell ill with TB which was a 4.5% increase from the 10.1 million recorded in 2020[2]. TB is one of the ten leading causes of death from a single infectious agent. It is estimated that one-fourth of the global population harbours the dormant of the TB bacilli. Most individuals who are infected with latent tuberculosis infection (LTBI) do not exhibit active TB until their immune system is compromised, while about 5 - 10% progress and develop active TB[5]. Thus, TB is an apparent problem and requires urgent attention. Several factors such as economic, social, and political add to the virulence of TB, and these factors directly or indirectly contribute to the spread of TB[6]. The physiological factors that contribute to the virulence of TB include malnutrition, comorbidities of conditions such as diabetes, tobacco smoking, and household air pollution among others[7]. Active TB is common in patients with compromised immune system. Therefore, caution is to be exercised for patients being treated with immunosuppressive medication. Treatment with anti-tumour necrosis factor (TNF) biologics and chronic corticosteroids also weaken the immune system and can result in one contracting *Mtb* and developing a TB infection[1].

1.2.1 *Mtb* biology

Mycobacteria are a group of bacteria, members of the order *Actinomycetales* and the only genus in the family *Mycobacteriaceae*. Tuberculosis, leprosy, and Buruli ulcer disease are some of the diseases that are caused by the *Mycobacterium* species[8]. Although not all *mycobacteria* are harmful to humans. *Mycobacterium tuberculosis* (*M. tuberculosis*) complex is a set of evolutionary closely related slow-growing mycobacterial species, containing the mobile insertion sequence IS6610 in their genome. There are more than 100 species of *mycobacteria* that are unique, including numerous pathogens, and saprophytic organisms of warm-blooded animals. The main causative agent *Mtb* is characterised as an acid-fast bacillus with a complex cell wall which consists of long-chain fatty acids (mycolic acids)[9]. *Mycobacteria* cells are slender and non-spore-forming. They are rod-shaped, thrive in aerobic environments,

are slow growing, and free-living in soil and water. A common characteristic of *Mycobacteria* is the lipid-rich cell envelope that encloses all the cell contents[10]. The cell wall structure makes the mycobacterium resist osmotic pressure and this increases their chances of survival in different environments. A firm exterior helps the bacterial cell withstand physical pressure or osmotic pressure[10]. *Mycobacteria* have typical genetic information like any normal bacteria, i.e., each cell contains a single large circular DNA highly concentrated with guanine (G) + cytosine (C)[11].

1.3 Transmission and pathology of TB

Mycobacterium tuberculosis is primarily transmitted via the airborne route. The air-droplets containing *Mtb* bacilli are expelled through coughing into the air by infected individuals, which are inhaled by uninfected people[12]. Patients with active TB, have a cavity in their lungs that have the highest chance of transmitting the disease[13]. Patients who are infected by *mycobacterium* and show symptoms of TB can be fully cured if they get treatment on time. Unfortunately, over time there has been the development of resistance to the treatment of TB. With all the advancement in the information around TB, scientists across different parts of the world are looking towards eradicating TB completely[14]. TB has a plethora of symptoms that may resemble other conditions. The common symptoms are a cough that lasts for three weeks or longer, chest pains, coughing of blood or mucus, feeling weak, unexplained weight loss, chills, fever, sweating at night and lack of appetite[15], among others. The reactivation from LTBI to active TB is difficult to quantify because of the challenge of the diagnosis of LTBI[16].

Under normal circumstances and in most patients the immune response will control any potential development of active TB in the initial stages of infection. The immune system is responsible for preventing LTBI from progressing to becoming an active form of TB[17]. When *Mtb* reaches the lungs, it is engulfed by alveolar macrophages and begins to replicate. The tubercule bacilli can also enter the parenchyma, infecting other macrophages and dendritic cells which will trigger the inflammatory pathways i.e., the production of inflammatory cytokines and chemokines, this will cause positive feedback, more inflammatory mediators, and immune response cells such as

monocytes (macrophages and neutrophils) to be released. The engulfed *Mtb* will migrate into the lungs, which activates the lymphatic system and releases T cells. All the above participate in granuloma formation. Granulomas have the most critical role to play in the pathophysiology of TB. Granulomas are complex spherical structures consisting of macrophages, lymphocytes, and neutrophils. At the centre of the granuloma is where caseous necrosis takes place, which is an attempt to halt and curb the infection of *mycobacterium*[18]. The success of the granuloma in destroying or inhibiting the tubercule bacilli growth and survival will result in the denaturing of bacilli[19]. This is all possible if the immune system is not compromised or under stress. The effective improvising of the immune system to protect the body is termed cell-mediated immunity (CMI). Research shows that CMI has an average potency of 90% in the curbing of a potential TB infection[18,20].

1.4 Stages of TB in the human body

TB progression is described in four stages. In the first stage within eight weeks, the *mycobacterium* is inhaled and exposed to the aerosols, and the bacteria is spread by the lymphatic system to regional lymph nodes in the lungs, which results in the formation of a Ghon complex. The lymph system inversion will also result in the reactivation of the bacteria (tuberculin). The second stage lasts approximately three months, and it is when the TB infection is spread to the rest of the lungs and other parts of the body. During this stage some people may develop symptoms of TB and some tubercular meningitis. At stage three, pleurisy or inflammation of the pleural surface takes place. This will last for three to seven months and can cause chest pains in the patient. The fourth stage is not involved with any disease progression and can last up to three years. At stage four the disease is not gone at all but will be manifested in certain areas of the body[21]. The stages above are only possible considering no interruptions (for example, taking medication) affecting the chain. In HIV-infected individuals, the progression of infection happens at a faster rate due to the compromised immune system of patients[22].

1.5 Clinical manifestation of TB

1.5.1 Primary pulmonary TB

The major known pathology in TB is necrotizing granulomatous inflammation and the lungs are the primary targets in 87% of the cases[23,24]. Lung function impairment is a major stage in the development of pulmonary TB[25]. It is characterised by lung tissue destruction and necrosis, differing from other lung infections in that it mainly targets the airways[26].

1.5.2 Miliary TB

Miliary TB is a spectrum of manifestations that are difficult to recognise and diagnose. There are still recordings of high mortality besides having effective therapy. This is a potentially fatal form of TB that is caused by the development of massive lymphohematogenous dissemination of *Mtb* bacilli[27]. Manifestation for diagnosis is seen by the presence of a diffuse miliary infiltrate on chest radiography or high-resolution computed tomography (HRCT). In some instances, there is evidence of miliary tubercles in multiple organs during laparoscopy, open surgery, or autopsy[27].

1.5.3 Extrapulmonary TB

In 2017, there was a 16% prevalence of Extrapulmonary TB (EPTB) among notified cases of TB recorded in Africa, and this was second to the 24% in the Eastern Mediterranean region[28]. It is difficult to diagnose because of the varied sites of infections. Samples for diagnosis are usually found in remote areas of the body, hence reducing the sensitivity of the tests[29]. An estimated 10-50% of TB patients reported having EPTB show pulmonary manifestations. Standard diagnosis is through *Mtb* staining and culture of a biopsy in some instances and this happens to be the most effective way of diagnosis of EPTB[30], during body fluid examination.

1.6 Diagnosis of TB

Though the primary onset of TB is pulmonary TB, *Mtb* can also be found in other areas of the body. Quick diagnosis is an area in the control of TB that has room for more development. It would make the process for the treatment a lot more efficient if there

could be tests that had quick, instant, and efficient results. However, that is not the case, getting accurate (reliable) results from tests conducted is cumbersome and it could take at least a full day to get results[31]. Different types of diagnostic tools are currently being used. Some are preferred more than others because of the cost, specificity, and sensitivity. The X-ray diagnosis method is a useful method when there is a need for a quick turnaround. However, there are limitations; X-ray images do not give specific results that are used to confirm TB without any other differential diagnosis. X-ray images can be of a person suffering from pneumonia and it is common for patients to be put on treatment for pneumonia before more specific tests are performed. Some people are infected by the *Mycobacterium* but in its latent state and are asymptomatic[32,33]. Sputum Smear Microscopy is the most rapid and inexpensive diagnostic tool, but it has a low sensitivity. The sensitivity is lower in patients with a low organism burden, such as children with primary TB and HIV-positive patients with paucibacillary disease[34]. The nucleic acid amplification (NAA) test is also a diagnosis tool for TB. This process has a higher specificity but a poor sensitivity and this means it does not ultimately rule out the disease after reporting a negative result[35]. NAA tests cannot be used to determine the progress of the disease, hence the only way to tell if a patient's disease burden is improving - is by doing a different test.[36] All samples (specimens) suspected of containing *Mycobacterium* should be cultured. A culture can detect as few as 10 bacteria/mL. Culture is also required for drug susceptibility testing. Sputum culture has sensitivity and specificity as high as 80% and 98%, respectively. Unfortunately, cultures take 2-6 weeks to obtain conclusive results[34]. The Xpert MTB/RIF assay is a novel, rapid, automated, and cartridge-based NAA test that can detect TB along with rifampicin resistance directly from sputum within two hours of collection[31].

1.7 Treatment and control of TB

The American Thoracic Society (ATS) in conjunction with the Centre for Disease Control and Prevention (CDC) developed international guidelines for the treatment of drug susceptible TB [37]. The guidelines are aimed at decreasing the burden of growing bacilli, preventing relapse, and decreasing drug resistance [38]. The development of resistance to *Mtb* is a major risk factor in the treatment and control of TB. Although

there is a great desire to design more drugs, there is also great fear of resistance developing against available treatment options. Additionally, non-adherence to taking medicine by the patients further undermine the efforts of treatment of TB. Treatment will be efficient and successful if identification, confirmation (diagnosis) and treatment are done quickly before the patient can infect other people[39]. The need to have a balance that exists between the design of new drugs and the risk of *Mtb* continuously developing resistance is an opportunity for more studies to be done. Closing the gap will ensure readily available treatment options.

Latent tuberculosis is the form of tuberculosis in which one is infected by *Mtb* but there are no immediate (active) signs or common symptoms. An estimated 23% (95% uncertainty interval 20.4% - 26.4%) of the global population harbour the infection in their bodies and these have the potential of becoming future active cases in the event of the weakening of the immune system leading to reactivation[40]. There is an investment towards the usage of preventive therapy for people who are receiving antiretroviral drugs. These are short doses of isoniazid and rifampicin that are used to treat latent tuberculosis in patients[40].

Monotherapy was part of the initial treatment plan, but it failed to yield sustainable results[39]. There are currently two phases in the treatment of TB, the initial phase (bactericidal) and the continuation phase (sterilizing). The first phase is responsible for killing actively growing bacteria undergoing rapid replication. This phase is crucial in reducing the risk of spreading the disease and patients become non-infectious. On the other hand, the continuous phase is responsible for killing the semi-dormant bacteria, and this phase is characterised by low replication rates. It is also responsible for minimizing the chances of the development of drug resistance. The regimen prescribed in the initial phase is made up of two bactericidal drugs, isoniazid with rifampicin (streptomycin in some instances) (**Figure 1.1**).

1.7.1 First-class TB drugs

Ethambutol is responsible for inhibiting non-resistant strains and reducing the *Mtb* burden. Pyrazinamide is more effective against semi-dormant bacteria. The intensive phase is two months long, and the sterilizing phase is four months of administering

rifampicin and isoniazid as preferred drugs. The intensive phase is crucial because it is responsible for reducing the number of *Mtb* bacilli[41,42]. The WHO classified drugs into different classes. The first class of drugs used in susceptible mycobacteria are ethambutol, isoniazid, pyrazinamide, and rifampicin **(Figure 1.1).**
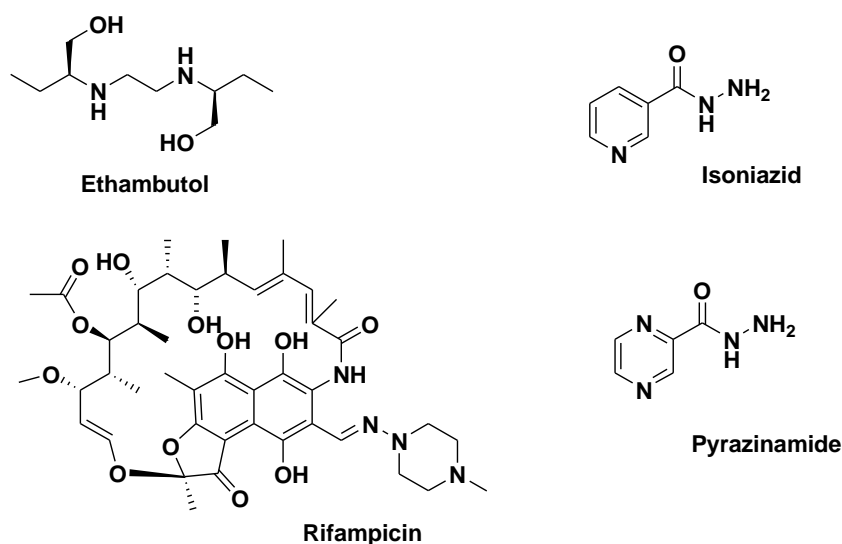
Figure 1.1: Chemical structures of the first-class drugs used in the treatment of TB.

The second class includes injectable drugs such as amikacin, capreomycin, kanamycin, and streptomycin. The third class includes a combination of new and old fluoroquinolones. The fourth class are cycloserine, ethionamide, para-aminosalicylic acid, prothionamide, terizidone, and thiacetazone. Finally, the fifth class contains drugs such as amoxicillin/clavulanate, clarithromycin, clofazimine, imipenem and linezolid[43]. All the drugs recommended for TB have different target sites (**Figure 1.2**) and work at different intensities and have different therapeutic outcomes. The recommended treatment plan by the WHO during the intensive phase is a combined dose of rifampicin, isoniazid, pyrazinamide, and ethambutol followed by a four-month regimen of rifampicin and isoniazid.

1.7.1.1 Ethambutol

Ethambutol is a derivative of *N,N'*-di-isopropyl ethylenediamine that was discovered through random screening[45]. Ethambutol is a narrow-spectrum bacteriostatic agent used against *Mtb* and has low activity against non-replicating microorganisms. It has little to no influence on shortening the duration of the treatment. Ethambutol is only

administered in the initial intensive two months, and it has the role of preventing the build-up of resistance to other treatment agents[46]. The mode of action of ethambutol is not fully understood. However, the existing evidence shows that ethambutol may act by targeting arabinosyltransferase, an enzyme encoded by the *emb*A and *amb*B genes, involved in the formation of cell walls[47]. Ethambutol is stereospecific with the (*S*,*S*)-(+) enantiomer responsible for its activity whereas the (*R*,*R*)-(-) ethambutol causes blindness[48].
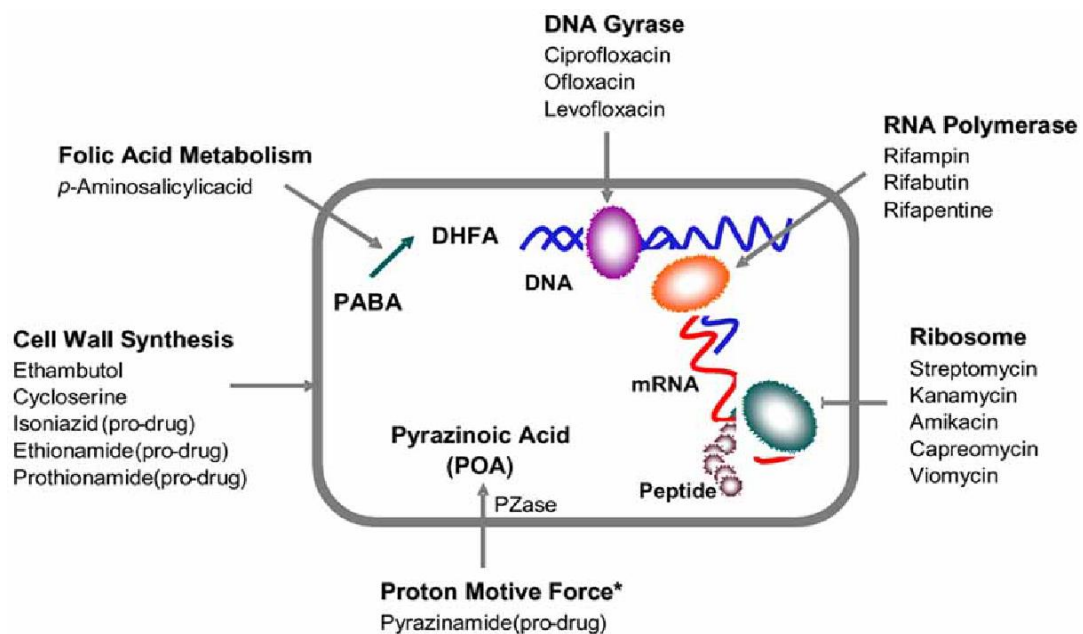
Figure 1.2: The different classes of drugs used in TB treatment and their target of action[44].

1.7.1.2 Isoniazid

Isoniazid is one of the most important and potent antitubercular drugs that have been developed to date. The development of resistance against isoniazid has been prevalent and is of great concern[49]. Isoniazid is a prodrug that is activated by the enzyme catalase-peroxidase, an enzyme regulated by *katG* to form highly reactive species such as reactive oxygen species, superoxide, peroxide, and hydroxyl radicals, nitric oxide, and reactive organic species such as isonicotinic acyl radical or anion that are bactericidal[50]. Isoniazid mainly works on the *InhA* enzyme (enoyl acyl carrier protein reductase), which aids in the elongation of fatty acids in mycolic acid synthesis which are found in the cell walls[51].

1.7.1.3 Rifampicin

Rifampicin has a half-life of 2-4 hours and other rifamycin derivatives have been developed with much longer serum half-lives such as Rifabutin[52]. Rifabutin has a half-life of 45 hours due to a high volume of distribution (> 9L/kg)[53]. Rifabutin is used as a first-line drug in some endemic areas, but it is mainly used as a substitute for Rifampicin in patients who are simultaneously treated with antiretroviral therapy as it interferes less with CYP-450 systems[54]. Rifampicin is bactericidal and works through the inhibition of DNA-dependent RNA polymerase (RNAP) either by sterically blocking the path of the elongating RNA at the 5' end or by diminishing the affinity of the RNAP for short transcripts[55].

1.7.1.4 Pyrazinamide (PZA)

Pyrazinamide is an amide derivative of pyrazinoic acid (pyrazine-2-carboxylic acid). It is a prodrug with pyrazinoic acid (POA) as the active compound. Pyrazinoic acid itself does not have any activity against *Mtb* possibly due to its hydrophilic nature. POA has one hydrogen bond donor and three hydrogen acceptors contributing to its polarity. This polarity makes passage through the cellular membranes difficult and almost impossible. Pyrazinoic acid is naturally ionized at physiological conditions[56]. Although the mechanism of action for pyrazinamide has not been fully understood, it is proposed that PZA is converted through hydrolysis to pyrazinoic acid by an enzyme pyrazinamidase **(Figure 1.3)**. Pyrazinamide has a unique quality, as it appears to kill a population of semi-dormant tubercle bacilli that survive the effects of other antitubercular drugs[57]. The inclusion of PZA as a first-line drug was critical in the reduction of the length of therapy from 9-12 months to 6 months[58,59]. PZA is given in the first two months of therapy because studies show the impact of PZA is minimal to none after 2 months of administering[60]. PZA works well in an acidic environment. Any infection will lead to inflammation and in this case, *Mtb* infection results in the formation of an acidic environment. Inflammation caused by TB is commonly observed in the lesions and it decreases after 2 months which concomitantly increases the pH of the environment to become less acidic[58]. Pyrazinoic acid has a dose-effect direct correlation activity against *Mtb*. The minimum inhibitory concentration (MIC) of POA is 8 – 16 times greater than that for PZA[61].
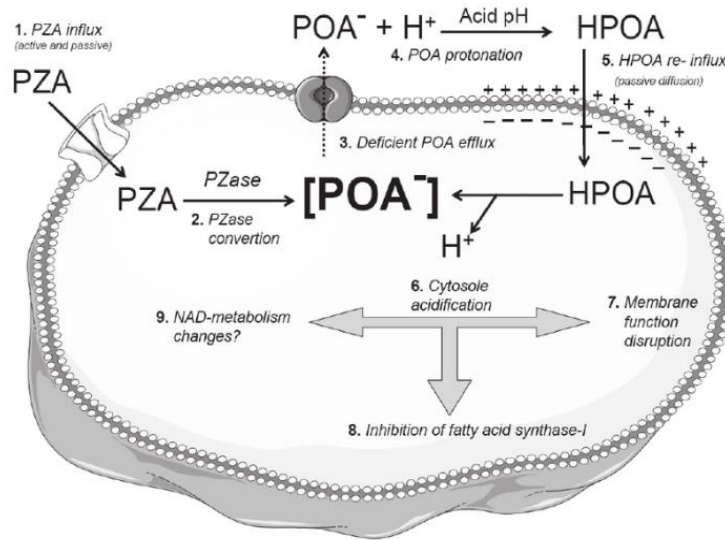
Figure 1.3: A scheme outlining the mode of action of PZA[67].

PZA has little to no activity against growing bacteria but is mainly lethal to dormant bacteria. PZA has high sterility against 'persisters'[62]. The enzyme pyrazinamidase is encoded by the *PncA* gene in *Mtb*. The recombinant *Mtb* gene *PncA* is a monomeric enzyme that contains Mn^{2+} and Fe^{2+} ions. The mechanism of PZA conversion to POA may be similar to the nitrilase enzyme superfamily, in which a nucleophilic attack by active site cysteine generates a tetrahedral intermediate that collapses with the loss of ammonia and subsequent hydrolysis of the thioester bond by water[63]. Some models have been designed to explain the progressions that PZA goes through when it enters the bacterial cells **(Figure 1.3)**. Through passive diffusion, pyrazinamide enters the bacilli and is converted to POA (pKa = 2.9) by cytoplasmic pyrazinamidase. The POA will diffuse out of the cell by passive diffusion and through a deficient efflux mechanism. This illustrates that PZA has ease of access to bacterial cells. The POA will be protonated (HPOA) under acidic extracellular conditions and readily crosses the membranes. This guarantees the maintenance of high HPOA concentration in the cells[64]. The accumulation of protons in the cells will cause cytoplasmic acidification such that vital enzymes can be inhibited. POA can also cause de-energizing of the membrane by collapsing proton motive force and affecting membrane transport, inhibiting RNA synthesis[65]. This mechanism is crucial, especially in non-growing persisters that have low metabolism production of acid. This hypothesis suggested that PZA works well in acidic conditions.

Diffusion of POA into cells is a passive process but its removal is through a pump (ATP-driven pump), hence bactericidal activity is greatest when bacterial energy sources are at their lowest[64]. The activity of PZA against persisters is supported because the efflux mechanism is weak in older cells[66]. The unique ability of PZA to be more active against semi-dormant bacteria is what prompted this research to explore the activity of PZA in combination with other bioactive molecular frameworks such as the quinolone moiety. Despite limited knowledge regarding the MOA of PZA, there is enough evidence to substantiate the fact that PZA is efficacious and is a very important drug in the first-line stage of treatment.

Although PZA has been successful in the treatment of TB, the emergence of drug resistance against PZA poses a serious health risk. Currently, the development of resistance at a molecular level for pyrazinamide has not been properly explored and explained [68]. The proposed mechanism of resistance has been suggested to result from mutations in the *PncA* gene [68]. The largely identified mutations are missense mutations causing amino acid substitution, however, other mutations have resulted from nucleotide insertions or deletions, and nonsense mutations on the structural *PncA* gene or in the putative promoter region. Certain areas are high targets, regions *PncA* (3-17, 61-85, 132-142) have been identified to be more prone to mutation as compared to the rest of the genetic code[69]. The three regions code for the amino acid sequence for active attachment sites, three of the four loops that contribute to the activity[69]. Studies have shown that 72-98% of PZA resistance is directly linked to *PncA* mutations, which are diverse[70]. However, there is not enough evidence to show that mutations would take place due to any specific causes, making it unpredictable. There are many theories behind the distribution of PZA resistance, and some have suggested the influence of geographical location, but all these suggestions are inconclusive. Furthermore, all the PZA susceptibility tests done to date are not reliable and result in false resistance results[71]. There is a possibility that much of the resistance is spread unexplained and undocumented[72].

Pyrazinamide is administered orally to both adult and paediatric patients at a maximum dosage of 2 g per day, there is evidence that higher doses would result in maximal effect[73]. However, high doses have also resulted in undesirable side effects. The side effects associated with PZA include hepatotoxicity and the high concentration of serum aminotransferase, which can lead to the development of secondary side effects such as jaundice and hepatitis[73-74]. Pyrazinamide is not given as monotherapy, particularly for the treatment of TB, but is given as a combination of drugs for the most part.

1.7.2 Second-class TB drugs

Multidrug-resistant tuberculosis (MDR-TB) is caused by *Mtb* isolates that are not responding to isoniazid and rifampicin. The second line drugs deployed to treat MDR-TB includes fluoroquinolones and aminoglycosides. Aminoglycosides are cheaper and injectable, and they are recommended by the WHO, especially in countries with limited resources[75]. The downside with injectable drugs is that in developing countries can be a constraint because they require handling by more trained personnel. Aminoglycosides are potent but are highly toxic and have caused irreversible hearing loss as an adverse event during usage[76,77]. Currently, kanamycin and amikacin (**Figure 1.4**) are commonly used drugs in the treatment of MDR-TB[78].
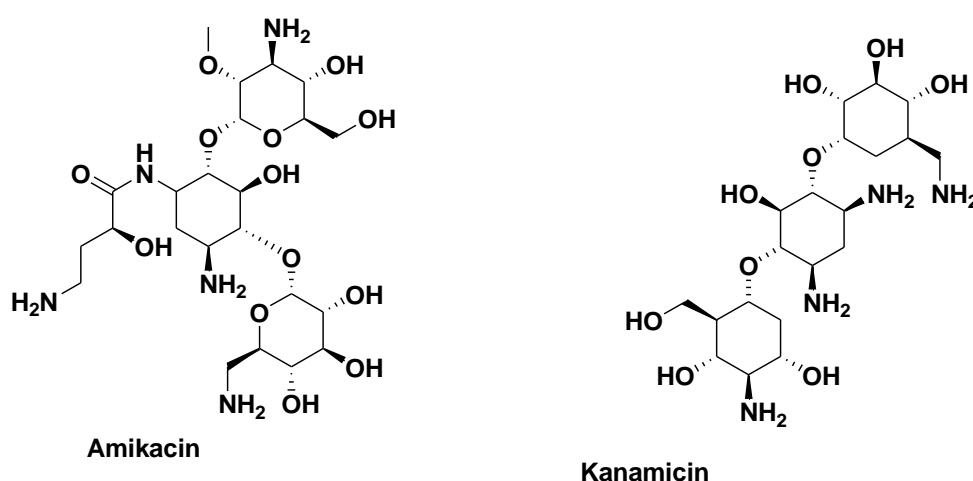

Amikacin

Kanamicin

Figure 1.4: Chemical structure of amikacin and kanamycin.

1.7.3 Third-class TB drugs

Fluoroquinolones are a critical option in the treatment of MDR-TB. This is a class of antibiotics that works by blocking the DNA gyrase, which inhibits bacterial DNA synthesis and leads to the denaturing of cells[79]. Recently, fluoroquinolones have been under scrutiny because of adverse effects that have been reported by patients taking them. Although they are well tolerated, fluoroquinolones such as moxifloxacin have the potential of causing prolongation of the start of the Q-wave and the end of the T-wave (QTc interval) which results delayed ventricular repolarisation[80]. Moxifloxacin and levofloxacin (**Figure 1.5**) are the two most used in the treatment of MDR-TB[79].

Moxifloxacin
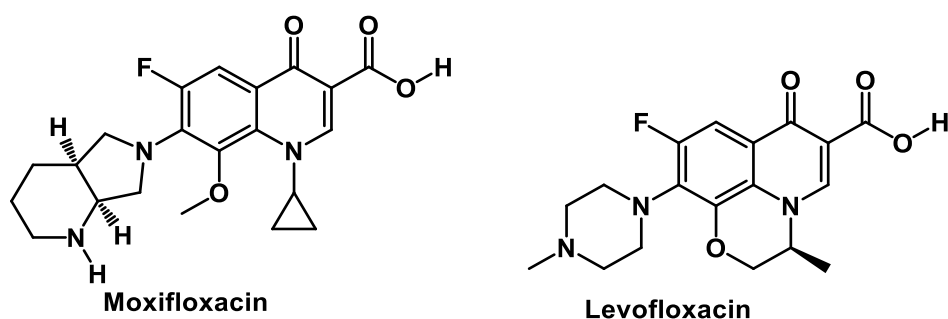
Levofloxacin

Figure 1.5: Chemical structures of fluroquinolones, moxifloxacin, and levofloxacin.

1.7.4 Fourth class TB drugs

In 2021, 71% of confirmed pulmonary TB cases were tested for Rifampicin resistance and of those tested, 141 953 were confirmed cases of MDR and 25 038 were cases of pre-XDR-TB or XDR-TB[81]. This level of resistance of TB is neither responsive to any fluoroquinolones nor at least one injectable second-line drug (capreomycin, kanamycin or amikacin)[82]. Group 4 drugs such as ethionamide, prothionamide, and cycloserine/terizidones (**Figure 1.6**) are core second-line drugs but they are associated with higher cases of adverse events as well.
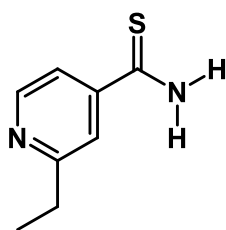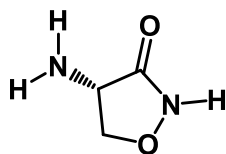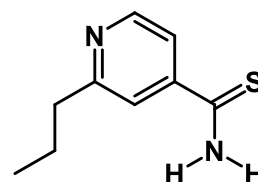
Figure 1.6: Chemical structures of ethionamide, prothionamide, and cycloserine.

1.7.5 Fifth-class TB drugs

These are mainly orally administered drugs available as new treatment options. Linezolid and clofazimine **(Figure 1.7)** have been added to the MDR-TB treatment regimen. Linezolid has good efficacy, but the downside is that it is expensive and has poor toxicity profile[82]. However, there is evidence that shows that tolerability can be managed with the adjustment of the initial doses[83].
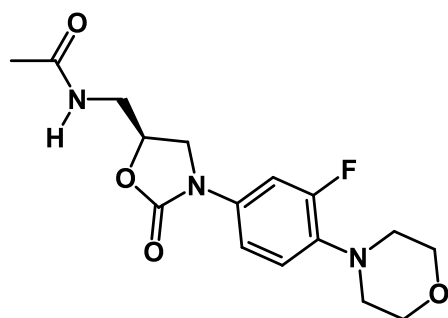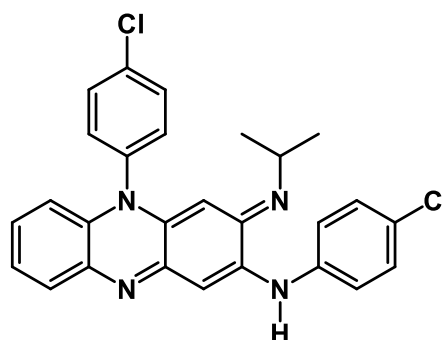
Figure 1.7: Chemical structures of linezolid and clofazimine

1.7.6 New TB drugs: Delamanid and bedaquiline

The latest TB drugs to be introduced follow recent approval by regulators are delamanid and bedaquiline (**Figure 1.8**), and they are still being studied and safety data collection is ongoing. In South Africa, these are the newest drug options to be cleared for usage and available as essential tools to be utilised against MDR-TB and XDR-TB. Bedaquiline targets replicating and dormant bacilli[82]. The most common adverse event of bedaquiline is a QTc interval increase in the electrocardiogram

(ECG). More importantly, bedaquiline shows cross-resistance to clofazimine [84]. Delamanid has bactericidal and sterilising activity, and it shows no evidence of cross-resistance with other anti-TB drugs[85]. Critically, there is evidence showing the safe usage of both bedaquiline and delamanid for a period of more than 6 months and delamanid usage in children is regarded as safe[86].
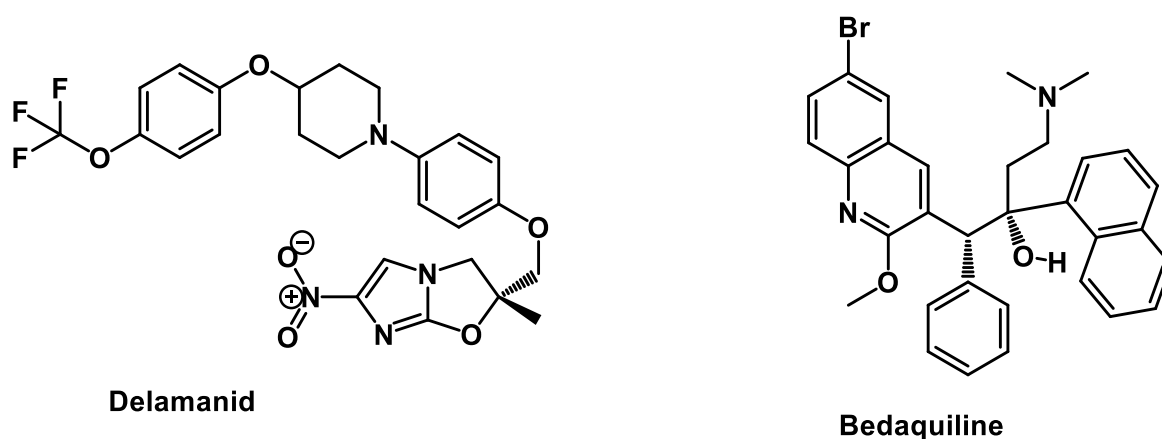
Figure 1.8: Chemical structures of Delamanid and Bedaquiline.

The WHO has made the eradication and control of the spread of TB disease a top priority. The current study attempts to contribute to an ongoing debate regarding the design of new drug molecules to be in line for treatment of TB. The emphasis is on using the molecular hybridisation strategy to conjugate PZA and quinolone nuclei to design novel compounds for the treatment of TB. This work is an extension of previous study conducted on quinolone-isoniazid hybrids that were synthesised from our laboratory[2].

1.8 References

(1)   Chakaya, J.; Khan, M.; Ntoumi, F.; Aklillu, E.; Fatima, R.; Mwaba, P.; Kapata, N.; Mfinanga, S.; Hasnain, S. E.; Katoto, P. D. M. C. Global Tuberculosis Report 2020–Reflections on the Global TB Burden, Treatment and Prevention Efforts. *Int. J. Infect. Dis.* **2021**, 113 (1), S7-S12.

(2)   World Health Organization. *Global Tuberculosis Report 2022*; Geneva, 2022.

(3)   Beteck, R. M.; Seldon, R.; Jordaan, A.; Warner, D. F.; Hoppe, H. C.; Laming, D.; Khanye, S. D. New Quinolone-Based Thiosemicarbazones Showing Activity against *Plasmodium falciparum* and *Mycobacterium tuberculosis*. *Molecules*

2019, *24* (9), 1740.

(4)   Barberis, I.; Bragazzi, N. L.; Galluzzo, L.; Martini, M. The History of Tuberculosis: From the First Historical Records to the Isolation of Koch's Bacillus. *J. Prev. Med. and Hyg*. **2017**, *58* (1), E9 – E12.

(5)   Sterling, T. R.; Njie, G.; Zenner, D.; Cohn, D. L.; Reves, R.; Ahmed, A.; Menzies, D.; Horsburgh Jr, C. R.; Crane, C. M.; Burgos, M. Guidelines for the Treatment of Latent Tuberculosis Infection: Recommendations from the National Tuberculosis Controllers Association and CDC, **2020**. Wiley Online Library 2020.

(6)   Hargreaves, J. R.; Boccia, D.; Evans, C. A.; Adato, M.; Petticrew, M.; Porter, J. D. H. The Social Determinants of Tuberculosis: From Evidence to Action. *Am. J. Public Health* **2011**, *101* (4), 654–662.

(7)   Dooley, K. E.; Chaisson, R. E. Tuberculosis and Diabetes Mellitus: Convergence of Two Epidemics. *Lancet Infect. Dis.* **2009**, *9* (12), 737–746.

(8)   van Ingen, J. Mycobacteria. In *Infectious Diseases*; Elsevier, **2017**; pp 1645–1659.

(9)   Lin, P. L.; Flynn, J. L. CD8 T Cells and *Mycobacterium Tuberculosis* Infection. In *Seminars in immunopathology*; Springer, **2015**; 37, pp 239–249.

(10)   Draper, P.; Daffé, M. The Cell Envelope of *Mycobacterium Tuberculosis* with Special Reference to the Capsule and Outer Permeability Barrier. In *Tuberculosis and the tubercle bacillus*; *AMS Journals*, **2005**; pp 261–274.

(11)   Brodin, P.; Demangel, C.; Cole, S. T. Introduction to Functional Genomics of the Mycobacterium Tuberculosis Complex. In *Tuberculosis and the tubercle bacillus*; *AMS Journals*, **2005**; pp 141–154.

(12)   Migliori, G. B.; D'Ambrosio, L.; Centis, R.; Van Den Boom, M.; Ehsani, S.; Dara, M. Guiding Principles to Reduce Tuberculosis Transmission in the WHO European Region. **2018**.

(13)   Nardell, E. A.; Piessens, W. F. Transmission of Tuberculosis in Tuberculosis: A Comprehensive International Approach. LB Reichman and ES Hershfield Ed. Marcel Dekker, New York 2000.

(14)   Dye, C.; Williams, B. G. Eliminating Human Tuberculosis in the Twenty-First Century. *J. R. Soc. Interface* **2008**, *5* (23), 653-662.

(15)   Cruz-Knight, W.; Blake-Gumbs, L. Tuberculosis: An Overview. *Primary Care -*

Clinics in Office Practice. **2013**, *40* (3), p743 – 756.

(16)   Cohen, A.; Mathiasen, V. D.; Schön, T.; Wejse, C. The Global Prevalence of Latent Tuberculosis: A Systematic Review and Meta-Analysis. *Eur. Respir. J.* **2019**, *54* (3), 1900655.

(17)   Churchyard, G. J.; Swindells, S. Controlling Latent TB Tuberculosis Infection in High-Burden Countries: A Neglected Strategy to End TB. *PLoS Med.* **2019**, *16* (4), e1002787.

(18)   Grosset, J. *Mycobacterium Tuberculosis* in the Extracellular Compartment: An Underestimated Adversary. *Antimicrob. Agents Chemother.* **2003**, *47* (3), 833– 836.

(19)   Gideon, H. P.; Phuah, J.; Myers, A. J.; Bryson, B. D.; Rodgers, M. A.; Coleman, M. T.; Maiello, P.; Rutledge, T.; Marino, S.; Fortune, S. M. Variability in Tuberculosis Granuloma T Cell Responses Exists, but a Balance of pro-and Anti-Inflammatory Cytokines Is Associated with Sterilization. *PLoS Pathog.* **2015**, *11* (1), e1004603.

(20)   Rook, G. A. W.; Bloom, B. R. Mechanisms of Pathogenesis in Tuberculosis. *Tuberc. Pathog. Prot. Control* **1994**, 485–501.

(21)   Wormser, G. P.; Belknap, R. W.; Cohn, D. L. Tuberculosis, Second Edition Edited by William N. Rom and Stuart M. Garay Philadelphia: Lippincott Williams & Wilkins, 2004. 944 Pp., Illustrated. $159.95 (Cloth). *Clin. Infect. Dis.* **2004**, *38 (10)*, 1509.

(22)   Smith, I. *Mycobacterium Tuberculosis* Pathogenesis and Molecular Determinants of Virulence. *Clin. Microbio.l Rev*. **2003**, *16* (3), 463 – 496.

(23)   Comas, I.; Coscolla, M.; Luo, T.; Borrell, S.; Holt, K. E.; Kato-Maeda, M.; Parkhill, J.; Malla, B.; Berg, S.; Thwaites, G. Out-of-Africa Migration and Neolithic Co-expansion of *Mycobacterium Tuberculosis* with Modern Humans. *Nat. Genet.* **2013**, *45* (10), 1176–1182.

(24)   Farer, L. S.; Lowell, A. M.; Meador, M. P. Extrapulmonary Tuberculosis in the United States. *Am. J. Epidemiol.* **1979**, *109* (2), 205–217.

(25)   Guirado, E.; Schlesinger, L. Modeling the *Mycobacterium Tuberculosis* Granuloma–the Critical Battlefield in Host Immunity and Disease. *Front. Immunol.* **2013**, *4*, 98 - 105.

(26) Elkington, P.; Lerm, M.; Kapoor, N.; Mahon, R.; Pienaar, E.; Huh, D.; Kaushal, D.; Schlesinger, L. S. In Vitro Granuloma Models of Tuberculosis: Potential and Challenges. *J. Infect. Dis.* **2019**, *219* (12), 1858–1866.

(27) Ray, S.; Talukdar, A.; Kundu, S.; Khanra, D.; Sonthalia, N. Diagnosis and Management of Miliary Tuberculosis: Current State and Future Perspectives. *Ther. Clin. Risk Manag.* **2013**, *9*, 9 – 26.

(28) Mohammed, H.; Assefa, N.; Mengistie, B. Prevalence of Extrapulmonary Tuberculosis among People Living with HIV/AIDS in Sub-Saharan Africa: A Systemic Review and Meta-Analysis. *HIV/AIDS (Auckland, NZ)* **2018**, *10*, 225 – 237.

(29) Lee, J. Y. Diagnosis and Treatment of Extrapulmonary Tuberculosis. *Tuberc. Respir. Dis.* **2015**, *78* (2), 47–55.

(30) Valdés, L.; Alvarez, D.; San José, E.; Penela, P.; Valle, J. M.; García-Pazos, J. M.; Suárez, J.; Pose, A. Tuberculous Pleurisy: A Study of 254 Patients. *Arch. Intern. Med.* **1998**, *158* (18), 2017–2021.

(31) Ryu, Y. J. Diagnosis of Pulmonary Tuberculosis: Recent Advances and Diagnostic Algorithms. *Tuberc. Respir. Dis*. **2015**, *78* (2), 64 - 71.

(32) Krysl, J.; Korzeniewska-Kosela, M.; Muller, N. L.; FitzGerald, J. M. Radiologic Features of Pulmonary Tuberculosis: An Assessment of 188 Cases. *Can. Assoc. Radiol. J.* **1994**, 45 (2), 101 - 107.

(33) Grossman, R. F.; Hsueh, P. R.; Gillespie, S. H.; Blasi, F. Community-Acquired Pneumonia and Tuberculosis: DIFFERENTIAL Diagnosis and the Use of Fluoroquinolones. *Int. J. Infect. Dis*. **2014**, *18*, 14 - 21.

(34) PILLAY, K. *TB DIAGNOSTICS*. https://www.lancet.co.za/wp-content/uploads/2015/07/N00146-South-Africa-TB-DIAGNOSTICS-FEB2016.pdf (accessed 2022-03-19).

(35) Greco, S.; Girardi, E.; Navarra, A.; Saltini, C. Current Evidence on Diagnostic Accuracy of Commercially Based Nucleic Acid Amplification Tests for the Diagnosis of Pulmonary Tuberculosis. *Thorax* **2006**, *61*, 783 - 790.

(36) Updated Guidelines for the Use of Nucleic Acid Amplification Tests in the Diagnosis of Tuberculosis. *J. Am. Med. Assoc.* **2009**, *58* (1), 7 - 10.

(37) C. Dela Cruz, P. Lyons, S. Pasnick, T. Weinstock, P. Nahid, K. Wilson, C.

Thomson; Treatment of drug-susceptible tuberculosis. *Ann. Am. Thorac. Soc.* **2016**, 13 (11), 2060 – 2063.

(38) Nahid, P.; Dorman, S. E.; Alipanah, N.; Barry, P. M.; Brozek, J. L.; Cattamanchi, A.; Chaisson, L. H.; Chaisson, R. E.; Daley, C. L.; Grzemska, M. Official American Thoracic Society/Centers for Disease Control and Prevention/Infectious Diseases Society of America Clinical Practice Guidelines: Treatment of Drug-Susceptible Tuberculosis. *Clin. Infect. Dis.* **2016**, *63* (7), e147–e195.

(39) D'Ambrosio, L.; Dara, M.; Tadolini, M.; Centis, R.; Sotgiu, G.; Van Der Werf, M. J.; Gaga, M.; Cirillo, D.; Spanevello, A.; Raviglione, M.; Blasi, F.; Migliori, G. B.; Hafizi, H.; Wanlin, M.; Oñate, W. A.; Groenen, G.; Janković, V. K.; Šimunović, A.; Wallenfels, J.; Voniatis, C.; Andersen, P. H.; Viiklepp, P.; Danilovits, M.; Kummik, T.; Ruutu, P.; Comolet, T. M.; Haas, W.; Korr, G.; Rüsch-Gerdes, S.; Bauer, T.; Hauer, B.; Brodhun, B.; Papavenstsis, K.; Papadima, S.; Pusztai, Z.; O'Donnell, J.; Chemtob, D.; Girardi, E.; Mehmeti, R.; Riekstina, V.; Asciak, A. P.; Arnesen, T. M.; Augustynowicz-Kopeć, E.; Korzeniewska-Kosela, M.; Miskiewicz, P. M.; Miecznikowska, D.; Duarte, R.; Correia, A. M.; Diniz, A. M. S. C.; Talevski, S.; Zakoska, M.; Popescu, G.; Chiotan, D.; Asic, G. R. J.; Solovic, I.; Ivanuša, M.; Košnik, M.; Valín, E. R.; Anchuela, O. T.; Jonsson, J.; Helbling, P.; Zellweger, J. P.; De Vries, G.; Erkens, C.; Anderson, L.; Laurenson, I. Tuberculosis Elimination: Theory and Practice in Europe. *Eur. Respir. J.* **2014**, *43* (5), 1410 - 1420.

(40) Sterling, T. R.; Villarino, M. E.; Borisov, A. S.; Shang, N.; Gordin, F.; Bliven-Sizemore, E.; Hackman, J.; Hamilton, C. D.; Menzies, D.; Kerrigan, A. Three Months of Rifapentine and Isoniazid for Latent Tuberculosis Infection. *N. Engl. J. Med.* **2011**, *365* (23), 2155–2166.

(41) Daniel, T. M. Toman's Tuberculosis. Case Detection, Treatment, and Monitoring. Questions and Answers. Second Edition. *Am. J. Trop. Med. Hyg.* **2005**, 62, 70.

(42) Sotgiu, G.; Centis, R.; D'Ambrosio, L.; Migliori, G. B. Medical Treatment of Pulmonary Tuberculosis. *Eur. Respir. Monogr.* **2013**, 61, 11 - 19.

(43) WHO. *Treatment of Tuberculosis: Guidelines for Treatment of Drug-Susceptible Tuberculosis and Patient Care. 2017 Update*; 2017.

(44) Laurenzi, M.; Ginsberg, A.; Spigelman, M. Challenges Associated with Current and Future TB Treatment. *Infect. Disord. Targets,* **2007**, *7* (2), 105–119.

(45) Shepherd, R. G.; Baughn, C.; Cantrall, M. L.; Goodstein, B.; Thomas, J. P.; Wilkinson, R. G. Design, Synthesis and Evaluation of Novel Ethambutol Analogues. *Ann. NY Acad. Sci* **1966**, *135*, 686–710.

(46) Zimmerman, M.; Lestner, J.; Prideaux, B.; O'Brien, P.; Dias-Freedman, I.; Chen, C.; Dietzold, J.; Daudelin, I.; Kaya, F.; Blanc, L. Ethambutol Partitioning in Tuberculous Pulmonary Lesions Explains Its Clinical Efficacy. *Antimicrob. Agents Chemother.* **2017**, *61* (9), e00924-17.

(47) Telenti, A.; Philipp, W. J.; Sreevatsan, S.; Bernasconi, C.; Stockbauer, K. E.; Wieles, B.; Musser, J. M.; Jacobs, W. R. The Emb Operon, a Gene Cluster of *Mycobacterium Tuberculosis* Involved in Resistance to Ethambutol. *Nat. Med.* **1997**, *3* (5), 567–570.

(48) Singh, N.; Sharma, L. Enantioseparation of D-and L-Isomers of Chiral Drugs for Improving Their Bioavailability: Some Techniques Including Micellization with Gemini Surfactants. *Indian J. Pharm. Educ* **2018**, *52*, 334–341.

(49) Jhun, B. W.; Koh, W.-J. Treatment of Isoniazid-Resistant Pulmonary Tuberculosis. *Tuberc. Respir. Dis.* **2020**, *83* (1), 20–30.

(50) Zhang, Y.; Heym, B.; Allen, B.; Young, D.; Cole, S. The Catalase—Peroxidase Gene and Isoniazid Resistance of *Mycobacterium Tuberculosis*. *Nature* **1992**, *358* (6387), 591–593.

(51) Zhang, Y *Tuberculosis*; Scott A. Waldman, Andre Terzic, Laurence J. Egan, Jean-Luc Elghozi, Arshad Jahangir, Garvan C. Kane, Walter K. Kraft, Lionel D. Lewis, Jason D. Morrow, Leonid V. Zingman, Darrell R. Abernethy, Arthur J. Atkinson, Neal L. Benowitz, D. Craig Brater, Jean Gr, R. L. W., Ed.; **2009**, provide the 1089 - 1106.

(52) O'Brien, R. J.; Lyle, M. A.; Snider Jr, D. E. Rifabutin (Ansamycin LM 427): A New Rifamycin-S Derivative for the Treatment of Mycobacterial Diseases. *Rev. Infect. Dis.* **1987**, *9* (3), 519–530.

(53) Skinner, M. H.; Blaschke, T. F. Clinical Pharmacokinetics of Rifabutin. *Clin. Pharmacokinet.* **1995**, *28* (2), 115–125.

(54) (CDC, C. for D. C. and P. Updated Guidelines for the Use of Rifabutin or Rifampin for the Treatment and Prevention of Tuberculosis among HIV-Infected Patients Taking Protease Inhibitors or Non-nucleoside Reverse Transcriptase Inhibitors.

MMWR. Morb. Mortal. Wkly. Rep. **2000**, *49* (9), 185–189.

(55) Suresh, A. B.; Rosani, A.; Wadhwa, R. Rifampin. In *StatPearls [Internet]*; StatPearls Publishing, **2022**.

(56) Fernandes, J. P. dos S.; Pavan, F. R.; Leite, C. Q. F.; Felli, V. M. A. Synthesis and Evaluation of a Pyrazinoic Acid Prodrug in *Mycobacterium Tuberculosis*. *Saudi Pharm. J.* **2014**, 22 (4), 376 - 380

(57) Heifets, L.; Lindholm-Levy, P. Pyrazinamide Sterilizing Activity in Vitro against Semidormant *Mycobacterium Tuberculosis* Bacterial Populations. *Am. Rev. Respir. Dis.* **1992**, 145 (5), 1223 - 1225.

(58) Zhang, Y.; Shi, W.; Zhang, W.; Mitchison, D. Mechanisms of Pyrazinamide Action and Resistance. *Microbiol. Spectr.* **2014**, 2 (4), MGM – 0023 - 2013.

(59) Mitchison, D. A. The Action of Antituberculosis Drugs in Short-Course Chemotherapy. *Tubercle* **1985**, *66* (3), 219–225.

(60) Fox, W.; Ellard, G. A.; Mitchison, D. A. Studies on the Treatment of Tuberculosis Undertaken by the British Medical Research Council Tuberculosis Units, 1946-1986, with Relevant Subsequent Publications. *Int. J. Tuber. Lung Dis.* **1999**, *3* (2), S231 – S279.

(61) Heifets, L. B.; Flory, M. A.; Lindholm-Levy, P. J. Does Pyrazinoic Acid as an Active Moiety of Pyrazinamide Have Specific Activity against Mycobacterium Tuberculosis? *Antimicrob. Agents Chemother.* **1989**, 33 (8), 1252 – 1254.

(62) McCune, R. M.; Feldmann, F. M.; Lambert, H. P.; McDermott, W. Microbial Persistence. I. The Capacity of Tubercle Bacilli to Survive Sterilization in Mouse Tissues. *J. Exp. Med.* **1966**, 123 (3), 445 - 468.

(63) Fyfe, P. K.; Rao, V. A.; Zemla, A.; Cameron, S.; Hunter, W. N. Specificity and Mechanism of Acinetobacter Baumanii Nicotinamidase: Implications for Activation of the Front-Line Tuberculosis Drug Pyrazinamide. *Angew. Chemie - Int. Ed.* **2009**, 48(48), 9176 - 9179.

(64) Zhang, Y.; Scorpio, A.; Nikaido, H.; Sun, Z. Role of Acid PH and Deficient Efflux of Pyrazinoic Acid in Unique Susceptibility of *Mycobacterium Tuberculosis* to Pyrazinamide. *J. Bacteriol.* **1999**, 181 (7), 2044 - 2049.

(65) Zhang, Y.; Wade, M. M.; Scorpio, A.; Zhang, H.; Sun, Z. Mode of Action of Pyrazinamide: Disruption of *Mycobacterium Tuberculosis* Membrane Transport

and Energetics by Pyrazinoic Acid. *J. Antimicrob. Chemother.* **2003**, 52(5), 790 - 795.

(66) Zhang, Y.; Mitchison, D. The Curious Characteristics of Pyrazinamide: A Review. *Int. J. Tuberc. and Lung Dis*. **2003**, 7(1), 6 - 21.

(67) Georgi Momekov1, Dilyan Ferdinandov, Yulian Voynikov, Georgi Stavrakov, Pyrazinamide – Pharmaceutical, Biochemical and Pharmacological Properties and Reappraisal of its Role in the Chemotherapy of Tuberculosis. *Pharmacia* **2014**, *61* (1), 38–67.

(68) Scorpio, A.; Zhang, Y. Mutations in *PncA*, a Gene Encoding Pyrazinamidase/Nicotinamidase, Cause Resistance to the Antituberculous Drug Pyrazinamide in Tubercle Bacillus. *Nat. Med.* **1996**, 2, 662 - 667.

(69) Scorpio, A.; Lindholm-Levy, P.; Heifets, L.; Gilman, R.; Siddiqi, S.; Cynamon, M.; Zhang, Y. Characterization of *PncA* Mutations in Pyrazinamide-Resistant *Mycobacterium Tuberculosis*. *Antimicrob. Agents Chemother.* **1997**, 41 (3), 540 - 543.

(70) Shi, J.; Su, R.; Zheng, D.; Zhu, Y.; Ma, X.; Wang, S.; Li, H.; Sun, D. Pyrazinamide Resistance and Mutation Patterns among Multidrug-Resistant *Mycobacterium Tuberculosis* from Henan Province. *Infect. Drug Resist.* **2020**, *13*, 2929 – 2941.

(71) Stehr, M.; Elamin, A. A.; Singh, M. Pyrazinamide: The Importance of Uncovering the Mechanisms of Action in Mycobacteria. *Exp. Rev. Anti-Inf. Ther*. **2015**, 13 (5), 593 - 603.

(72) Syre, H.; Øvreås, K.; Grewal, H. M. S. Determination of the Susceptibility of *Mycobacterium Tuberculosis* to Pyrazinamide in Liquid and Solid Media Assessed by a Colorimetric Nitrate Reductase Assay. *J. Antimicrob. Chemother.* **2010**, 65 (4), 704 - 712.

(73) Gumbo, T.; Dona, C. S. W. S.; Meek, C.; Leff, R. Pharmacokinetics-Pharmacodynamics of Pyrazinamide in a Novel in Vitro Model of Tuberculosis for Sterilizing Effect: A Paradigm for Faster Assessment of New Antituberculosis Drugs. *Antimicrob. Agents Chemother.* **2009**, 53 (8), 3197 - 3204.

(74) Lacroix, C.; Phan Hoang, T.; Nouveau, J.; Guyonnaud, C.; Laine, G.; Duwoos, H.; Lafont, O. Pharmacokinetics of Pyrazinamide and Its Metabolites in Healthy Subjects. *Eur. J. Clin. Pharmacol.* **1989**, 36, 395 - 400.

(75) World Health Organisation.; Multidrug-Resistant Tuberculosis (MDR-TB) 2013 Update. *Geneva, Switz. WHO* **2014**.

(76) Fischel-Ghodsian, N.; Prezant, T. R.; Chaltraw, W. E.; Wendt, K. A.; Nelson, R. A.; Arnos, K. S.; Falk, R. E. Mitochondrial Gene Mutation Is a Significant Predisposing Factor in Aminoglycoside Ototoxicity. *Am. J. Otolaryngol.* **1997**, *18* (3), 173–178.

(77) Pandya, A.; Xia, X.; Radnaabazar, J.; Batsuuri, J.; Dangaansuren, B.; Fischel-Ghodsian, N.; Nance, W. E. Mutation in the Mitochondrial 12S RRNA Gene in Two Families from Mongolia with Matrilineal Aminoglycoside Ototoxicity. *J. Med. Genet.* **1997**, *34* (2), 169–172.

(78) Reeves, A. Z.; Campbell, P. J.; Sultana, R.; Malik, S.; Murray, M.; Plikaytis, B. B.; Shinnick, T. M.; Posey, J. E. Aminoglycoside Cross-Resistance in Mycobacterium Tuberculosis Due to Mutations in the 5′ Untranslated Region of WhiB7. *Antimicrob. Agents Chemother.* **2013**, *57* (4), 1857–1865.

(79) Schluger, N. W. Fluoroquinolones in The Treatment of Tuberculosis: Which Is Best? *Am. J. Respir. Crit. Care Med*. **2013**, *188* (7), 768 - 769.

(80) Grosjean, P.; Urien, S. Reevaluation of Moxifloxacin Pharmacokinetics and Their Direct Effect on the QT Interval. *J. Clin. Pharmacol.* **2012**, *52* (3), 329–338.

(81) WHO. *Global Tuberculosis Report* **2022**. https://doi.org/.1037//0033-2909.I26.1.78.

(82) Rendon, A.; Tiberi, S.; Scardigli, A.; D'Ambrosio, L.; Centis, R.; Caminero, J. A.; Migliori, G. B. Classification of Drugs to Treat Multidrug-Resistant Tuberculosis (MDR-TB): Evidence and Perspectives. *J. Thorac. Dis.* **2016**, *8* (10), 2666.

(83) Srivastava, S.; Peloquin, C. A.; Sotgiu, G.; Migliori, G. B. Therapeutic Drug Management: Is It the Future of Multidrug-Resistant Tuberculosis Treatment? *Eur. Respir. J*. **2013**, *49*, 1449–1453.

(84) Cox, H.; Ford, N. Linezolid for the Treatment of Complicated Drug-Resistant Tuberculosis: A Systematic Review and Meta-Analysis. *Int. J. Tuberc. Lung Dis.* **2012**, *16* (4), 447–454.

(85) Skripconoka, V.; Danilovits, M.; Pehme, L.; Tomson, T.; Skenders, G.; Kummik, T.; Cirule, A.; Leimane, V.; Kurve, A.; Levina, K. Delamanid Improves Outcomes and Reduces Mortality in Multidrug-Resistant Tuberculosis. *Eur. Respir. J.* **2013**,

41 (6), 1393–1400.

(86)   Tadolini, M.; Garcia-Prats, A. J.; D'Ambrosio, L.; Hewison, C.; Centis, R.; Schaaf, H. S.; Marais, B. J.; Ferreira, H.; Caminero, J. A.; Jonckheere, S. Compassionate Use of New Drugs in Children and Adolescents with Multidrug-Resistant and Extensively Drug-Resistant Tuberculosis: Early Experiences and Challenges. *Eur. Respir. J.* **2016**, *48* (3), 938–943.

Chapter Two

Quinolones and related structural chemistry

2.1   Introduction

The goal of the study is to find molecules that could destabilize normal living conditions of bacterial cells. Most antibacterial drugs mainly target the cell wall synthesis, protein synthesis, RNA synthesis, DNA synthesis and metabolic pathways[1]. Herein, a brief review of some of the recent developments in the synthesis and medicinal chemistry of quinolones and their application for the treatment of tuberculosis (TB) is presented. Previous work on the hybridisation of isoniazid and quinolone pharmacophores through the hydrazine linker yielded compounds that showed promising *in vitro* antitubercular activity[2]. Isoniazid and pyrazinamide have structures that are very similar and have similar chemical properties. The emphasis of this chapter will be on the synthesis and pharmacology of quinolones and their related compounds.

2.2   Quinolones and their derivatives

Heterocyclic molecules are organic compounds with a ring structure that contains elements such as nitrogen (N), oxygen (O) and sulphur (S). Most of the compounds contain five or six-member ring structures which are inherently more stable than the three, four, seven or larger-member rings.[3] The ring systems can be aromatic or non-aromatic, and the non-aromatic structures have the same chemical properties as their acyclic counterparts[4]. Heterocycles are very significant in today's drug discovery, and they are widely used in medicinal chemistry and biochemistry fields[5]. Some heterocycles are traditionally derived from naturally occurring sources[5]. Heterocyclic chemistry constitutes a large group of chemical compounds that are used in drug discovery, agriculture, veterinary products, etc[6]. Typical examples of important heterocyclic ring member systems are quinolones and quinolines.

Quinolones and quinolines are compounds which belong to the same family. Quinoline was first isolated from coal tar in 1834 and it was found to be a pyrolytic degradation product of cinchonamine, an alkaloid closely related to quinine[7]. Many antimalarial

drugs such as chloroquine (CQ) (**Figure 2.1**) contain a quinoline scaffold. Fluoroquinolones are derivatives of the quinoline structure.
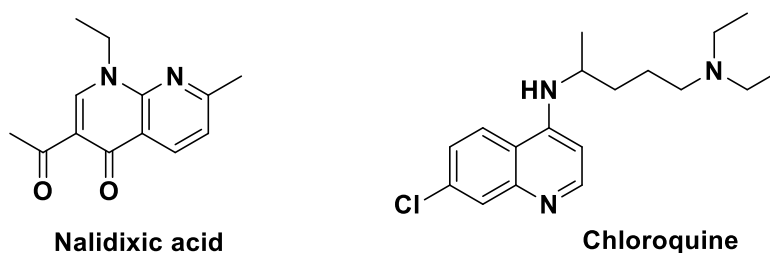

Figure 2.1 The chemical structures of nalidixic acid and chloroquine.

The parent heterocycle for all quinolones and fluoroquinolones is quinones. 2 and 4–Hydroxyquinoline was isolated from plant sources, and they exist as 2(1*H*)-quinolone and 4(1*H*)-quinolone, respectively[8]. Nalidixic acid (**Figure 2.1**) is the first quinolone that was administered as a drug, and it became a prototype in which all first-generation quinolones were designed. Nalidixic acid was identified as a by-product during the synthesis of the antimalarial agent CQ, and it showed activity against gram-negative bacteria[9]. Compounds that were efficient against gram-negative bacteria led to the new derivatives such as pipemidic acid, piromidic acid, oxolinic acid, cinoxacin and flumequine (**Figure 2.2**), which are regarded as the first generation of antibacterial quinolones[10]. Initially, quinolones had a narrow spectrum, they were efficacious against gram-negative bacteria and minimum activity was noticed in gram-positive bacteria. Consequently, these compounds were only used in the treatment of urinary tract infections caused by *Escherichia coli* and other gram-negative bacteria. With further studies involving quinolones, researchers managed to unlock more potential in quinolones and structure-activity relationship studies led to derivatives with various substituents at the specific positions on the quinolone scaffold. Notable substitutions were made on position 6 by inserting a fluorine atom to yield the next generation of quinolone-containing compounds, fluoroquinolones. Fluoroquinolones exhibit activity against organisms such as *Pseudomonas aeruginosa,* an organism that is mostly transmitted in the hospital environment [9].
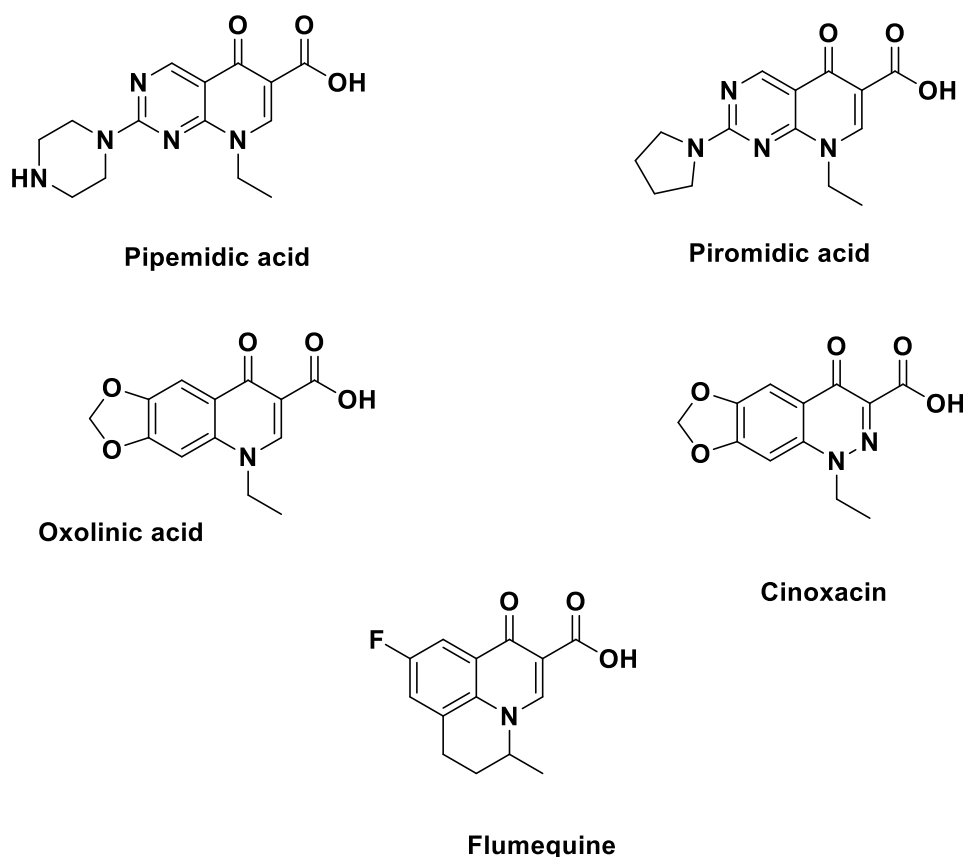
Pipemidic acid

Piromidic acid

Oxolinic acid

Cinoxacin

Flumequine

Figure 2.2: Chemical structures derivatives active against gram-negative bacteria.

Although quinolones are derived from natural sources,[11] most of them are accessible through synthesis. 6-Fluoroquinolones and 4-quinolones are synthetic antibacterial agents related to nalidixic acid and oxolinic acid[12]. It is estimated that over 10000 analogues of nalidixic acid or fluoroquinolones have been synthesised[13]. The nitrogen atom occupies position one and it allows the attachment of alkyl groups such as methyl, ethyl, or benzyl groups. The ethyl and methyl groups have been found to influence the pharmacokinetic properties of quinolones and membrane permeability in living cells[13]. The same impact is noticed when alkyl groups are added to the para position of the piperazinyl ring. A carboxylic acid group in position three is a key structural feature of quinolones and it is required for antimicrobial activity. The fluorine atom in position six broadens the scope in terms of the biological activity bacterial species. Quinolone compounds can permeate through the cellular membranes since they possess both acidic and basic properties in their structure resembling the zwitterionic structure[12].

2.2.1 Mechanism of action of quinolones

Quinolones are bactericidal hence they induce the death of bacterial cells. They work by inhibiting DNA synthesis, thereby causing cleavage of bacterial DNA in the DNA-enzyme complexes of the DNA gyrase and type IV topoisomerase which unequivocally result in cell death[12-14]. Bacteria have type II topoisomerase also known as DNA gyrase, a tetrameric bacterial enzyme that folds and coils 1.0-0.3 m (length) of the bacterial circular DNA to make it compact[12]. DNA gyrase is responsible for keeping the DNA structure in a comfortable state with less risk of damage during replication. The DNA is coiled around an RNA core in a series of loops. According to Sarkozy each loop or domain is then negatively supercoiled by nicking both strands of DNA and passing that broken strand "behind" the accompanying double-strand and then resealing the double nick', a process facilitated by the DNA gyrase. Quinolones inhibit the A sub-unit of DNA gyrase (coded by the *gyr* A gene), interfering with the DNA re-joining step. As a result, genetic material is liberated, and some fragments keep piling as more replication is taking place [15]. Bacterial DNA gyrase is exclusively susceptible to 4-quinolone antimicrobials which uniquely spare the human (mammalian) DNA gyrase. The fragments will be destroyed by exonucleases, this is a mechanism that naturally exists in cellular environments[16]. Generally, activity against gram-negative bacteria correlates with the inhibition of DNA gyrase, and activity against gram-positive is linked with inhibition of DNA type IV topoisomerase[17].

2.3   Synthetic pathways for quinolones

Although quinolones are derived from natural sources, most quinolone-containing molecules are completely synthetic compounds[18]. The first commercially synthesised quinolone, nalidixic acid (1,8-naphthyridine carboxylic acid) and the structural variations were systematically synthesised until the end of the 1970s[19]. There has been various campaign to develop new methods for the synthesis and the improvement of the older approaches to the synthesis of quinolones.

2.3.1 Gould Jacob's reaction

This reaction process is used to make heterocyclic frameworks. Until the 1970s, this method was commonly used in the synthesis of 1,4-dihydro-4-oxoquinoline-3-carboxylic acid derivatives and is now used in the synthesis of some quinolones such as norfloxacin[19]. The Gould-Jacob's reaction is carried out between -78 and 250°C at 0.01 and 100 bar pressure[20]. This method is the most efficient route for the synthesis of quinolones. Gould-Jacob's reaction demonstrated the pyrolysis technique in the construction of heterocyclic systems that require high-energy transfers[20]. The initial step involves the condensation of an arylamine with diethyl ethoxymethylenamalonate at 80-120 °C to form an arylaminomethylenemalonic ester (**Scheme 2.1**). This step is followed by a heat-induced cyclization of boiling in diphenyl ether or Dowtherm A, at 250-270 °C [21,19]. More importantly, scientists have managed to improve the Gould-Jacobs reaction through the discovery of improved reaction conditions and outcomes. Substitution of aniline with either alkoxy methylene malonic ester or acyl malonic ester results in an anilinomethylenemalonic ester. This method of approach for the synthesis of quinolones is cheap and all the raw materials are easily acquired. This study was performed using the traditional Gould Jacobs approach for the synthesis of quinolones.
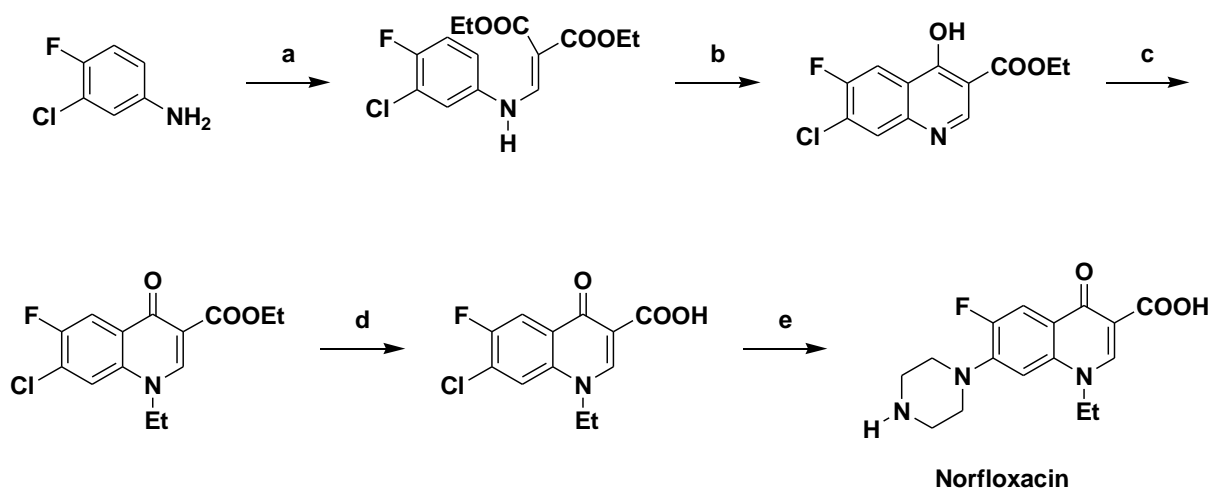
Scheme 2.1: Synthesis of norfloxacin[19] (a) EtOCH=C(CO$_2$Et)$_2$; (b) Dowtherm A, heat (c) EtI, K$_2$CO$_3$, DMF; (d) H$_3$O$^+$ or OH$^-$; (e) piperazine.

2.3.2 Conrad-Limpach synthesis of quinolones

Conrad-Limpach synthesis is one of the traditional techniques used to synthesize the quinoline system. However, this approach can be used in combinatorial chemistry to produce quinolones that are substituted at various positions with methane sulfonic acid as a catalyst[22]. In classical quinolone synthesis, the formation of intermediates will involve the use of high-boiling point solvents[23]. The substrate for cyclization to take place must be a high-energy imine enol tautomer. The cyclization into the hemiketal which is a substructure that is formed when the alcohol oxygen atom attaches to the carbonyl carbon atom of an aldehyde or ketone breaks the aromaticity of the phenyl ring. Solvents with very high boiling points are traditionally used. Reference solvents used are diphenyl ether (BP = 259 °C) and Dowtherm A (BP = 259 °C). Studies have shown that the usage of solvents of boiling points above 250 °C will result in high yields of 4-hydroxyquinolines (**Scheme 2.2**)[23]. The synthesis of 4-quinolones using the Conrad-Limpach synthesis method will often result in the isomerization of the quinolone to 4-hydroxyquinolines. High temperatures are required so the cis stereochemical relationship of the ester groups will undergo isomerization before ring closure[24].
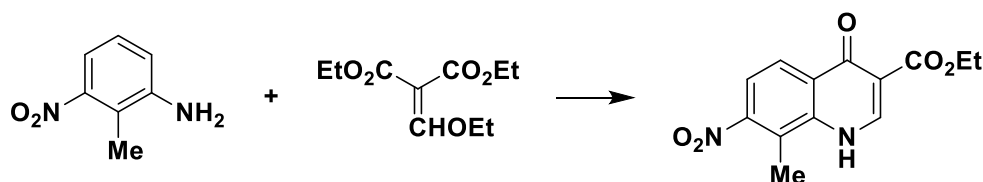
Scheme 2.2: Quinolone synthesis by the Conrad-Limpach method.

2.3.3 Camps quinolone synthesis

In 1901, Camps described the cyclo-condensation of 2-formamide-acetophenone in an alkaline medium to form 4-hydroxyquinoline. Camps achieved this by heating the ethyl ester of 2-formamido-propynoic acid with aqueous alcoholic sodium hydroxide (**Scheme 2.3**)[19]. The Camps quinolone synthesis is based on a metal-catalysed synthesis of N-containing heterocycles[25]. Unlike traditional approaches that use transitional metals, such as palladium-catalysed carbonylation, titanium-mediated reductive coupling and ruthenium-catalysed reduction reactions, Camps synthesis is

a metal-free method to access quinoline (enol form) and quinolone (keto form). This method is carried out in basic reaction conditions during the cyclisation of *N*-(ketoaryl) amides[26]. Camps precursors, *N*-(ketoaryl) amides*,* are accessible through condensation of *o*-aminoacetophenone and carboxylic acids or acid chlorides, Friedel-Crafts acylation of anilides. 4-Quinolones have two tautomeric forms, and they can either be 4-hydroxyquinoline in the enol form or 4-quinolones in the keto-form[26].
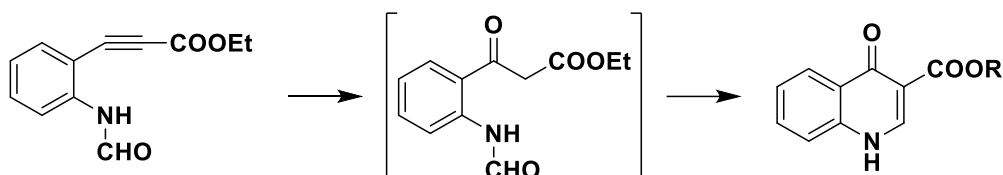
Scheme 2.3: Chemical illustration of the Camps quinolone synthesis route.

2.3.4 Biere and Seelen synthesis of quinolones

This process involves the addition of esters of *o*-aminobenzoic acid and esters of acetylene dicarboxylic acids to yield enamino esters. The resulting enamino ester intermediates undergo cyclisation to form dicarboxylic acid esters (**Scheme 2.4**). This process takes place in the presence of a strong base, i.e., sodium hydride or potassium *tert*-butoxide in dimethylformamide. Ester acids or dicarboxylic acids are obtained from regioselective or complete alkaline hydrolysis. The carboxylic acid group at position two is eliminated by thermal decarboxylation. The products can then be *N*-alkylated. However, this synthetic approach is not commonly used because it is a very expensive process and requires high temperatures. This method is not used to manufacture fluoroquinolones[27].
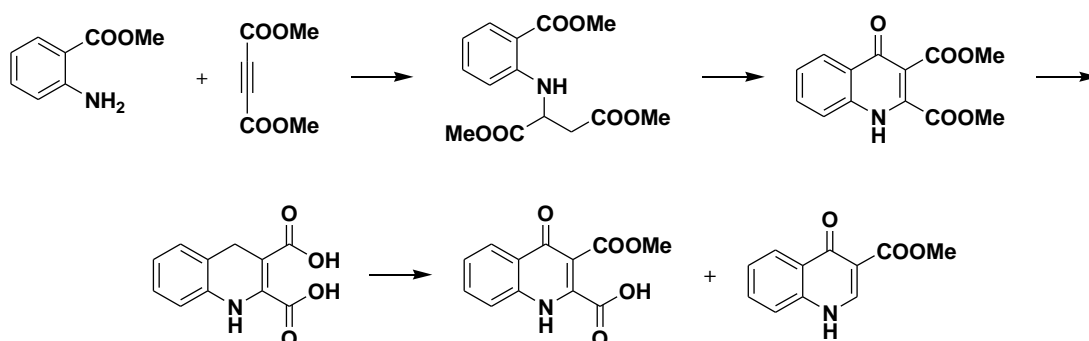
Scheme 2.4: Chemical illustration of Biere-Seelen synthesis of quinolones.

2.3.5 Dieckmann cyclisation of diester

Dieckmann cyclisation is a procedure used in the synthesis of *aza-* and diazaquinolone carboxylic acids derivatives[28]. This method like the above synthetic procedure will take place conveniently in basic conditions. The synthesis of enoxacin is an example of *aza-*quinolone accessible using this method. Regioselective reaction of 2,6-dichloro-5-fluoronicotinic acid ester at position 6 with *N*-acetyl piperazine yield 6-piperazinyl compound **2.3.5b**. The piperazinyl compound **2.3.5b** is treated with 3-ethylaminopropionic acid as ethyl ester to make a diester **2.3.5c**. The diester will undergo intramolecular ring closure with potassium *tert*-butylate to form the ethyl ester of tetrahydro-naphthyridine carboxylic acid **2.3.5d** (**Scheme 2.5**). Dehydrogenation of tetrahydronapthyridine carboxylic acid **2.3.5d** by chloranil yields the ethyl ester of naphthyridine carboxylic acid which will be hydrolysed to give fluoroquinolones in this case enoxacin **2.3.5e**[27]. The double bond between C2 and C3 can be formed by heating with chloranil in ethanol or dioxane or by using thionyl chloride[19].
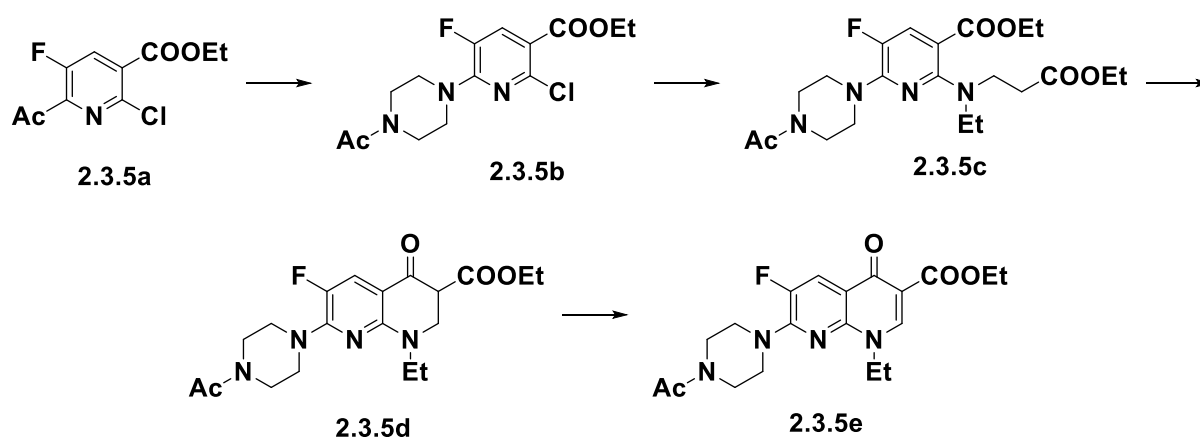
Scheme 2.5: Chemical illustration of the Dieckmann cyclisation of diesters.

2.3.6 Cycloaracylation

The cycloaracylation procedure was developed by Grohe *et al* in the mid-1970s[29,19]. The procedure is illustrated in the synthesis of ciprofloxacin, the first commercially produced fluoroquinolone with a cyclopropyl group at position N1 of the quinolone ring. 2,4-Dichloro-5-fluorobenzoyl chloride is reacted with ethyl 3-cyclopropyl-aminoacrylate in the presence of triethylamine giving an acrylated intermediate

(Scheme 2.6). The acylate intermediate undergoes cyclisation under the influence of potassium carbonate producing ethyl ester of the quinolone carboxylic acid[19].
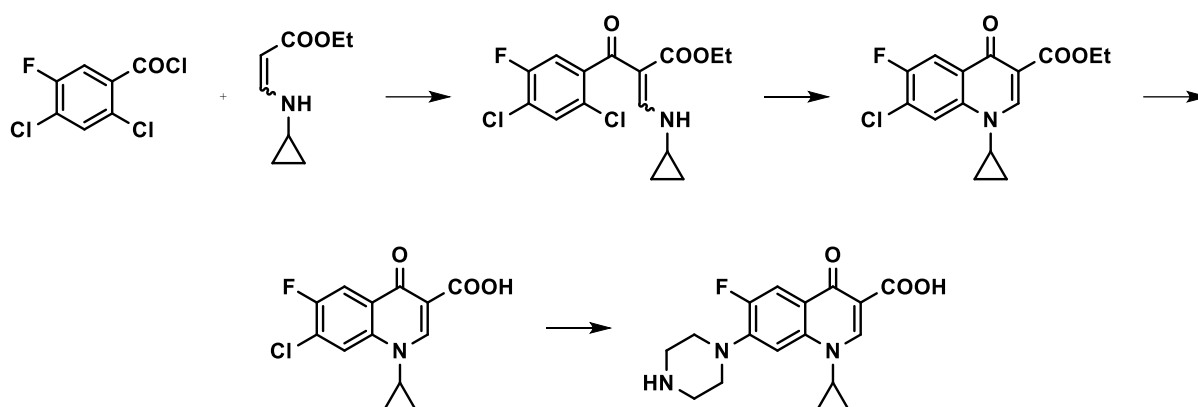
Scheme 2.6: Cycloacrylation method of synthesis of ciprofloxacin.

2.4   Therapeutic application of quinolones

The early quinolones discovered, i.e., nalidixic acid, are mainly effective against gram-negative bacteria. These were used to treat urinary tract infections because they are excreted mainly by micturition, hence they are found in high concentrations in genitourinary organs. However, there are complicated urinary tract infections in patients with kidney stones or obstructive uropathies and patients with catheters. These infections are usually nosocomial and are highly prone to causing the development of drug resistance. These types of infections are treated by the later-designed quinolones mainly ciprofloxacin, ofloxacin and lomefloxacin[30]. Quinolones have adequate permeability into prostatic tissue; hence they are used to treat prostatitis. Successful treatment is noticed in long-term therapy which ranges from four-six weeks. Levofloxacin is used as the first-line treatment and ciprofloxacin are used in complicated cases of prostatitis[31]. Although quinolones have high efficacy in the treatment of respiratory infections, there is a high chance of bacteria developing resistance[14]. The following sections are a summary of biomedical applications of quinolones and areas where quinolones have shown promise and could contribute to future treatment.

2.4.1 Quinolones in the treatment of tuberculosis

Fluoroquinolones (**Figure 2.2**) are mainly administered for the treatment of multidrug-resistant TB (MDR-TB)[32]. Due to their unique mode of action compared to the current first-line treatment, fluoroquinolones are becoming a regular preference in the treatment of multidrug-resistant TB. To avoid the widespread development of resistance by *mycobacterium* against fluoroquinolones [33], the WHO recommended the usage of levofloxacin and moxifloxacin in the treatment of MDR-TB. The two fluoroquinolones are an attractive choice because they showed activity against *Mtb* as compared to ciprofloxacin and have minimal side effects [32].
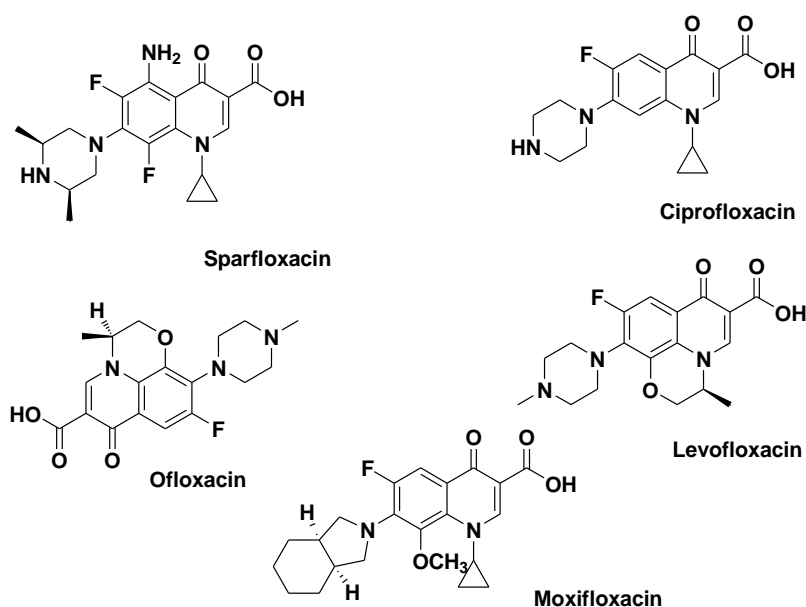
Figure 2.2: Commonly prescribed fluoroquinolones for the treatment of TB.

Studies on patients after they are prescribed levofloxacin and moxifloxacin showed positive results. However, there are patients previously being treated with levofloxacin who reported musculoskeletal abnormalities [32]. Levofloxacin is well tolerated during the first month of therapy when used in children, but one in four of these children had incidences of predefined musculoskeletal disorders. Thus, caution needs to be considered when prescribing levofloxacin to children[34]. With adverse events associated with fluoroquinolones that are being reported in young children and older patients, this is highlighting a gap in the research on fluoroquinolones. Despite their success, there is not enough evidence to substantially crown fluoroquinolones as the

future treatment plan for TB. Lately, fluoroquinolones are being used as first-line treatment, in patients that are suffering from TB caused by susceptible *Mycobacterium tuberculosis*[35].

South Africa has the highest per capita cases of MDR-TB and XDR-TB, and the prevalence of rifampicin resistance has doubled in the 2012-2014 period as compared to 2001-02[36]. Fluoroquinolones are providing new hope in the fight against MDR-TB[37]. Ciprofloxacin, ofloxacin, levofloxacin, and sparfloxacin (**Figure 2.2**) are commonly used in the treatment of TB. More importantly, fluoroquinolones have favourable bioavailability, pharmacokinetic properties, toxicity profiles, and drug-enhanced interaction profiles [38]. FQs drug agents have a minimum inhibitory concentration (MICs) range of 0.1 - 4 µg/mL[39]. Furthermore, fluoroquinolones induce activity within the human macrophage, where many tuberculosis bacilli reside[40,41]. Fluoroquinolones are widely distributed in the body including being found in the intracellular cavities, where they target tubercle bacilli[38]. FQs such as sparfloxacin in combination with other treatment agents such as rifabutin have synergistic properties in both susceptible strains and MDR-TB[42]. However, mycobacteria have evolved and developed resistance against fluoroquinolones. Ongoing studies suggest that resistance is a result of the mutation of genes, *gyrA* and *gyrB*, encoding the gyrase proteins. Resistance can manifest as cross-resistance, where resistance to a certain medicinal agent will result in the development of resistance to another treatment option[43]. This is common with antibiotics. Although fluoroquinolones are marvellous in the treatment of TB, they are still inferior to first-line treatment options, i.e., isoniazid and rifampicin. They are mostly used primarily as second-line options in combination with two or more antituberculosis agents[39].

The hybridization of quinolone with antibacterial compounds is a strategy that a lot of researchers have been exploiting to design novel antimycobacterial compounds. The investigation is centred around developing safe and highly effective antibacterial agents (antimicrobial) with potential multiple target sites and synergistic properties[44]. Quinolone and cephalosporin hybrid Ro 23-9424 (**Figure 2.3**) showed the potential of broad-spectrum activity against various bacteria including ESKAPE (*Escherichia coli,*

Staphylococcus aureus, Klebsiella pneumonia, Acinetobacter Baumannii, Pseudomonas aeruginosa) pathogens [44].
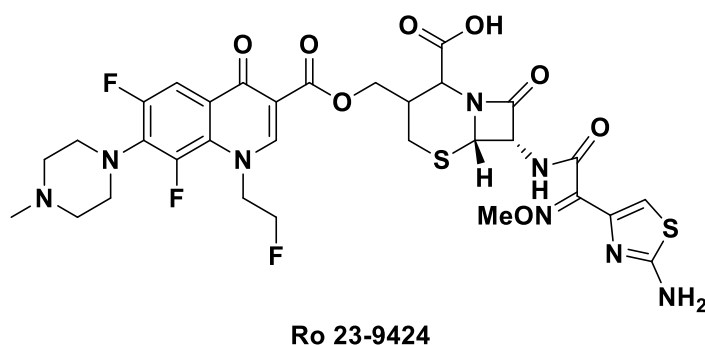
Ro 23-9424

Figure 2.3: Cephalosporin-quinolone hybrid.

Some research has been looking at exploiting the flexible core structure of quinolones. Beteck et al synthesised quinolone-isoniazid hybrid derivatives and tested them for antitubercular activity[2]. In their study, they incorporated hydrazine hydrazone as a link between isoniazid and quinolone framework (**Figure 2.4**). According to their findings, substitution at position-1 and -3 of the quinolone nucleus influences anti-MTB activity[2]. The compounds that showed high activity demonstrated activities comparable to isoniazid (INH).
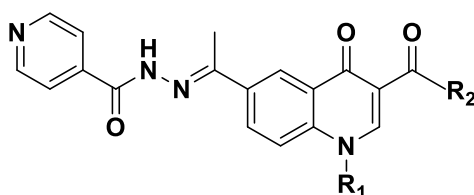
Figure 2.4: Core structure of isoniazid quinolone hydrazone hybrid.

2.4.2 Quinolones activity against protozoa

Due to the positive results that have been noted in the usage of quinolones, there have also been studies that reported the activity of quinolones against malaria and other protozoan parasites[45,46]. Endochin (**Figure 2.5**) is a 4-(1*H*)-quinolone compound which was initially synthesised and tested for antimalarial activity but did not yield any positive results when tested in humans[47]. Further research was later conducted to explore the synthesis of similar compounds referred to as endochin-like quinolones (ELQs). These compounds showed potency in the inhibition of *Toxoplasma gondii* proliferation *in vitro* and animal models[48]. ELQ-316 was identified as a lead compound (**Figure 2.5**) for

toxoplasmosis and has shown oral efficacy when administered orally in systemic mouse models of malaria and babesiosis[49,50].
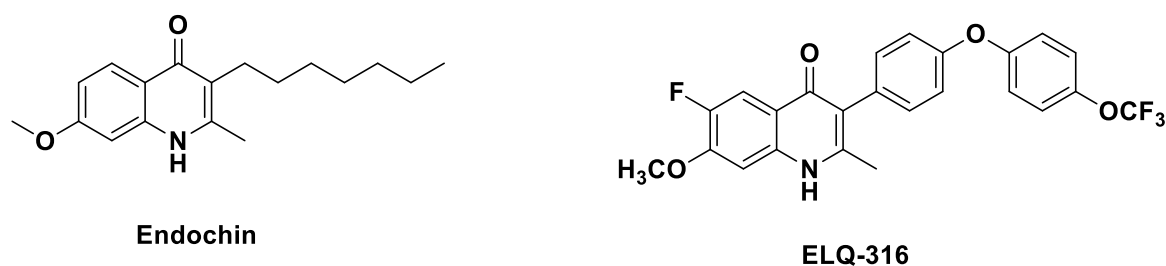

Figure 2.5: Chemical structure of Endochin and Endochine-like Quinolone derivative.

Fluoroquinolones and related quinolone compounds have shown potential *in vitro* antiplasmodial activities against erythrocytic and hepatic stages of chloroquine-sensitive (CQS) and chloroquine-resistant (CQR) strains of *Plasmodium falciparum*[51]. Organometallic fragments or units such as ferrocene have been used to enhance the anti-plasmodial activity of fluoroquinolone such as ciprofloxacin (**Figure 2.6**)[52]. The combining of bioorganometallic chemistry and bioactive ciprofloxacin resulted in the formation of achiral compounds that were found to be 10-100-fold more active than ciprofloxacin against *Plasmodium falciparum*[53].
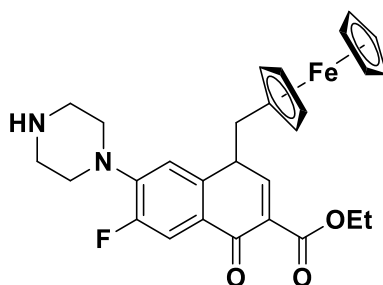
Figure 2.6: Structure of the derivative ciprofloxacin attached to a ferrocene group.

Quinolones and fluoroquinolones show a progressive inhibitory effect corresponding to the duration of the incubation with the drug for the screening for activity against the *T. gondii*, an organism of protozoa classification[54]. Grepafloxacin was the most active drug in the screening for malaria. Grepafloxacin, piromidic acid and trovafloxacin (**Figure 2.7**) resulted in a reduction in the causative agents in the culture[51]. Studies by Fournet *et al* reported quinolones activity against Leishmaniasis. 2,3-Substitution of quinolones, alkenyl and alkynyl quinolones are active against cutaneous and visceral

leishmaniasis, African trypanosomiasis, and Chaga's disease[55]. The vast amount of research that has been done on quinolones; is the reason why there has been the development of more ways of using them as treatment options. There is little research on the cardiovascular activity of quinolones.
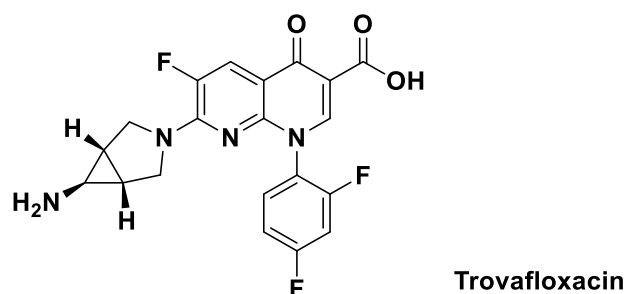
Figure 2.7: Candidate for repurposing FQs as an anti-protozoal.

2.4.3 Anti-fungal quinolones

Quinolones have been screened for antifungal activity and some have shown promising, and positive results against .*C albicans, A. fumigatus, A. clavatus A. niger*[52]. All positions of the quinolone structure can be modified. Variations can be made at positions N-1, C-5, C-6, C-7, and C-8 and this can result in structures that differ in activity and potency[52]. Preclinical models show that fluoroquinolones are active against *Candida albicans*.

Figure 2.8: Chemical structures of 2-quinolone derivatives

2-Quinolone (carbostyrils or 1-aza coumarins) (**Figure 2.8**) derivatives are under clinical trials for infections caused by bacteria. 2-Quinolone-thiazole hybrids **(Figure 2.9)** that have been studied showed activity but were less potent than the more established antifungal agent, fluconazole. Evidence also showed that the compounds

with an electron-withdrawing group such as a phenyl group on position N-1 had significant improvement in activity against fungal species[52]. The combined usage of the curren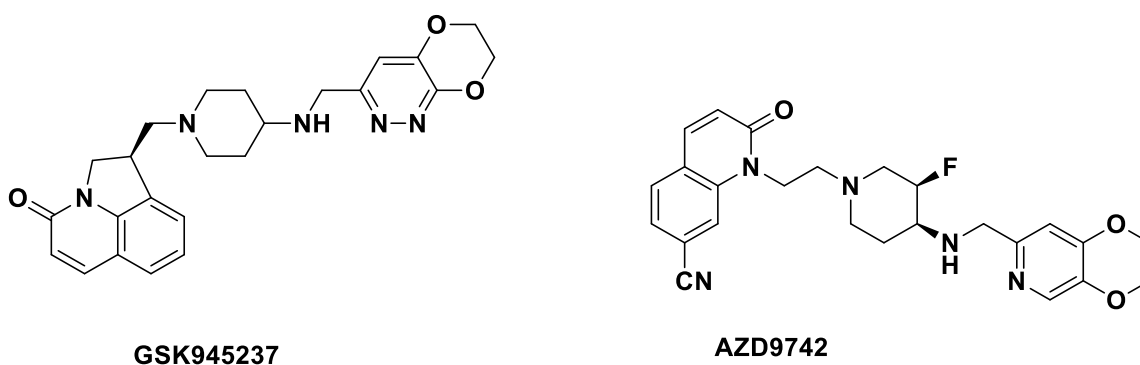t antifungal drugs and quinolone antibiotics such as trovafloxacin has the potential to improve therapeutic outcomes[56].
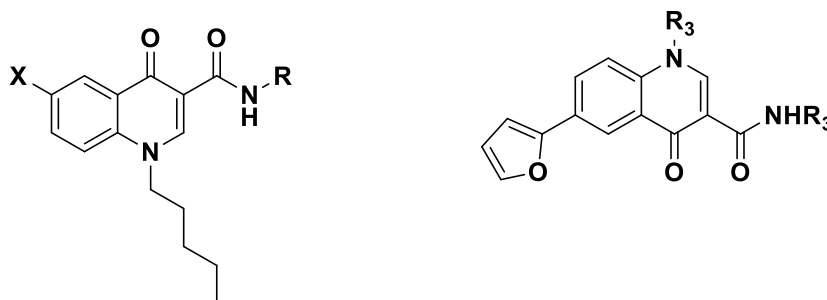

Figure 2.9: Synthesised compounds containing the quinolone scaffold for anti-fungal usage.

2.4.4 Antiviral quinolones

Commercially available quinolones used in the treatment of bacterial infections have been repurposed for the treatment of viral infections. The broadening of the activity of quinolones is aligned with their ability to inhibit type II topoisomerase or the inhibition of viral helicase [57]. Studies show that at similar dosages, quinolones are clinically effective against viral and parasitic infections[58]. Quinolones possess antiviral activity by binding with the nucleic acid of viruses or viral nucleoprotein complexes. They exhibit activity against viruses such as the vaccinia virus and papoviruses[59]. Ciprofloxacin, ofloxacin, levofloxacin and gatifloxacin are clinically effective in the treatment of the single-stranded ribonucleotide acid (RNA) hepatitis C virus (HCV) and the non-capsulated DNA polyomavirus BK[58]. Patients with HCV-induced chronic hepatitis and compensated liver cirrhosis were treated with 100-900 mg of ofloxacin per day for eight weeks and one in three of the patients recorded positive outcomes[60]. The activity of quinolone derivatives has been proposed to have a different mode of action. Structures containing the basic quinolone carboxylic acid template and different lipophilic substituents were patented as antiviral agents with most of them being tested against HIV-1 and showed effective results in the treatment or prophylaxis of Acquired Immune Deficiency Syndrome (AIDS). However, the mechanism of action

was not reported[61]. Some compounds were analysed using molecular modelling techniques to predict structural interaction of the drug and new target. That included the addition of an amine group on position 6 which is usually reserved for F in fluoroquinolones. Compound WM5 (**Figure 2.10**) was the most active in inhibiting HIV-1 on the novo-infected human lymphoblastoid cell lines. This compound had an EC_{50} of 0.1 µM[62].
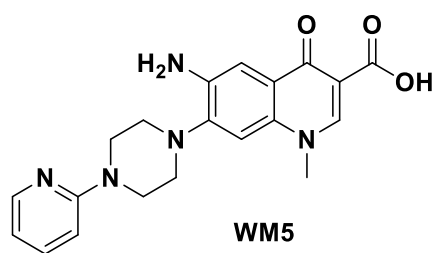

Figure 2.10: 6-Amino-Quinolones that have been tested against HIV-1

2.4.5 Quinolones as anti-cancer agents

There has been a great surge in the research involving the repurposing and repositioning of drugs[63]. Anticancer drugs are broadly grouped into two main categories i.e., cytotoxic (cell-killing drugs) or as cytostatic (antiproliferative drugs)[63]. Fluoroquinolones have the potential of being used as anticancer agents. It was discovered that the two main changes that switch the activity of quinolones from antibacterial to anti-cancer are disruption of the zwitterionic properties of the compounds through modification of the C7 substituted basic properties or changing the C3 carboxyl group. The other is increasing the extent of aromatic/condensed rings to increase affinity to quinolones for double stranded DNA[61]. These quinolones show different activities such as anti-proliferative activity, some show pro-apoptotic activity and others have anti-epithelial-mesenchymal-transition[64]. Fluoroquinolones have activity as inducers of cell cycle arrest. Fluoroquinolones can manipulate the cell cycle primarily in the S and G_2 phases of progression. Ciprofloxacin was able to suppress the proliferation of human prostate cancer, and these are promising outcomes[65]. Ciprofloxacin, gatifloxacin and moxifloxacin show results of downregulation in the levels of cyclin-CDK[66]. Fluoroquinolones possess apoptosis-inducing ability in varied cell lines[67]. Quinolone derivatives such as Voreloxin, AT-3639 and quarfloxin (**Figure 2.11**) has been used in clinics or under clinical trials for the treatment of cancer [68,69].
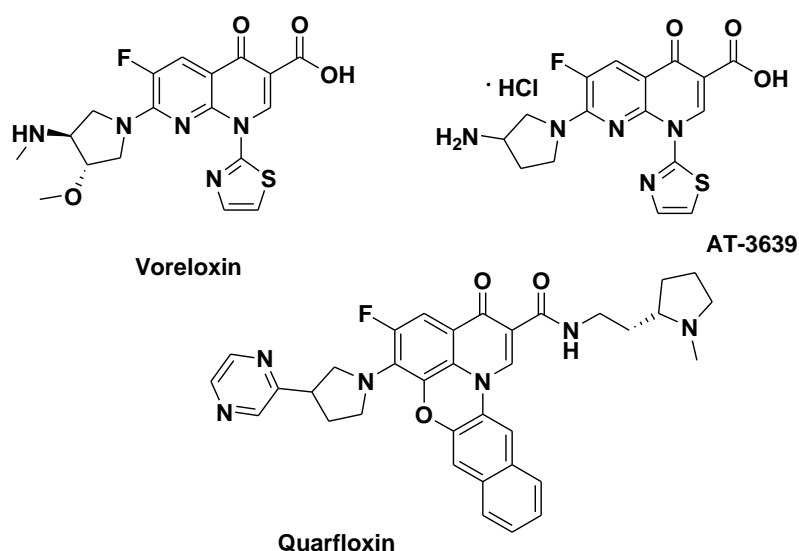
Figure 2.11: Quinolone derivatives that have been tested for anti-cancer activity.

The hybridisation of the quinolone pharmacophore is also being exploited for future cancer treatment options[70]. Symadex (C-1311) (**Figure 2.12**) is an acridinone-imidazole hybrid that has shown great activity against breast cancer and progressed to phase II clinical trials[71]. A derivative of symadex has also shown activity when tested against tumour cells and is expected to have better pharmacological properties than symadex[71]. These compounds have the quinolone pharmacophore (**Figure 2.12**).
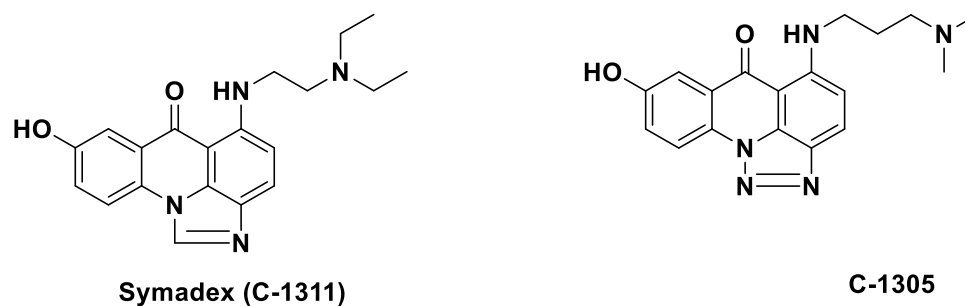
Figure 2.12: Acridinone-triazole/imidazole hybrids.

2.4.6 Analgesic properties of quinolones

Cannabinoid receptors and their endogenous ligands and proteins responsible for endocannabinoid cellular uptake and inactivation are promising drug targets that present opportunities for the design of new treatment options for pain, loss of appetite in patients with AIDS, obesity, chemotherapy-induced nausea and vomiting, immune and inflammatory disorders, cardiovascular and gastrointestinal disorders, and

neurodegenerative diseases[72]. Agonists of cannabinoid receptor subtypes (selective CB$_2$) result in antinociceptive effects in animal models of chronic neuropathy, persistent inflammatory pain, post-operative pain, and cancer pain[73]. These agonists are investigated as a potential new analgesic and inflammatory agents[74]. 6-Substituted 4-quinolone-3-carboxamide derivatives (**Figure 2.13**) were synthesised and tested for their potential to bind cannabinoid ligand receptors. They were reported to be highly selective CB$_2$ ligands with K$_i$ values in the low nanomolar or sub-nanomolar range and selectivity index values > 14000[72]. Compound **1** showed agonistic properties while **2** showed promising inverse agonist-like activity.
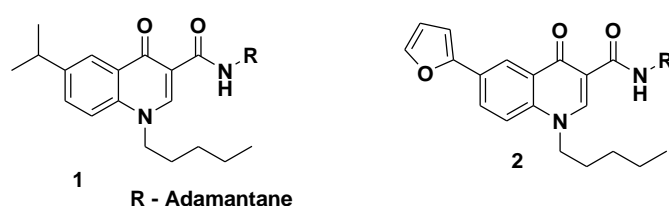
Figure 2.13: Chemical structures of 4-quinolone-3-carboxamides.

The study reported an excellent affinity of a number of quinolones derivatives for cannabinoid receptor 2 (CB2) ligands during *in vitro* studies[72]. Amongst other pharmacological properties that quinolones possess, chronic inflammation is a manifestation of many types of cancers. Most tumour appearance is accompanied by inflammatory indicators. Inflammatory cytokines such as tumour necrosis factor (TNF)-α and interleukin 6 (IL-6) are produced mainly by activated macrophages and are involved in the up-regulation of inflammation. These inherently are target sites for the control of inflammation and pain. Alkaloids with pyrano[3,2-*c*] quinolone moieties (**Figure 2.14**) reveal a broad spectrum of biological activities and promising anticancer activity through the inhibition of this inflammatory markers[75].
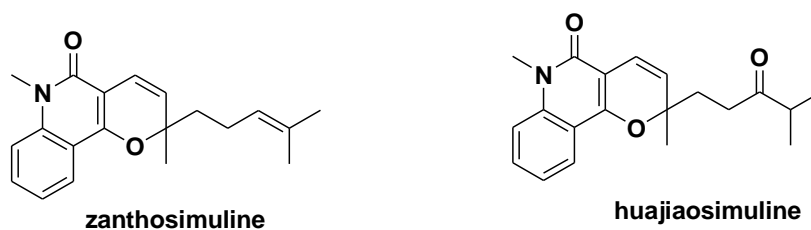
Figure 2.14: Pyrano[3,2-*c*] pyridine- and pyrano [3,2-*c*] quinolone-based alkaloids.

2.5   Hydrazone-containing compounds

Hydrazones are compounds that contain an azomethine -NHN=CH- structural feature. Compounds possessing this structural feature are the backbone of this project. The hydrazones, related to ketones and aldehydes, belong to a group of compounds with the structure $R_1R_2C=NNH_2$[76]. Compounds containing the hydrazone moiety possess a broad spectrum of potential pharmacological properties including antimicrobial, anti-inflammatory, analgesic, antifungal, anti-tubercular, antiviral, anticancer, antiplatelet, antimalarial, anticonvulsant, cardioprotective, anthelmintic, antiprotozoal, anti-trypanosoma and anti-schistosomiasis activities[77]. Hydrazones have the C=N functionality which is conjugated with lone pairs of electrons on the nitrogen atom of azomethine C=N functionality. The hydrazones that are a result of aldehyde condensation are more potent than the hydrazine derived from ketone. The alpha H atom of hydrazone is more nucleophilic because it is 10 times more acidic than ketones[78].

The chemistry of hydrazine dates to the 19th century[79]. Hydrazine derivatives were used in a variety of ways in the pharmaceutical industry in the 20th century. The reduction in the usage is linked to harsh side effects that were being experienced. Today hydrazine and its derivatives are also used as high-energy rocket fuel which is not a safer option, it leads to undesirable effects on nature and people. Hydrazines are also found in tobacco and edible mushrooms [80]. Hydralazine (**Figure 2.15**) is a drug that belongs to the hydrazine family and it is used as an arterial vasodilator during the treatment of hypertension and congestive heart failure [80]. The usage of hydralazine is reported to cause toxic side effects such as DNA damage and may cause severe lupus erythematosus[80].
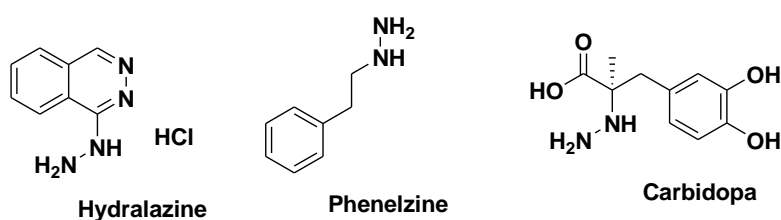

Figure 2.15: Chemical structure of hydralazine, carbidopa and phenelzine.

2.5.1 Hydrazine CNS drugs

Carbidopa is an anti-Parkinson agent, and phenelzine, (**Figure 2.15**) an antidepressant are successful examples of drugs that contain the hydrazine moiety. Phenelzine is a monosubstituted alkyl hydrazine which is a monoamine oxidase inhibitor[81]. The impact on the central nervous system (CNS) is generally attributed to its ability to inhibit the monoamine oxidase enzyme. There is evidence to show that monoamine oxidase inhibitors primarily affect symptoms of depression, resulting in a lift of mood[79].

2.5.2 Hydrazine in anti-cancer drugs

Procarbazine (*N*-isopropyl-α-(2-methyl-hydrazine)-*p*-toluamide hydrochloride) (PCZ) **Figure 2.16**, is an anticancer drug that is part of a cocktail of drugs used for the treatment of Hodgkin's lymphoma, malignant melanoma and bronchogenic carcinoma and brain tumours in children[82]. Chemotherapeutic agents such as nitrofurazone, furazolidone and nitrofurazone (**Figure 2.16**) contain the hydrazine-hydrazone moiety[83].
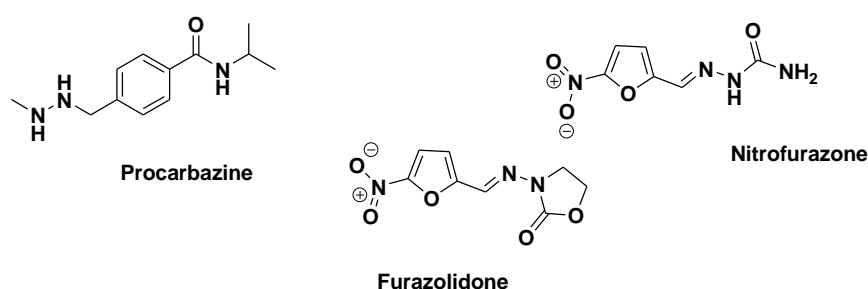
Figure 2.16: Chemical structures of anticancer agents containing hydrazine hydrazone moiety.

2.5.3 Antibacterial activity of hydrazine-hydrazone-containing compounds

Hydrazone derivatives have been tested and investigated for their antibacterial activity. Some derivatives are complex materials that contain transition metals[6]. Hydrazones are used to combat different bacterial strains. Other studies have shown that efficacy is favourable against fungal, protozoal, and viral disease-causing organisms [83]. Isoniazid, a tuberculostatic antibiotic, is used as a crucial first-line drug in the treatment of TB. Hydrazone derivatives are very active and are of biological importance. Hydrazone-based coupling methods are used in biotechnology to couple drugs to

target antibodies. The hydrazone bond is stable in neutral pH but destroyed in acidic conditions, such as those of the lysosomes of the cell. On other hand, the hydrazone is a suitable delivery system because the drug is released at the cellular level [84]. Effective compounds such as iproniazid (**Figure 2.17**) are used as antitubercular drugs, nifuroxazide is an oral nitrofuran antibiotic, that is used as anti-dehydration and colitis treatment, and has a spectrum that covers a lot of enteropathogenic micro bacteria, *Shigella, Escherichia coli, Salmonella, Staphylococci, Klebsiella, Yersinia.*

Iproniazide   **Isocarboxazide**

Figure 2.17: Hydrazone derivatives with antibacterial activity.

2.6   Physicochemical properties in anti-TB drug discovery

Modern drug discovery and development looks at the pharmacodynamics of the compound at the target site while at the same time considers the pharmacokinetic properties of the compound. Novel compounds that are being designed are expected to have appropriate pharmacokinetic profiles before they can be tested at the clinical phase. The number of potential drug compounds that end up not reaching the clinical trials due to undesirable bioavailability or poor pharmacokinetic or pharmacodynamic properties is astronomically high[86,87]. Subsequent to the identification of the drug target, the next step is the identification of lead compounds to compliment the drug target. During the optimisation phase, the lead compound is subjected to various structural modifications to eliminate any potential liabilities that may impact the progression of a compound along the drug discovery pipeline to reach clinical candidate stage[88]. An ideal drug candidate binds selectively to the receptor site while producing the desired functional response, and it must have sufficient bioavailability and volume distribution. A drug candidate designed for use in human should be evaluated *in vitro* and *in vivo* for formal toxicity effects[89].

Pfizer scientists developed a rule of five (RoF) for screening leads and drug candidates for suitable physicochemical properties[90]. The ROF guidelines state that a drug-like agent must have a molecular weight of less than 500 g/mol, a partition coefficient (log P, a measure of hydrophobicity) of less than 5, hydrogen bond donors no more than 5, and a maximum of 10 hydrogen acceptors[89]. Most TB drugs and other antibacterial agents do not follow the ROF[91]. The physicochemical properties have implications on the Administration, Distribution, Metabolism, Excretion and Toxicity (ADMET) of a drug in early drug discovery projects. Although ADMET properties are primarily aimed at in vivo dosing and pharmacokinetics, they are also important properties in in vitro biological assays[89]. The toxicity of a drug compound is equally important as those of the above-mentioned parameters. One of the main reasons why antimycobacterial molecules fail is their inability to cross the largely impermeable *Mtb* cell envelope, preventing most therapeutics from reaching their periplasmic or intracellular targets[92-93]. Historically, the drug discovery activities have put more emphasis on the *in vitro* pharmacological activity of compounds while neglecting the physicochemical and pharmacokinetic parameters to later[94]. For TB treatment to be efficacious, bioactive molecules must penetrate the microbe effectively to reach the site of infection (e.g., lung tissue and lesions for pulmonary TB) and inhibit an essential process and must reach the site of infection[91].

With the advancement in technology, the rise *in silico* softwares and databases have enabled the development of useful computational tools for predicting the ADMET properties. These tools assist in predicting favourable or unfavourable ADMET properties including the physicochemical parameters[85]. Drug discovery scientists in Africa and other developing worlds rely on the evaluation of ADMET properties using online-based *in silico* prediction tools such as regression-based and classification-based approaches, machine learning (ML) methods, and artificial intelligence[95]. Researchers can embark on rational synthesis instead of wasting time and resources on compounds that will never reach the market[85]. The *in silico* tools have ADMET prediction platforms, including multiple quantitative-structure-activity-relationships (QSAR) and ML models that can exclude undesirable drug candidates[96]. Considering that only 10% of all synthesised compounds that reach phase 1 clinical trials progress

to the market, software tools in the early drug discovery phases will help reduce the associate costs of resources that would have been spent in the laboratory[97]. Organisations such as the U.S. Environmental Protection Agency (USEPA) has been advocating *in silico* modelling to study the toxicities of the investigational compounds, which is in line with efforts to minimise the usage of animals in research by 2035[85].

Some of the commercial *in silico* tools commonly used include CASE ULTRA, DEREK, META-PC, METEOR, PASS, GUSAR, etc. On other hand, open access tools include ADMETLab, admetSAR, pkCSM, and SwissADME[98], which have been extensively used in early drug discovery. Physicochemical properties are important in the early stages of determining potential drug candidates. PK/PD properties, as well as bioavailability, are dependent on the prediction of ADMET information[99]. Pharmacological properties such as the site of metabolism and the type of enzymes involved in the biotransformation of the drugs can be identified with computerized models; CypReact, Xenosite[100,101]. CypReact is an open access *in silico* tool used to predict a compound's interaction with the CYP450 enzyme. CypReact helps determine whether the potential drug compound will react with any of the nine prominent CYP450 enzymes, namely CYP1A2, CYP2A6, CYP2B6, CYP2C8, CYP2C9, CYP2C19, CYP2D6, CYP2E1, and CYP3A4[101]. SwissADME is another popular web tool that is convenient for its fast prediction of physicochemical properties, a diverse range of pharmacokinetics parameters and medicinal chemistry friendliness[98].

2.7   Justification, aims and objectives

With the significant impact of TB on developing countries, including millions of cases of infection and more than 1 million deaths annually coupled with drug resistance to common antitubercular drugs, there is a great need to continue to identify and develop new compounds for treatment of TB. The current project emanated from previous work conducted in our laboratory involving the synthesis of novel quinolone-isoniazid hybrid compounds which exhibited significant antimycobacterial activity against *Mtb* H37Rv with MIC_{90} values in the range 0.2 – 8 µM without any noticeable cytotoxic effects[2]. This prompted us to explore the antimycobacterial effects of replacing the isoniazid

unit with the pyrazinamide pharmacophore while retaining the same quinolone framework.

2.7.1 Project aim

The overall purpose of this project was to synthesise a focus library of quinolone-pyrazinamide hybrid molecules with *in vitro* activity against the *Mtb* H37Rv sensitive strain.

2.7.2 Objectives

- To synthesise and fully characterised quinolone-pyrazinamide hybrid molecules as potential antimycobacterial agents.
- To pharmacologically evaluate the synthesised compounds for their antimycobacterial activity against the *Mtb* H37Rv sensitive strain.

  To apply *in silico* tools to assess the physicochemical and ADMET properties of achieved quinolone-pyrazinamide hybrid compounds to determine their likelihood to be drug-like compounds.

2.8   References

(1)   Hooper, D. C. Mechanisms of Action of Antimicrobials: Focus on Fluoroquinolones. *Clin. Infect. Dis.* **2001**, *32* (Supplement_1), S9–S15.

(2)   Beteck, R. M.; Seldon, R.; Jordaan, A.; Warner, D. F.; Hoppe, H. C.; Laming, D.; Legoabe, L. J.; Khanye, S. D. Quinolone-Isoniazid Hybrids: Synthesis and Preliminary in Vitro Cytotoxicity and Anti-Tuberculosis Evaluation. *MedChemComm* **2019**, *10* (2), 326–331.

(3)   Smith, M. B.; March, J., March's Adavanced Organic Chenistry Reactions, Mechanisms, and Structure, 6th Edition, John Wiley and Sons Inc, Hoboken, New Jersey, **2007**, pp 54-67.

(4)   Moldoveanu, S. C. *Pyrolysis of Organic Molecules: Applications to Health and Environmental Issues*; 2nd Edition; Elsevier Science; **2018**, 715 - 762.

(5)   Mishra, B. B.; Kumar, D.; Mishra, A.; Mohapatra, P. P.; Tiwari, V. K. Cyclo-Release Strategy in Solid-Phase Combinatorial Synthesis of Heterocyclic Skeletons. *Advances in Heterocyclic Chemistry*; **2012**, *107*, 41 - 99.

(6)   Mahajan, N. D.; Jain, N. Heterocyclic Compounds And Their Applications In The Field Of Biology: A Detailed Study. Nat. *Volatiles & Essent. Oils*. **2021**, 13223–13229.

(7)   Godge, R. K.; Kunkulol, R. Synthesis of Novel Heterocyclic Quinolone Compound for Anti -Tubercular Activity. *Int. J. Clin. Biomed. Res.* **2018**, *4* (3), 44 - 49.

(8)   Aly, A. A.; El-Sheref, E. M.; Mourad, A. F. E.; Bakheet, M. E. M.; Bräse, S. 4-Hydroxy-2-Quinolones: Syntheses, Reactions and Fused Heterocycles. *Mol. Divers*. **2019**, *24*, 477 - 524.

(9)   Bisacchi, G. S. Origins of the Quinolone Class of Antibacterials: An Expanded "Discovery Story." *J. Med. Chem*. **2015**, *58* (12), 4874 - 4882.

(10)   Ball, P. The Quinolones: History and Overview. In *The quinolones*; Elsevier, **2000**; pp 1–31.

(11)   Liu, M.; Ohashi, M.; Tang, Y. Engineered Biosynthesis of Fungal 4-Quinolone Natural Products. *Org. Lett.* **2020**, *22* (16), 6637–6641.

(12)   Sárközy, G. Quinolones: A Class of Antimicrobial Agents. *Vet. Med*. **2001**, *9* (10), 257 - 274.

(13)   Tillotson, G. S. Quinolones: Structure-Activity Relationships and Future Predictions. *J. Med. Microbiol.* **1996**, *44* (5), 320–324.

(14)   Oliphant, C. M.; Green, G. M. Quinolones: A Comprehensive Review. *Am. Fam. Physician*. **2002**, 65 (3), 455 - 464.

(15)   Neu, H. C. Quinolones: A New Class of Antimicrobial Agents with Wide Potential Uses. *Med. Clin. North Am.* **1988**, 72 (3), 623 - 636.

(16)   Smith, J. T. The Mode of Action of 4-Quinolones and Possible Mechanisms of Resistance. *J. Antimicrob. Chemother.* **1986**, 18 (Supplement_D), 21 - 29.

(17)   Bennett, J. E.; Dolin, R.; Blaser, M. J. *Mandell, Douglas, and Bennett's Principles and Practice of Infectious Diseases E-Book*; 9th Ed, Elsevier Health Sciences, **2019**, 426 – 449.

(18)   Albrecht, R. Development of Antibacterial Agents of the Nalidixic Acid Type. *Prog. Drug Res. der Arzneimittelforschung/ Prog. Drug. Res.* **1977**, 9–104.

(19)   Grohe, K. The Chemistry of the Quinolones: Methods of Synthesizing the Quinolone Ring System. In *Quinolone antibacterials*; Springer, **1998**; pp 13–62.

(20)   Lengyel, L. C.; Sipos, G.; Sipöcz, T.; Vágó, T.; Dormán, G.; Gerencsér, J.; Makara,

G.; Darvas, F. Synthesis of Condensed Heterocycles by the Gould-Jacobs Reaction in a Novel Three-Mode Pyrolysis Reactor. *Org. Process Res. Dev.* **2015**, 19 (3), 399 - 409.

(21) Bella, M.; Schultz, M.; Milata, V.; Koariková, K.; Breza, M. Application of the Gould-Jacobs Reaction to 4-Amino-2,1,3-Benzoselenadiazole. *Tetrahedron* **2010**, *66* (41), 8169 - 8174.

(22) Boteva, A. A.; Krasnykh, O. P. The Methods of Synthesis, Modification, and Biological Activity of 4-Quinolones. *Chem. Heterocycl. Comp.* **2009**, *45* (7), 757–785.

(23) Brouet, J. C.; Gu, S.; Peet, N. P.; Williams, J. D. Survey of Solvents for the Conrad-Limpach Synthesis of 4-Hydroxyquinolones. *Synth. Commun.* **2009**, *39* (9), 1563 - 1569.

(24) Zewge, D.; Chen, C. Y.; Deer, C.; Dormer, P. G.; Hughes, D. L. A Mild and Efficient Synthesis of 4-Quinolones and Quinolone Heterocycles. *J. Org. Chem.* **2007**, *72* (11), 4276 - 4279.

(25) Pozharskii, A. F.; Soldatenkov, A. T.; Katritzky, A. R. *Heterocycles in Life and Society: An Introduction to Heterocyclic chemistry, Biochemistry and Applications; 2nd Ed*; John Wiley and Sons; West Sussex, United Kingdom; **2011**,146 – 155.

(26) Jones, C. P.; Anderson, K. W.; Buchwald, S. L. Sequential Cu-Catalyzed Amidation-Base-Mediated Camps Cyclization: A Two-Step Synthesis of 2-Aryl-4-Quinolones from o-Halophenones. *J. Org. Chem.* **2007**, *72* (21), 7968 - 7973.

(27) Kuhlmann, J. Dalhoff, A., Zeiler, H, -J.; Zeiler; *Quinolone Antibacterials*; **1998**, 13 – 52.

(28) Pesson, M.; Antoine, M.; Chabassier, S.; Geiger, S.; Girard, P.; Richer, D.; De Lajudie, P.; Horvath, E.; Leriche, B.; Patte, S.; A ANTIBACTERIENS DERIVES DES ACIDES ALKYL-8-OXO-5-DIHYDRO-5, 8 PYRIDO (2, 3-D) PYRIMIDINE-6-CARBOXYLIQUES. I. NOUVEAU PROCEDE DE PREPARATION;**1974**; *9* (6); 585 – 590.

(29) *The Grohe Method and Quinolone Antibiotics*; Leverkusen; https://www.bayer.com/sites/default/files/the-grohe-method-and-quinolone-antibiotics.pdf

(30)   Bennett, J. E.; Dolin, R.; Blaser, M. J. *Mandell, Douglas, and Bennett's Principles and Practice of Infectious Diseases*; **2014**, 1-2.

(31)   Sabbaj, J.; Hoagland, V. L.; Cook, T. Norfloxacin versus Co-Trimoxazole in the Treatment of Recurring Urinary Tract Infections in Men. *Scand. J. Infect. Dis.* **1986**, *18* (48), 1 – 91.

(32)   Schluger, N. W. Fluoroquinolones in The Treatment of Tuberculosis: Which Is Best? *Am. J. Respir. Crit. Care. Med*. **2013**, *188* (7), 763 - 886.

(33)   Migliori, G. B.; Langendam, M. W.; D'Ambrosio, L.; Centis, R.; Blasi, F.; Huitric, E.; Manissero, D.; Van Der Werf, M. J. Protecting the Tuberculosis Drug Pipeline: Stating the Case for the Rational Use of Fluoroquinolones. *Eur. Respir. J*. **2012**, *40*, 814 - 822.

(34)   Noel, G. J.; Bradley, J. S.; Kauffman, R. E.; Duffy, C. M.; Gerbino, P. G.; Arguedas, A.; Bagchi, P.; Balis, D. A.; Blumer, J. L. Comparative Safety Profile of Levofloxacin in 2523 Children with a Focus on Four Specific Musculoskeletal Disorders. *Pediatr. Infect. Dis. J.* **2007**, *26* (10), 879 - 891.

(35)   Sarathy, J.; Blanc, L.; Alvarez-Cabrera, N.; O'Brien, P.; Dias-Freedman, I.; Mina, M.; Zimmerman, M.; Kaya, F.; Liang, H. P. H.; Prideaux, B.; Dietzold, J.; Salgame, P.; Savic, R. M.; Linderman, J.; Kirschner, D.; Pienaar, E.; Dartois, V. Fluoroquinolone Efficacy against Tuberculosis Is Driven by Penetration into Lesions and Activity against Resident Bacterial Populations. *Antimicrob. Agents Chemother.* **2019**, *63* (5).

(36)   Mahla, R. S. Prevalence of Drug-Resistant Tuberculosis in South Africa. *Lancet Infect. Dis.* **2018**, *18* (8), 836.

(37)   Gillespie, S. H.; Kennedy, N. Fluoroquinolones: A New Treatment for Tuberculosis? *Int. J. Tuberc. Lung Dis.* **1998**, *2* (4), 265–271.

(38)   Turnidge, J. Pharmacokinetics and Pharmacodynamics of Fluoroquinolones. *Drugs* **1999**, *58* (2), 29–36.

(39)   Berning, S. E. The Role of Fluoroquinolones in Tuberculosis Today. *Drugs* **2001**, *61* (1), 9–18.

(40)   Crowle, A. J.; Elkins, N.; May, M. H. Effectiveness of Ofloxacin against *Mycobacterium Tuberculosis* and *Mycobacterium Avium*, and Rifampin against M. Tuberculosis in Cultured Human Macrophages. *Am. J. Respir. Crit. Care Med.*

1988, *137* (5), 1141–1146.

(41) Mor, N.; Vanderkolk, J.; Heifets, L. Inhibitory and Bactericidal Activities of Levofloxacin against *Mycobacterium Tuberculosis in Vitro* and in Human Macrophages. *Antimicrob. Agents Chemother.* **1994**, *38* (5), 1161–1164.

(42) Rastogi, N.; Goh, K. S.; Bryskier, A.; Devallois, A. In Vitro Activities of Levofloxacin Used Alone and in Combination with First-and Second Line Antituberculous Drugs against *Mycobacterium Tuberculosis*. *Antimicrob. Agents Chemother.* **1996**, *40* (7), 1610–1616.

(43) Alangaden, G. J.; Bone, S. A. The Clinical Use of Fluoroquinolones for the Treatment of Mycobacterial Diseases. *Clin. Infect. Dis.* **1997**, *25* (5), 1213–1221.

(44) Gao, J.; Hou, H.; Gao, F. Current Scenario of Quinolone Hybrids with Potential Antibacterial Activity against ESKAPE Pathogens. *Eur. J. Med. Chem.* **2022**, 115026.

(45) Beteck, R. M.; Smit, F. J.; Haynes, R. K.; N'Da, D. D. Recent Progress in the Development of Anti-Malarial Quinolones. *Malar. J.* **2014**, *13* (1), 1–10.

(46) Dube, P. S.; Legoabe, L. J.; Beteck, R. M. Quinolone: A Versatile Therapeutic Compound Class. *Mol. Divers.* **2022**, 1–26.

(47) Van Schalkwyk, D. A.; Riscoe, M. K.; Pou, S.; Winter, R. W.; Nilsen, A.; Duffey, M.; Moon, R. W.; Sutherland, C. J. Novel Endochin-like Quinolones Exhibit Potent *In Vitro* Activity against *Plasmodium Knowlesi* but Do Not Synergize with Proguanil. *Antimicrob. Agents Chemother.* **2020**, *64* (5), e02549-19.

(48) Doggett, J. S.; Schultz, T.; Miller, A. J.; Bruzual, I.; Pou, S.; Winter, R.; Dodean, R.; Zakharov, L. N.; Nilsen, A.; Riscoe, M. K. Orally Bioavailable Endochin-like Quinolone Carbonate Ester Prodrug Reduces *Toxoplasma Gondii* Brain Cysts. *Antimicrob. Agents Chemother.* **2020**, *64* (9), e00535-20.

(49) McConnell, E. V; Bruzual, I.; Pou, S.; Winter, R.; Dodean, R. A.; Smilkstein, M. J.; Krollenbrock, A.; Nilsen, A.; Zakharov, L. N.; Riscoe, M. K. Targeted Structure–Activity Analysis of Endochin-like Quinolones Reveals Potent Qi and Qo Site Inhibitors of *Toxoplasma Gondii* and *Plasmodium Falciparum* Cytochrome Bc 1 and Identifies ELQ-400 as a Remarkably Effective Compound against Acute Experimental T. *ACS Infect. Dis.* **2018**, *4* (11), 1574–1584.

(50) Doggett, J. S.; Nilsen, A.; Forquer, I.; Wegmann, K. W.; Jones-Brando, L.; Yolken,

R. H.; Bordón, C.; Charman, S. A.; Katneni, K.; Schultz, T. Endochin-like Quinolones Are Highly Efficacious against Acute and Latent Experimental Toxoplasmosis. *Proc. Natl. Acad. Sci.* **2012**, *109* (39), 15936–15941.

(51) Mahmoudi, N.; Ciceron, L.; Franetich, J.-F.; Farhati, K.; Silvie, O.; Eling, W.; Sauerwein, R.; Danis, M.; Mazier, D.; Derouin, F. In Vitro Activities of 25 Quinolones and Fluoroquinolones against Liver and Blood Stage Plasmodium Spp. *Antimicrob. Agents Chemother.* **2003**, *47* (8), 2636–2639.

(52) Zhang, B. Quinolone Derivatives and Their Antifungal Activities: An Overview. *Arch. Pharm.* **2019**, *352* (5), 1800382.

(53) Dubar, F.; Anquetin, G.; Pradines, B.; Dive, D.; Khalife, J.; Biot, C. Enhancement of the Antimalarial Activity of Ciprofloxacin Using a Double Prodrug/Bioorganometallic Approach. *J. Med. Chem.* **2009**, *52* (24), 7954–7957.

(54) Khan, A. A.; Araujo, F. G.; Brighty, K. E.; Gootz, T. D.; Remington, J. S. Anti-Toxoplasma Gondii Activities and Structure-Activity Relationships of Novel Fluoroquinolones Related to Trovafloxacin. *Antimicrob. Agents Chemother.* **1999**, *43* (7), 1783–1787.

(55) Fakhfakh, M. A.; Fournet, A.; Prina, E.; Mouscadet, J.-F.; Franck, X.; Hocquemiller, R.; Figadère, B. Synthesis and Biological Evaluation of Substituted Quinolines: Potential Treatment of Protozoal and Retroviral Co-Infections. *Bioorg. Med. Chem.* **2003**, *11* (23), 5013–5023.

(56) Vitale, R. G.; Afeltra, J.; De Hoog, G. S.; Rijs, A. J.; Verweij, P. E. In Vitro Activity of Amphotericin B and Itraconazole in Combination with Flucytosine, Sulfadiazine and Quinolones against Exophiala Spinifera. *J. Antimicrob. Chemother.* **2003**, *51* (5), 1297–1300.

(57) Sales, E. M.; Figueroa-Villar, J. D. Recent Studies about Synthesis and Biological Activity of Quinolones and Derivatives: A Review. *World J Pharm Pharm Sci* **2016**, *5* (8), 253–268.

(58) Dalhoff, A. Antiviral, Antifungal, and Antiparasitic Activities of Fluoroquinolones Optimized for Treatment of Bacterial Infections: A Puzzling Paradox or a Logical Consequence of Their Mode of Action? *Eur. J. Clin. Microbiol. Infect. Dis.* **2015**, *34* (4), 661–668.

(59) Kaur, P.; Chandra, A.; Tanwar, T.; Sahu, S. K.; Mittal, A. Emerging Quinoline-and

Quinolone-based Antibiotics in the Light of Epidemics. *Chem. Biol. Drug Des.* **2022**, *100* (6), 765 – 785.

(60) Takada, A.; Takase, S.; Tsutsumi, M.; Sawada, M. Effects of Ofloxacin for Type C Hepatitis. *Int. Hepatol. Commun.* **1993**, *1* (5), 272–277.

(61) Richter, S.; Parolin, C.; Palumbo, M.; Palù, G. Antiviral Properties of Quinolone-Based Drugs. *Curr. Drug Targets-Infectious Disord.* **2004**, *4* (2), 111–116.

(62) Cecchetti, V.; Parolin, C.; Moro, S.; Pecere, T.; Filipponi, E.; Calistri, A.; Tabarrini, O.; Gatto, B.; Palumbo, M.; Fravolini, A. 6-Aminoquinolones as New Potential Anti-HIV Agents. *J. Med. Chem.* **2000**, *43* (20), 3799–3802.

(63) Yadav, V.; Talwar, P. Repositioning of Fluoroquinolones from Antibiotic to Anti-Cancer Agents: An Underestimated Truth. *Biomed. Pharmacother.* **2019**, *111*, 934–946.

(64) Gao, Y.; Shang, Q.; Li, W.; Guo, W.; Stojadinovic, A.; Mannion, C.; Man, Y.; Chen, T. Antibiotics for Cancer Treatment: A Double-Edged Sword. *J. Cancer* **2020**, *11* (17), 5135.

(65) Aranha, O.; Grignon, R.; Fernandes, N.; McDonnell, T. J.; Wood, D. P.; Sarkar, F. H. Suppression of Human Prostate Cancer Cell Growth by Ciprofloxacin Is Associated with Cell Cycle Arrest and Apoptosis. *Int. J. Oncol.* **2003**, *22* (4), 787–794.

(66) Aranha, O.; Wood Jr, D. P.; Sarkar, F. H. Ciprofloxacin Mediated Cell Growth Inhibition, S/G2-M Cell Cycle Arrest, and Apoptosis in a Human Transitional Cell Carcinoma of the Bladder Cell Line. *Clin. Cancer Res.* **2000**, *6* (3), 891–900.

(67) Herold, C.; Ocker, M.; Ganslmayer, M.; Gerauer, H.; Hahn, E. G.; Schuppan, D. Ciprofloxacin Induces Apoptosis and Inhibits Proliferation of Human Colorectal Carcinoma Cells. *Br. J. Cancer* **2002**, *86* (3), 443–448.

(68) Musiol, R. An Overview of Quinoline as a Privileged Scaffold in Cancer Drug Discovery. *Expert Opin. Drug Discov.* **2017**, *12* (6), 583–597.

(69) Makhanya, T. R.; Gengan, R. M.; Pandian, P.; Chuturgoon, A. A.; Tiloke, C.; Atar, A. Phosphotungstic Acid Catalyzed One Pot Synthesis of 4, 8, 8-Trimethyl-5-phenyl-5, 5a, 8, 9-tetrahydrobenzo [b][1, 8] Naphthyridin-6 (7H)-one Derivatives and Their Biological Evaluation Against A549 Lung Cancer Cells. *J. Heterocycl. Chem.* **2018**, *55* (5), 1193–1204.

(70) Gao, F.; Zhang, X.; Wang, T.; Xiao, J. Quinolone Hybrids and Their Anti-Cancer Activities: An Overview. *Eur. J. Med. Chem.* **2019**, *165*, 59–79.

(71) Fedejko-Kap, B.; Bratton, S. M.; Finel, M.; Radominska-Pandya, A.; Mazerska, Z. Role of Human UDP-Glucuronosyltransferases in the Biotransformation of the Triazoloacridinone and Imidazoacridinone Antitumor Agents C-1305 and C-1311: Highly Selective Substrates for UGT1A10. *Drug Metab. Dispos.* **2012**, *40* (9), 1736–1743.

(72) Pasquini, S.; Ligresti, A.; Mugnaini, C.; Semeraro, T.; Cicione, L.; De Rosa, M.; Guida, F.; Luongo, L.; De Chiaro, M.; Cascio, M. G. Investigations on the 4-Quinolone-3-Carboxylic Acid Motif. 3. Synthesis, Structure− Affinity Relationships, and Pharmacological Characterization of 6-Substituted 4-Quinolone-3-Carboxamides as Highly Selective Cannabinoid-2 Receptor Ligands. *J. Med. Chem.* **2010**, *53* (16), 5915–5928.

(73) Mugnaini, C.; Nocerino, S.; Pedani, V.; Pasquini, S.; Tafi, A.; De Chiaro, M.; Bellucci, L.; Valoti, M.; Guida, F.; Luongo, L. Investigations on the 4-Quinolone-3-Carboxylic Acid Motif Part 5: Modulation of the Physicochemical Profile of a Set of Potent and Selective Cannabinoid-2 Receptor Ligands through a Bioisosteric Approach. *ChemMedChem* **2012**, *7* (5), 920–934.

(74) Pertwee, R. G. Emerging Strategies for Exploiting Cannabinoid Receptor Agonists as Medicines. *Br. J. Pharmacol.* **2009**, *156* (3), 397–411.

(75) Upadhyay, K. D.; Dodia, N. M.; Khunt, R. C.; Chaniara, R. S.; Shah, A. K. Synthesis and Biological Screening of Pyrano [3, 2-c] Quinoline Analogues as Anti-Inflammatory and Anticancer Agents. *ACS Med. Chem. Lett.* **2018**, *9* (3), 283–288.

(76) Uppal, G.; Bala, S.; Kamboj, S.; Saini, M. Therapeutic Review Exploring Antimicrobial Potential of Hydrazones as Promising Lead. *Der Pharma Chem.* **2011**, *3* (1), 250–268.

(77) Verma, G.; Marella, A.; Shaquiquzzaman, M.; Akhtar, M.; Ali, M. R.; Alam, M. M. A Review Exploring Biological Activities of Hydrazones. *J Pharm Bioallied Sci*. **2014**, 6 (2), 69 - 80.

(78) Singh, N.; Ranjana, R.; Kumari, M.; Kumar, B. A Review on Biological Activities of Hydrazone Derivatives. *Int J Pharm Clin Res* **2016**, *8* (3), 162–166.

(79) Jucker, E. Recent Pharmaceutical Research on Hydrazine Derivatives. *Pure Appl. Chem.* **1963**, *6* (3), 409–434.

(80) Sinha, B. K.; Mason, R. P. Biotransformation of Hydrazine Derivatives in the Mechanism of Toxicity. *J. Drug Metab. Toxicol.* **2014**, *5* (3).

(81) Gamberini, M.; Cidade, M. R.; Valotta, L. A.; Armelin, M. C.; Leite, L. C. Contribution of Hydrazines-Derived Alkyl Radicals to Cytotoxicity and Transformation Induced in Normal c-Myc-Overexpressing Mouse Fibroblasts. *Carcinogenesis* **1998**, *19* (1), 147–155.

(82) DeVita Jr, V. T.; Serpick, A. A.; Carbone, P. P. Combination Chemotherapy in the Treatment of Advanced Hodgkin's Disease. *Ann. Intern. Med.* **1970**, *73* (6), 881–895.

(83) Popiołek, Ł. Hydrazide–Hydrazones as Potential Antimicrobial Agents: Overview of the Literature since 2010. *Med. Chem. Res.* **2017**, *26* (2), 287–301.

(84) Wu, A. M.; Senter, P. D. Arming Antibodies: Prospects and Challenges for Immunoconjugates. *Nat. Biotechnol.* **2005**, *23* (9), 1137–1146.

(85) Kar, S.; Leszczynski, J. Open Access in Silico Tools to Predict the ADMET Profiling of Drug Candidates. *Expert Opin. Drug Discov.* **2020**, *15* (12), 1473–1487.

(86) Fleming, N. Computer-Calculated Compounds. *Nature* **2018**, *557* (7707), S55-7.

(87) Fleming, N. How Artificial Intelligence Is Changing Drug Discovery. *Nature* **2018**, *557* (7706), S55–S55.

(88) Teague, S.; Valko, K. How to Identify and Eliminate Compounds with a Risk of High Clinical Dose during the Early Phase of Lead Optimisation in Drug Discovery. *Eur. J. Pharm. Sci.* **2017**, *110*, 37–50.

(89) Edward H. Kerns, Li Di, Guy T. Carter, ADMET in vitro profiling: Utility and applications in lead discovery, Burger's Medicinal Chemistry, Drug Discovery and Development, Discovering Lead Molecules, Chapter 2, John Wiley and Sons, Eds. DJ Abraham, and DP Rotella, **2003**, Volume 2, pp 47 – 72.

(90) Lipinski, C. A.; Lombardo, F.; Dominy, B. W.; Feeney, P. J. Experimental and Computational Approaches to Estimate Solubility and Permeability in Drug Discovery and Development Settings. *Adv. Drug Deliv. Rev.* **1997**, *23* (1–3), 3–

25.

(91) Koul, A.; Arnoult, E.; Lounis, N.; Guillemont, J.; Andries, K. The Challenge of New Drug Discovery for Tuberculosis. *Nature* **2011**, *469* (7331), 483–490.

(92) Cole, St.; Brosch, R.; Parkhill, J.; Garnier, T.; Churcher, C.; Harris, D.; Gordon, S. V; Eiglmeier, K.; Gas, S.; Barry, C. E. 3rd. Deciphering the Biology of *Mycobacterium Tuberculosis* from the Complete Genome Sequence. *Nature* **1998**, *396* (6707), 190.

(93) Batt, S. M.; Minnikin, D. E.; Besra, G. S. The Thick Waxy Coat of Mycobacteria, a Protective Layer against Antibiotics, and the Host's Immune System. *Biochem. J.* **2020**, *477* (10), 1983–2006.

(94) Lakshminarayana, S. B.; Huat, T. B.; Ho, P. C.; Manjunatha, U. H.; Dartois, V.; Dick, T.; Rao, S. P. S. Comprehensive Physicochemical, Pharmacokinetic and Activity Profiling of Anti-TB Agents. *J. Antimicrob. Chemother.* **2015**, *70* (3), 857–867.

(95) Bhhatarai, B.; Walters, W. P.; Hop, C. E. C. A.; Lanza, G.; Ekins, S. Opportunities and Challenges Using Artificial Intelligence in ADME/Tox. *Nat. Mater.* **2019**, *18* (5), 418–422.

(96) Roy, K.; Kar, S.; Das, R. N. *Understanding the Basics of QSAR for Applications in Pharmaceutical Sciences and Risk Assessment*; Academic press, **2015**, 427 – 453.

(97) Jia, C.-Y.; Li, J.-Y.; Hao, G.-F.; Yang, G.-F. A Drug-Likeness Toolbox Facilitates ADMET Study in Drug Discovery. *Drug Discov. Today* **2020**, *25* (1), 248–258.

(98) Daina, A.; Michielin, O.; Zoete, V. SwissADME: A Free Web Tool to Evaluate Pharmacokinetics, Drug-Likeness and Medicinal Chemistry Friendliness of Small Molecules. *Sci. Rep.* **2017**, *7* (1), 1–13.

(99) Agoram, B.; Woltosz, W. S.; Bolger, M. B. Predicting the Impact of Physiological and Biochemical Processes on Oral Drug Bioavailability. *Adv. Drug Deliv. Rev.* **2001**, *50*, S41–S67.

(100) Matlock, M. K.; Hughes, T. B.; Swamidass, S. J. XenoSite Server: A Web-Available Site of Metabolism Prediction Tool. *Bioinformatics* **2015**, *31* (7), 1136–1137.

(101) Tian, S.; Djoumbou-Feunang, Y.; Greiner, R.; Wishart, D. S. CypReact: A

Software Tool for in Silico Reactant Prediction for Human Cytochrome P450 Enzymes. *J. Chem. Inf. Model.* **2018**, *58* (6), 1282–1291.

Chapter 3

Synthesis and characterization of quinolone-hydrazine hybrids derivatives

3.1 Introduction

A lot of the research that is currently being done around TB is aimed at identifying new drugs, new drug targets and novel mechanisms of action[1-3]. Approximately one quarter (2 billion people) of the global population are infected with latent TB and are regarded as a reservoir of further infection upon reactivation. It is difficult to treat latent TB with the current forms of therapy partly because of the difficulty of diagnosis, and the prevalence of resistance to current drugs[4-5]. The development of treatment options that target latent TB is a gap in TB drug discovery that requires to be filled. Therefore, this project is attempting to contribute to the existing gap by designing novel hybrid molecules for the treatment of *Mycobacterium tuberculosis* (*Mtb*), a causative agent of TB. This chapter is presenting the synthetic pathways of quinolone pyrazine hydrazine derivatives including their acquisition and the characterisation. Synthesis followed a stepwise process depending on the availability of raw materials. The characterisation was done through routine spectroscopic techniques.

3.2 Rationale for the synthesis of quinolone pyrazinamide derivatives

From drug design and development viewpoint, it would take roughly 15-20 years to replace all current treatment options one by one and come up with a completely new TB regimen[4]. In the last decade, there has been an improvement in the number of new drug candidates cleared for clinical trials and an increase in the number of repurposed drugs for the treatment of TB[6]. The urgency for improved treatment is critical considering the lack of proper control and management of TB mainly in areas with poor health infrastructure and or high HIV incidences[7]. A complete overhaul of all drugs in the current treatment of TB is almost not feasible[7]. In 2012, the United States Food and Drug Administration approved bedaquiline (**Figure 3.1**) brand name Sirturo for the treatment of MDR-TB[1]. Subsequently, a few new anti-Tb drugs i.e., delamanid, and pretomanid have also been cleared for human trials [8-9].
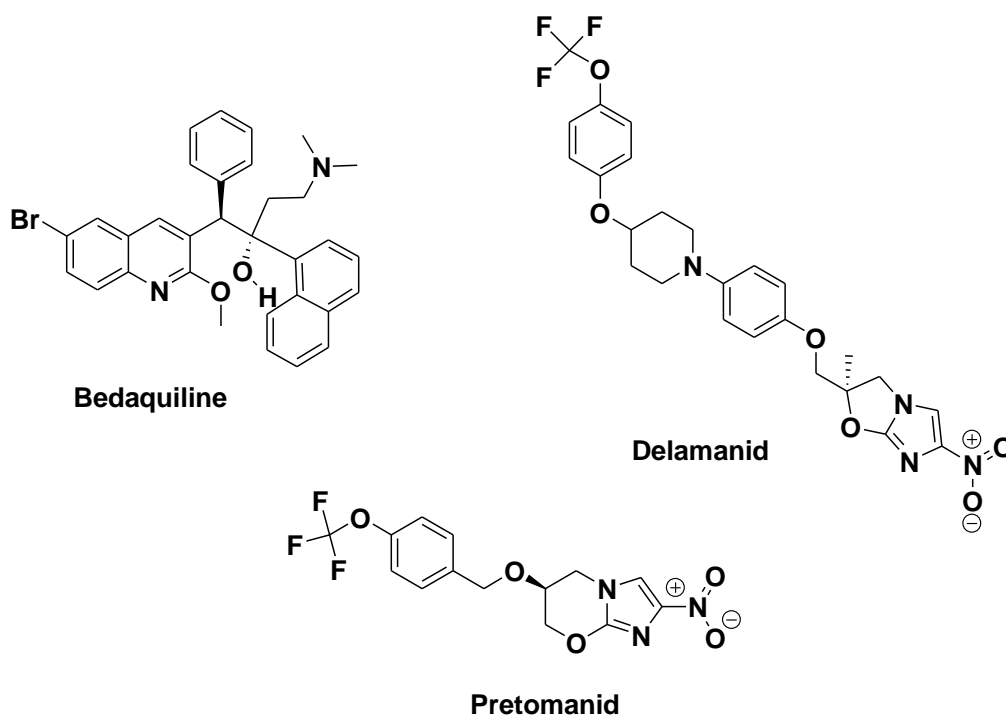
Figure 3.1: Chemical structures of recently approved TB drugs.

This project is an extension of the work that was previously conducted at Rhodes University by Beteck et al[10]. Beteck and co-workers investigated the amalgamation of quinolone scaffold and isoniazid using a hydrazine-hydrazone linker to generate a series of quinolone-isoniazid hybrids (**Figure 3.2**) as antimycobacterial agents. The synthesised compounds were screened for their potential anti-TB activity against *Mtb* H37Rv. Generally, the compounds showed activity in the range of 0.2-8.0 μM. From the series, compounds **3.1a** (MIC_{90}; 0.9 μM), **3.1b** (MIC_{90}; 0.2 μM), **3.1c** (MIC_{90}; 0.8 μM) and **3.1d** (MIC_{90}; 0.8 μM) emerged as the most active compounds[10]. More importantly, these compounds showed activity that was comparable to the activity of isoniazid INH and superior to those reported for the flouroquinolones against the *Mtb* H37Rv strain. None of the compounds from the series displayed a potential cytotoxicity risk.
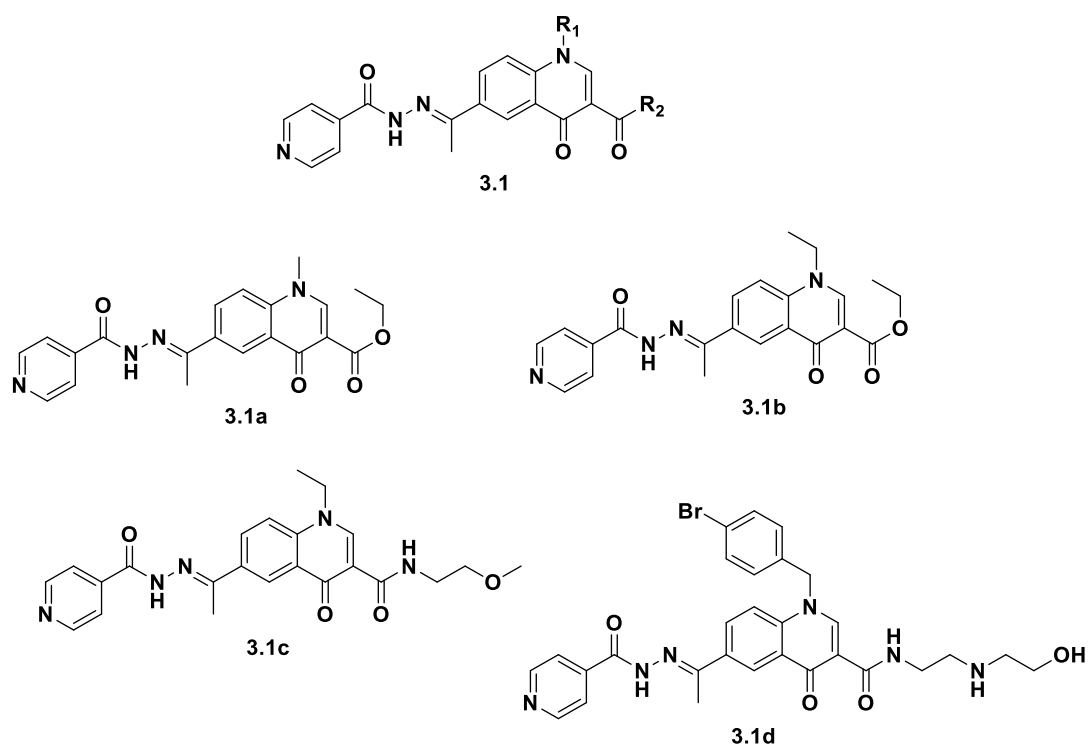
Figure 3.2: Quinolone-isoniazid hybrids reported by Beteck and co-workers showing enhanced anti-TB activity.

This work prompted us to explore the pharmacological effects of replacing isoniazid with another first line antitubercular pyrazinamide form quinolone-pyrazinamide hybrid compounds (**Figure 3.3**).
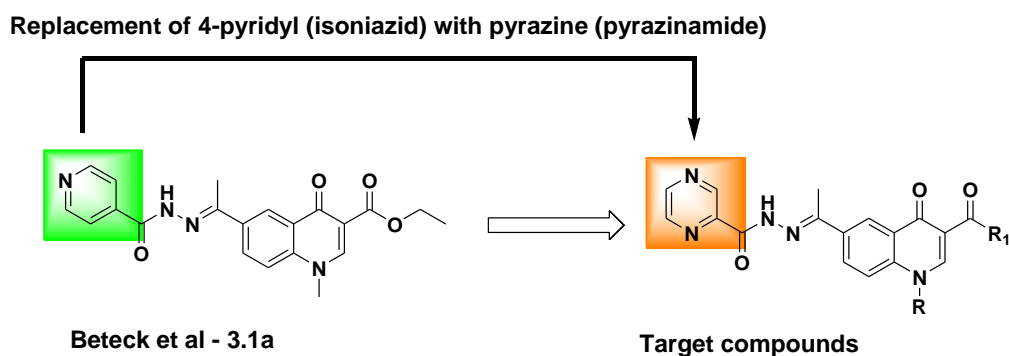

**Figure 3.3**: Design of target quinolone-pyrazinamide hybrid molecules.

Quinolone-containing compounds are deployed as key drugs for the treatment of resistant strains of TB[4]. The attachment of quinolone to pyrazinamide using a hydrazine moiety is a promising strategy considering the individual anti-tubercular activity of quinolones and pyrazinamide, respectively. Having more treatment options in the

arsenal of TB treatment will provide extra tools to address the problem drug resistance and ultimately, the eradication of *Mtb*.

3.3   Results and discussion

### 3.3.1 Retrosynthetic analysis of target compounds

A summary of the retrosynthetic analysis of our targeted compounds is shown in (**Scheme 3.1**). The quinolone-pyrazinamide hybrids **3.8** could be accessed from pyrazinamide **3.7** and the quinolone intermediate **3.6**. Pyrazinamide **3.7** is accessible from the commercial pyrazinoic acid **3.5** via ester intermediate and hydrazine hydrate. In turn, the quinolone intermediate **3.6** could be achieved by condensation of *p*-aminoacetophenone **3.3**, which is obtained by reduction of *p*-nitroacetophenone **3.2** using iron powder and ammonium chloride, and diethylethoxymethylenemalonate **3.4.** Subsequently, this was followed by a classical Gould-Jacobs cyclization method for synthesis of quinolone[11].
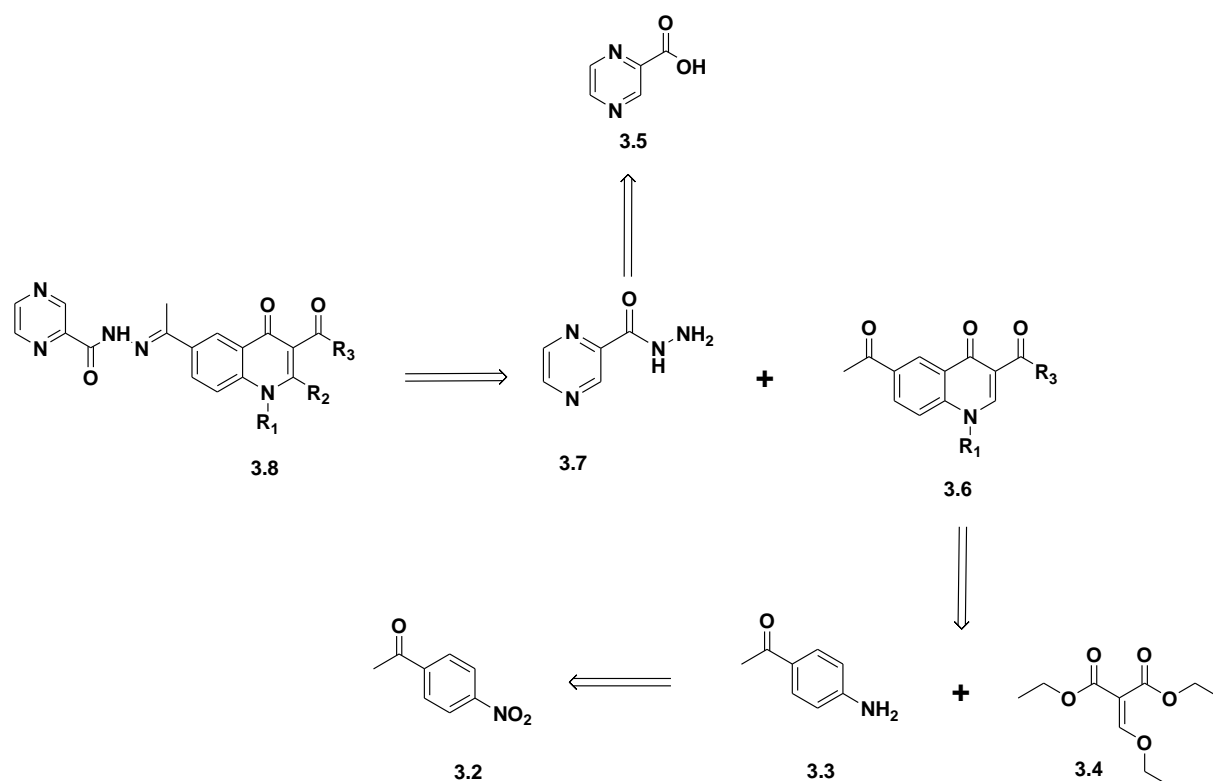
Scheme 3.1: Retrosynthetic pathway of the proposed quinolone-pyrazinamide derivatives **3.8**.

3.3.2 Synthesis of the pyrazinamide, 3.7

Pyrazine carboxylic acid **3.5** was reacted with ethanol under reflux for 10 hours in concentrated sulphuric acid as a catalyst. The TLC (DCM: MeOH; 90%:10%) indicated the completion of the reaction. The ester was collected as yellow white solid product with percentage yield of 44%. The synthesis of the hydrazine amide of pyrazine carboxylic acid theoretically could follow different pathways. Direct amidation of pyrazinoic acid **3.5** with hydrazine hydrate using *N, N'*-carbonyldiimidazole (CDI) coupling agent[12] yielded no desired product. Then, we opted for an accelerative coupling agent, 1-hydroxy benzotriazole (HOBt), with hydrazine hydrate as the amine, and this attempt did not yield desirable results. Thereafter, T3P was used as a coupling agent to facilitate the amidation reaction, but it did not yield any positive results. Then, we resolved to convert the acid **3.5** to an ester **3.5a** intermediate (**Scheme 3.2**), which was subsequently treated with hydrazine as described in the literature[13]. Thereafter, the ethyl pyrazinoate **3.5a** was dissolved in ethanol at room temperature and treated with excess hydrazine and the reaction mixture stirred for at least 2 hours. The solid product which precipitated at room temperature was isolated through filtration and allowed to dry in the open air. The resulting pyrazinamide **3.7** was obtained in 64% yield as a yellow solid upon purification.
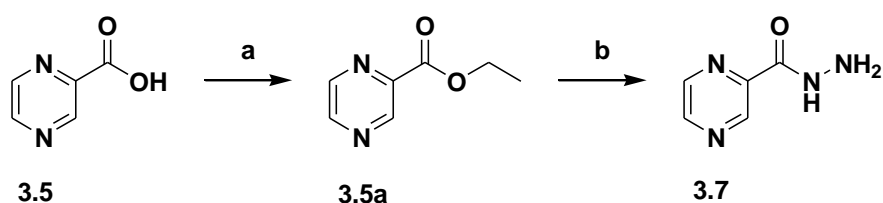
Scheme 3.2: *Reagents and conditions*: a) Dry EtOH, *conc* H_2SO_4, reflux 10 h; b) EtOH, NH_2NH_2 (10 equiv), r.t, 2h.

3.3.2.1 Spectroscopic characterisation of 3.7

The ^{1}H-NMR spectrum of compound **3.7** (**Figure 3.4**) confirmed the successful formation of the hydrazide. The appearance of a singlet at δ 10.14 ppm shows the amide NH which resulted from the conversion of the $-NH_2$ during amidation. The remaining hydrazine NH_2 appeared singlet peak integrating for 2H at δ 4.65 ppm. The aromatic protons could be observed appeared in the aromatic region.

The ^{13}C-NMR (**Figure 3.5**) showed the expected number of C atoms that are consistent with the skeletal structure of the proposed hydrazide. The signal peak at δ 161.53 ppm represents the amide functionality, which appeared slightly up-field compared to the carbonyl carbon of the starting ethyl pyrazinoate **3.5a**.
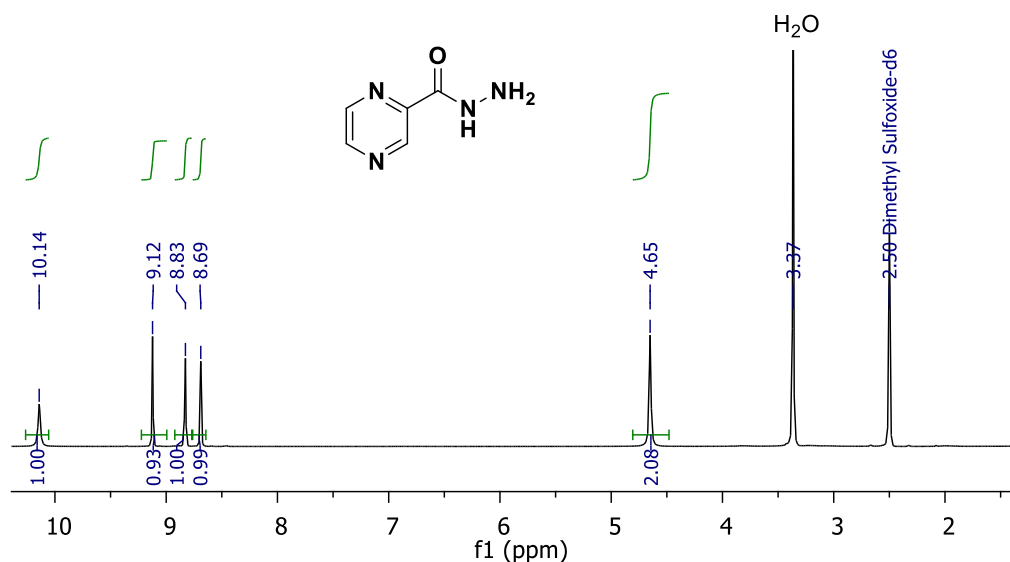

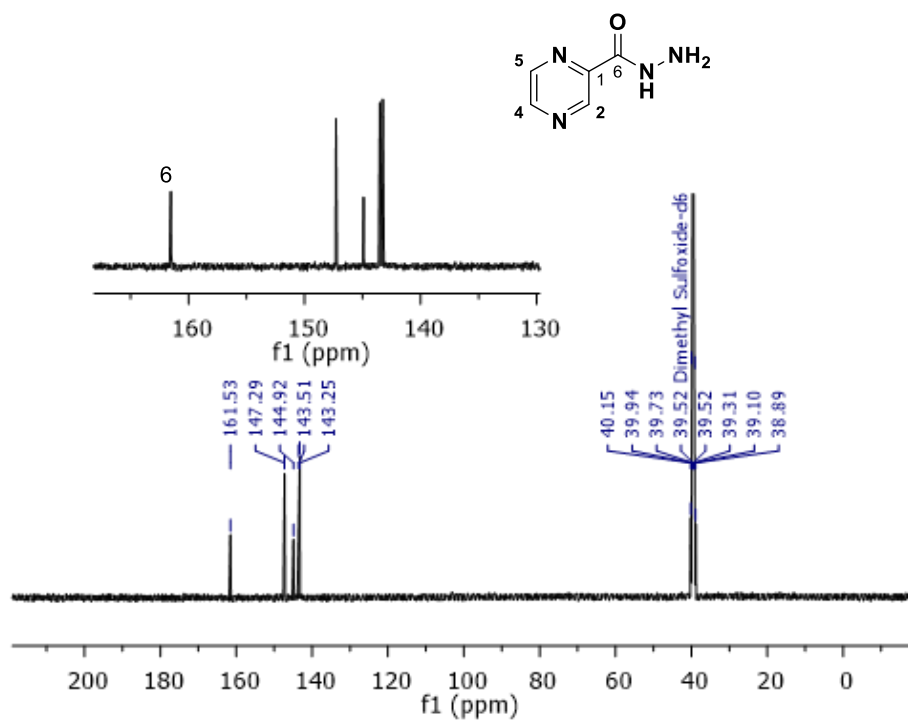**Figure 3.4**: 400 MHz ^{1}H-NMR spectrum of compound **3.7** in DMSO-d_6.

Figure 3.5: 400 MHz ^{13}C-NMR spectrum of compound **3.7** in DMSO-d_6.

3.3.3 Overall reaction scheme for the synthesis of target quinolone hybrids

Scheme 3.1 above illustrated the retrosynthetic analysis of target compounds. The complementary overall multi-step synthesis of quinolone-based derivatives is displayed in (**Scheme 3.3**) below.
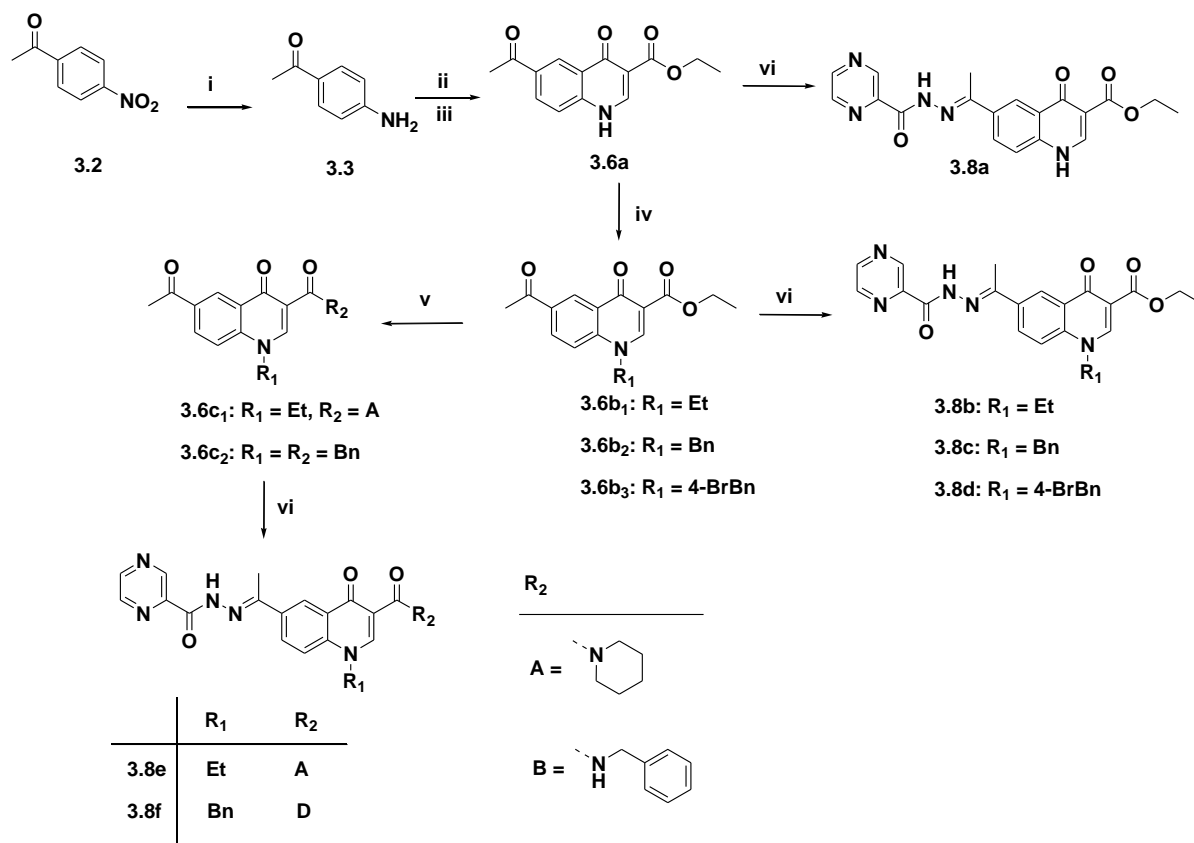
Scheme 3.3[10]: *Reagents and conditions*: i) Reduced iron (Fe) powder, ethanol, HCl; ii) Acetonitrile, diethyl ethoxylmethylenemalonate, reflux 12 h; iii) Diphenyl ether, 250-253 °C, < 5 mins; iv) K_2CO_3, $CHCl_3$/THF (2:1), alkyl/benzyl halide (1.2 Equiv), 12 h; v) Amine (5 equiv), DBU (1.2 equiv), $CHCl_3$, reflux 12 h; vi) Pyrazinamide **3.7**, Ethanol, cat. HAc, reflux overnight.

3.3.4 Synthesis of ethyl 6-acetyl-1,4-dihydro-4-oxoquinoline-3-carboxylate

Following the synthesis of desired pyrazinamide **3.7**, the next step involved the synthesis of ethyl 6-acetyl-1,4-dihydro-4-oxoquinoline-3-carboxylate intermediate **3.4**, which undergoes cyclisation to form the desired quinolone **3.6a**. Reduction of 4-nitro-acetophenone **3.2** using iron powder (**Scheme 3.3**) under reflux in ethanol and concentrated hydrochloric acid (HCl) yielded *p*-aminoacetophenone **3.3** in 65% yield.

The ^{1}H-NMR (**Figure 3.6**) showed the presence of a broad peak at δ 4.16 ppm integrating for 2 H which was attributed to the NH_2 functional group. The observed chemical shifts were consistent with the values reported in the literature[14].
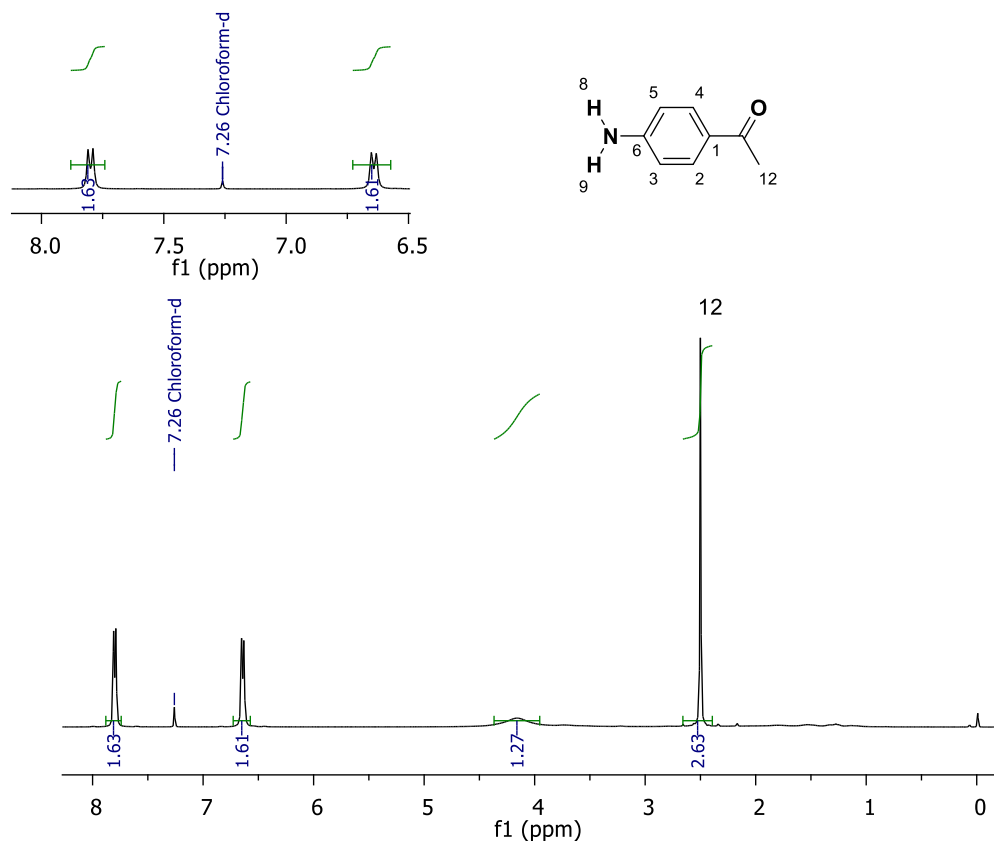

Figure 3.6: 400 MHz ^{1}H-NMR spectrum for compound **3.6** in $CDCl_3$.

The conversion of *p*-aminoacetophenone **3.3** by refluxing with diethyl ethoxymethylenemalonate in acetonitrile for 12 hours led to the formation of intermediate **3.4** (not shown in **Scheme 3.3**). The TLC (EtOAc: Hex) analysis showed the completion conversion of the reaction to form a product. The acetonitrile was evaporated in vacuo resulting in the precipitation of a solid product. The solid was isolated through filtration in a good percentage yield of 75%. The ^{1}H NMR spectrum (**Figure 3.7**) showed all expected protons signals consistent with the proposed intermediates. The appearance of additional chemical shifts in the alkyl region (δ 3.5-4.5 ppm) of the spectrum is an indication of the symmetrical ethyl ester groups.

The ^{13}C-NMR spectrum (**Figure 3.8**) of **3.4** showed the appearance of more than one signal consistent with the carbonyl group appearing in the region δ160 – 170 ppm, thus confirming the ester functionality. The C-atom of the ketone signal appeared at δ_C 196.61 ppm. The rest of the other signals confirmed the skeletal structure of the ester intermediate **3.4**.
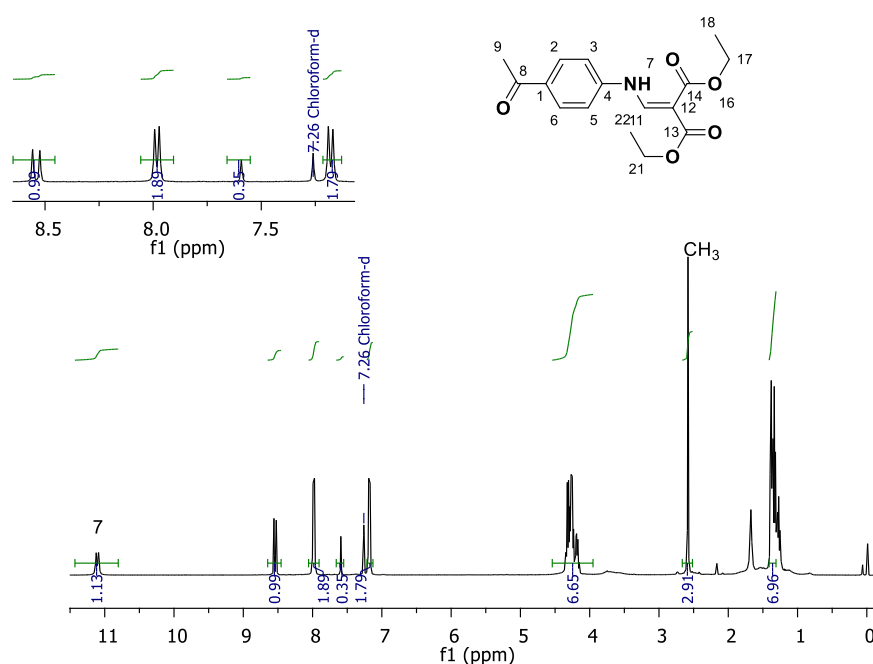

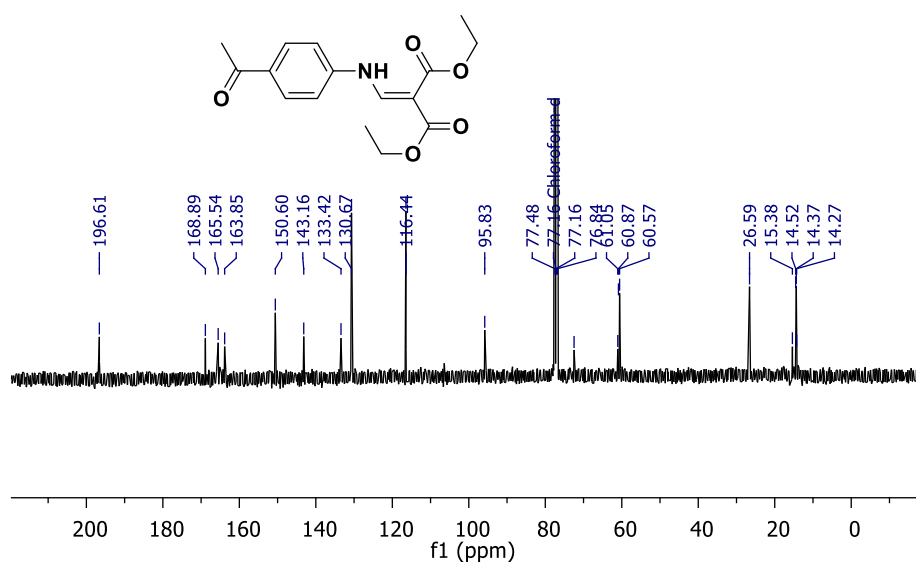**Figure 3.7**: 400 MHz ^{1}H-NMR spectrum of compound **3.4** in CDCl$_3$.

Figure 3.8: 100 MHz ^{13}C-NMR spectrum of compound **3.4** in CDCl$_3$.

After the successful synthesis of **3.4**, the next step was the cyclisation (step iii) of the achieved intermediate to yield the desired key starting quinolone intermediate **3.6a** (**Scheme 3.3**). Thus, cyclisation of the anilinomethylenemalonate **3.4** in diphenyl ether at a temperature range of 240 – 254 °C to yield intermediate **3.6a**[15]. The process of cyclisation is temperature dependent. Conducting the cyclisation at temperatures above 260 °C results in the formation of unidentifiable compounds as judged by TLC[10]. Thus, the reaction was maintained at 240 – 254 °C for approximately one hour. After cooling, the reaction contents were poured into cold hexane resulting in a solid precipitate. The precipitate was separated from the solvent by gravity filtration. After drying in the open air a light brown solid, which was further purified by silica gel column chromatography using 90-100% ethyl acetate:hexane gave a yellow fine amorphous solid powder of quinolone **3.6a** in 63% yield. The mechanism of the formation of compound **3.6a** is illustrated below.
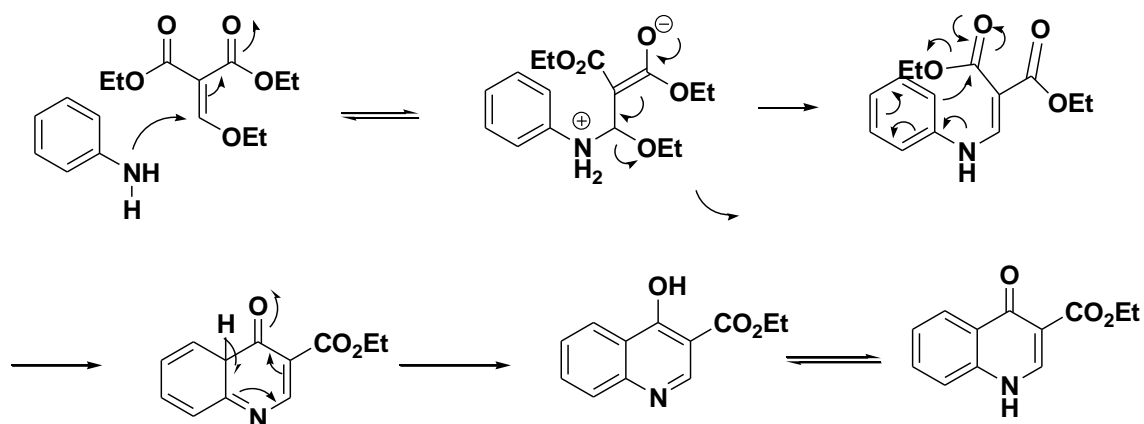
Scheme 3.4: The proposed reaction mechanism for the formation of the quinolone framework.

The Gould-Jacobs reaction is the reaction that is commonly used in the synthesis of quinolines, 4-hydroxyquinoline and in this case 4-quinolones[16]. The step-by-step sequence starts with the formation of an anilidomethylenemalonic ester through the condensation of the aniline with an alkoxy, a methylene malonic ester or an acyl malonic ester (**Scheme 3.4**). Followed the formation of 4-hydroxy-3-carboalkoxy quinoline, which usually occurs in the 4-oxo form through the 6-electron cyclisation process. The formation of the acid occurs from saponification. More importantly, the

Gould-Jacobs is more effective with meta-position anilines, with electron-donating groups[17].

3.3.4.1   Spectroscopic analysis of ethyl 6-acetyl-4-oxo-1,4-dihydroquinoline-3-carboxylate, 3.6a

The ^{1}H-NMR (**Figure 3.9**) analysis confirmed the structural identify of quinolone **3.6a**. The ^{1}H NMR that was run in DMSO and showed a broad singlet peak appearing downfield corresponding to NH of the quinolone framework.
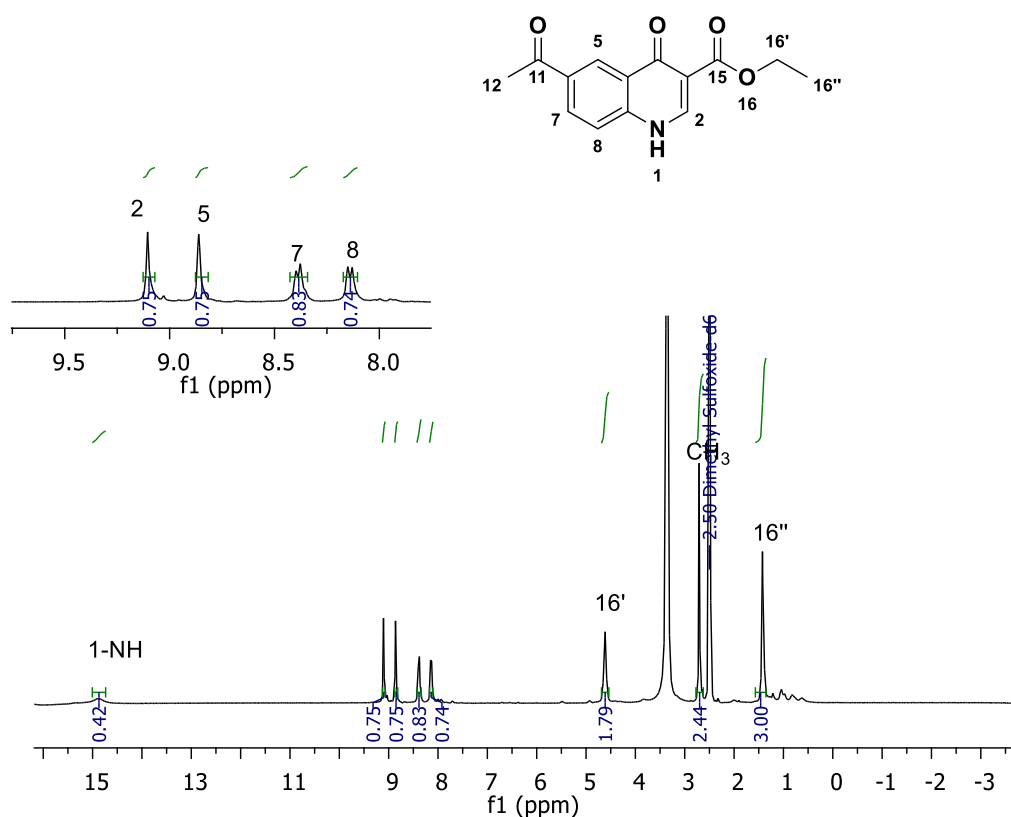
Figure 3.9: ^{1}H NMR spectrum (400 MHz, CDCl₃) of quinolone **3.6a**.

The observed proton signals in the aromatic regions confirmed the cyclisation of the methylene malonate ester **3.4** to form the desirable quinolone intermediate **3.6a**. The upfield regions (δ 1.00 – 2.00 ppm and 4.50 – 5.00 ppm) of the spectra are consistent with the ethyl ester protons (16' and 16''). The ketone protons (i.e., H12) could be observed at δ 2.60 – 3.00 pm. The ^{13}C NMR spectrum (**Figure 3.10**) confirmed the successful formation of quinolone **3.6a**. The C peaks in the range of δ160 – 200 ppm

provided evidence of the presence of carbonyl carbons (C4, C11 and C15). The alkyl region of the spectrum also showed evidence of three C peaks consistent with the ethyl ester at position 3 and the methyl group (C12) on the position 6 of the quinolone scaffold. The rest of other carbons could be observed in the aromatic region confirming the skeletal structure of the proposed compound **3.6a**.
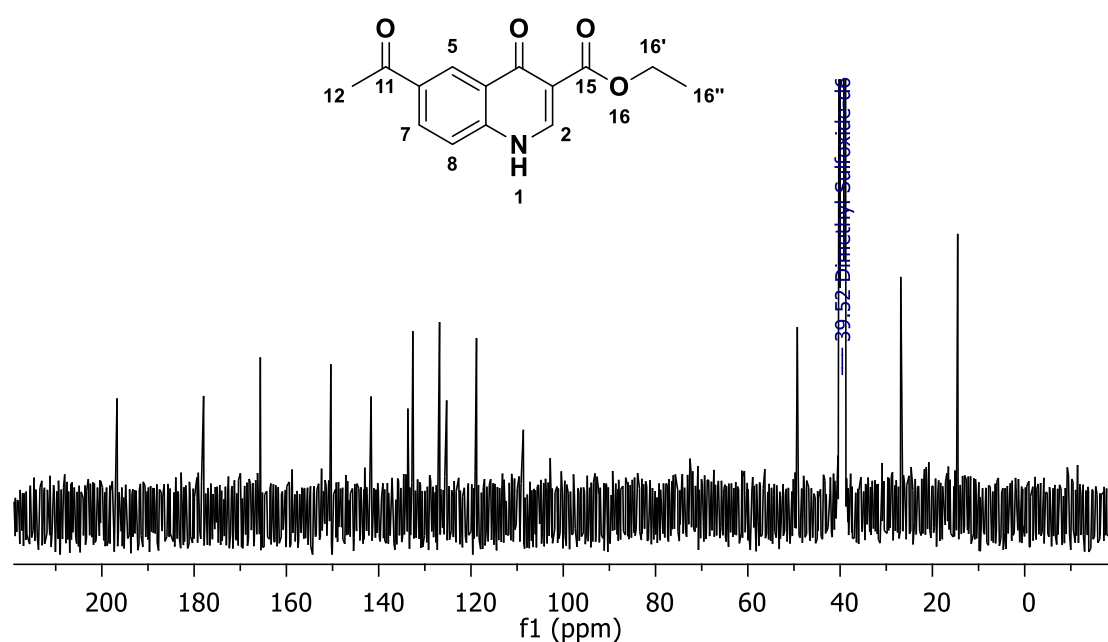

Figure 3.10: ^{13}C NMR spectrum (100 MHz, CDCl$_3$) of quinolone **3.6a**.

3.3.5 Synthesis of amide and *N*-alkylated derivatives, 3.6b$_{1-3}$

The literature evidence indicates that position one of the quinolones is very critical for their activity as an antimicrobials[15]. It has been observed by other researchers that the substituted group on the position N-1 can either improve or impair the activity of the quinolone scaffold[18]. In this study, we modified the position N-1 of the quinolone by attaching the alkyl or benzyl group as part of exploring the structural activity relationship of proposed quinolone pyrazinamide hybrid molecules. Thus, alkylation or benzylation of the quinolone **3.6a** with alkyl halide or benzyl halide in the presence of K$_2$CO$_3$ base (**Scheme 3.3**) in a solvent mixture of chloroform and tetrahydrofuran (1:2) afforded compounds **3.6b$_1$** – **3.6b$_3$** in yields of 64 – 70%. The proposed structures of compounds **3.6b$_1$** – **3.6b$_3$** were confirmed (see Chapter 5) by ^1H and ^{13}C NMR spectroscopic techniques.

Amidation of the esters can either be performed through hydrolysis of the ester followed by amide coupling using agents such as *N, N'*-carbonyldiimidazole (CDI) and propylphosphonic acid anhydride (T3P). However, we opted to use a one-pot reaction with 1,8-diazabicyclo [5.4.0] undec-7-ene (DBU) as a nucleophilic catalyst to the reaction of the ester with an amine. Thus, amide coupling of the esters **3.6b₁ – 3.6b₃** with piperidine or benzylamine using DBU in chloroform yielded, upon purification by silica gel column chromatography, the amides **3.6c₁** and **3.6c₂** in 35% and 22% yields. The achieved intermediates were also analysed using routine spectroscopic techniques and characterisation details of a representative compound **3.6c₁** are discussed below.

3.3.5.1 Spectroscopic characterisation of quinolones 3.6c₁

The ^{1}H NMR (**Figure 3.11**) spectrum of **3.6c₁** confirmed the successful amidation of **3.6b₁** to form compound **3.6c₁**. The synthesis involves the substitution of the ethyl ester moiety with piperidine to form the target compound **3.6c₁**.

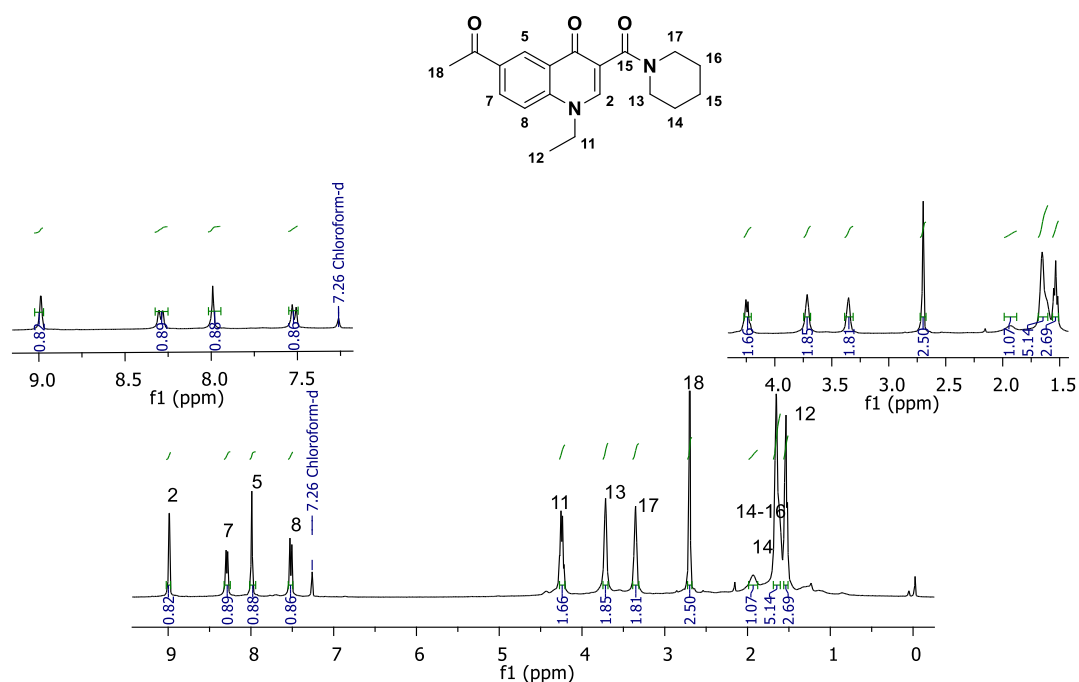**Figure 3.11**: ^{1}H NMR spectrum (400 MHz, CDCl₃) of quinolone derivative **3.6c₁**.

The ^{1}H NMR spectrum showed multiple signal peaks observed in the alkyl regions. The observed peaks were assigned to the cyclohexyl ring of the piperidine. The presence

of an unresolved quartet at δ 4.00 - 4.50 ppm range and integrating for 2H showed the successful synthesis of the *N*-ethyl derivative **3.6c₁**. The ^{13}C NMR spectrum (**Figure 3.12**) confirmed the proposed structure of **3.6c₁**. The carbon signals corresponding to the piperidine (C13 – 17), ethyl (C11 and C12) and methyl ketone moiety (C18) could be observed in the range between δ14.0 and 49.0 ppm. Whereas the three carbonyl (C4, C15 and C17) peaks appeared between δ165.1 and 197.2 ppm. The remaining carbon signals appeared in the aromatic region with the chemical shifts in range δ116.1 – 145.2 ppm.
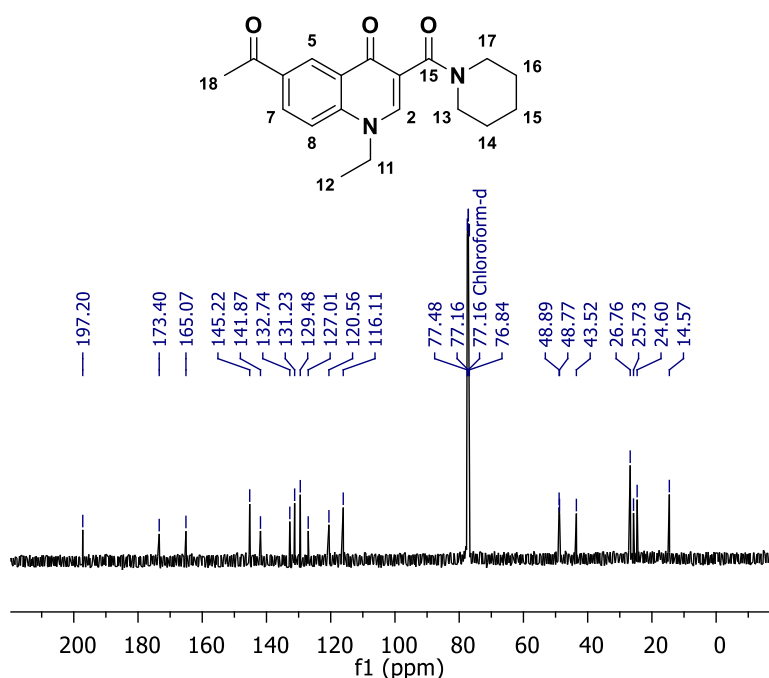

Figure 3.12: ^{13}C NMR spectrum (100 MHz, CDCl₃) of quinolone derivative **3.6c₁**.

3.3.6 Synthesis of quinolone pyrazinamide hybrids 3.8a-f

After successfully synthesising the required quinolone intermediates **3.6a**, **3.6b₁₋₃** and **3.6c₁₋₂**, the next step was appending the pyrazinamide **3.7** to these quinolones through a Schiff base reaction. Schiff base condensation reaction normally involves the condensation of primary amines and active carbonyl groups[18]. The pyrazine-2-carboxylic acid hydrazide **3.7** and the quinolone intermediates **3.6a**, **3.6b₁₋₃** and **3.6c₁₋₂** were refluxed in ethanol overnight in the presence of a catalytic amount of acetic acid (**Scheme 3.3**). Schiff base reactions are sensitive to pH, where slightly acidic conditions accelerate the reaction, and excessively acidic environments halt the

reaction[19]. Ideally water should be expelled as the reaction takes place to shift the equilibrium towards the products and avoid diassociation[19]. The reaction can take place in non-acidic environments mainly for primary amines but will take a longer reaction time. Acid catalysis is believed to follow more than one pathway of the reaction mechanism. Mechanistically, the Schiff base proceeds primarily through the formation of a carbinolamine intermediate followed by the removal of water to give the imine, which is the rate-determining step[20]. Sometimes during the reaction desired compounds precipitate and isolated by gravitational filtration. Where there was no precipitate formation during the reaction, the final compounds were obtained by evaporating the solvent to yield crude products, which were purified using silica gel column chromatography. The resulting compounds were achieved in yields ranging between 22 and 40%. The details are provided in the experimental chapter.

3.3.6.1   Spectroscopic analysis of synthesised compounds

All the synthesised compounds were characterised using ^{1}H and ^{13}C NMR, IR, and mass spectrometry. The ^{1}H and ^{13}C NMR spectra for a representative compound **3.8e** are shown in (**Figure 3.13**) and (**Figure 3.14**).
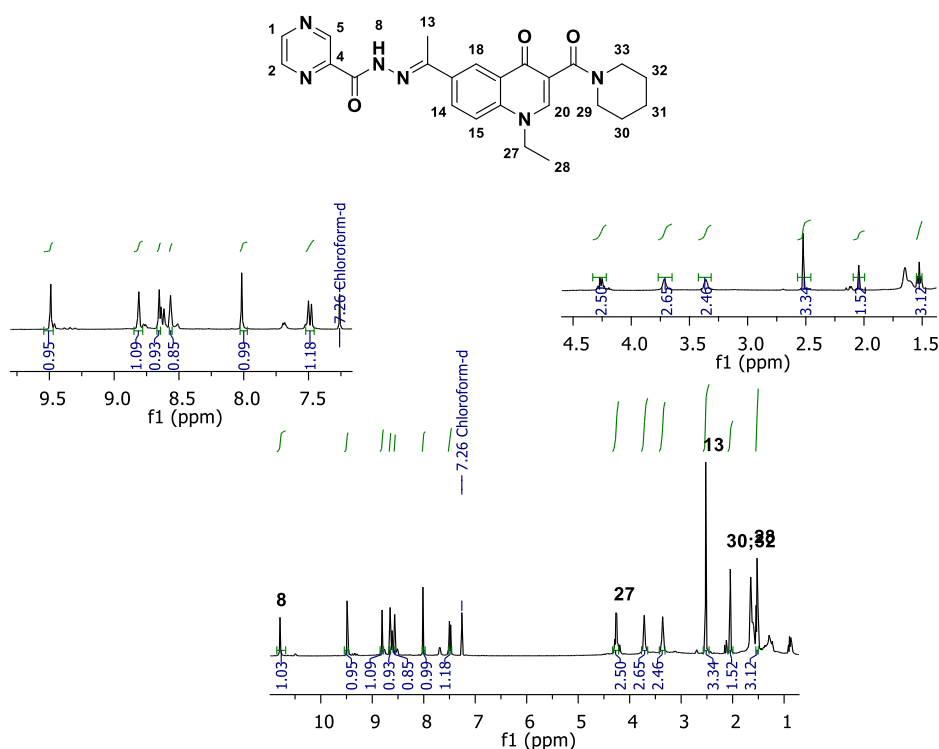

Figure 3.13: ^{1}H NMR spectrum (400 MHz, CDCl$_3$) for compound **3.8e**.

Upfield, the 1H NMR spectrum showed signal peaks consistent with the piperidine moiety (H29-33), N-1 ethyl group (H-27 and H-28) and methyl group (H13) attached to the imine. The appearance of NH signal peak at δ10.79 ppm further confirmed the formation of compound **3.8e**. The aliphatic carbons are also confirmed by the ^{13}C NMR spectrum (**Figure 3.14**), which showed the presence of 6 signal peaks that are consistent with the number of carbons for the piperidine moiety (C29-33), N-1 ethyl group (C-27 and C-28) and methyl group (C13) attached to the imine. Compared to the intermediate **3.6c$_1$**, which showed 11 carbons in its aromatic region, compound **3.8e** ^{13}C spectrum showed additional carbons in the aromatic region further confirming the successful Schiff condensation of **3.7** with **3.6c$_1$** to form **3.8e**. Additionally, the disappearance of carbonyl (C=O) peak at δ197.2 ppm (**Figure 3.12**) accompanied by the appearance of new C=N peak at δ158.8 ppm is a clear evidence of the existence of imine functionality in the proposed structure of **3.8e**. Compound **3.8e** also has three carbonyl carbons which are evident from the ^{13}C spectrum provided (**Figure 3.14**).
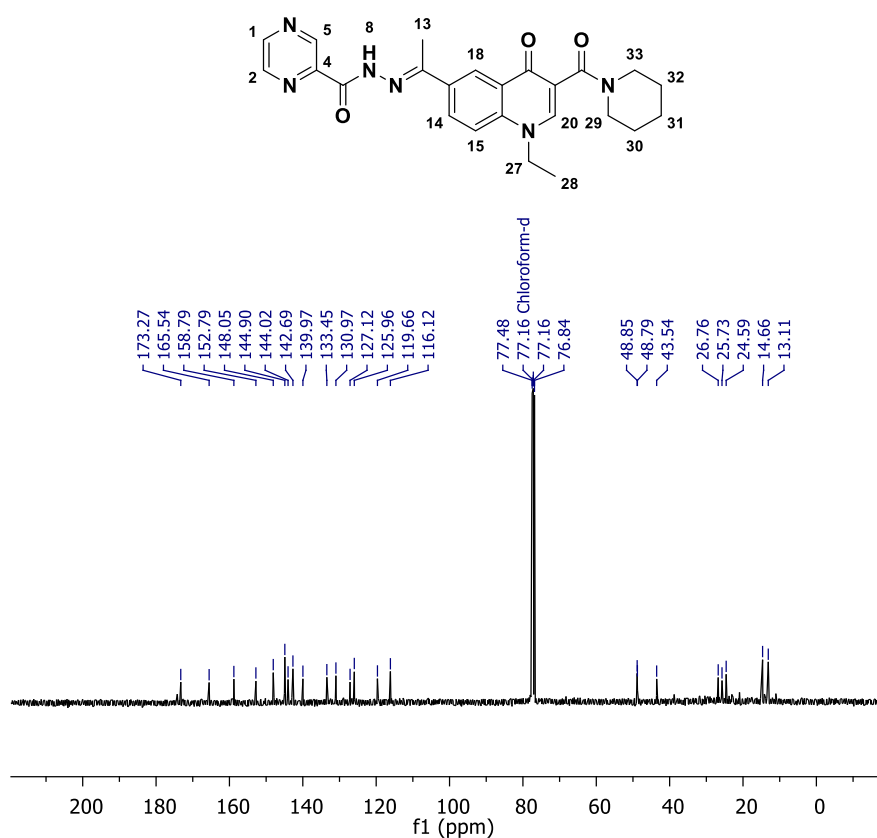

Figure 3.14: ^{13}C NMR spectrum (100 MHz, CDCl$_3$) of quinolone pyrazinamide derivative **3.8e.**

The final compounds were further analysed by liquid chromatography-mass spectrometry (LCMS) to determine their corresponding molecular weights. **Figure 3.15** illustrates the high-resolution mass spectrometry spectrum of compound **3.8e** obtained using electron spray ionisation (ESI) in positive mode. The ESI mass spectrum showed an intense signal of the molecular ion peak at *m/z* 447.2148 consistent with the proposed structure of compound **3.8e**. FT-IR spectrum (Figure 3.15) obtained showed diagnostic bands in the regions 3000 – 2800, 1700 – 1600 and 1500-1400 cm^{-1}, which were attributed to NH, C=O and C=N stretches, respectively.
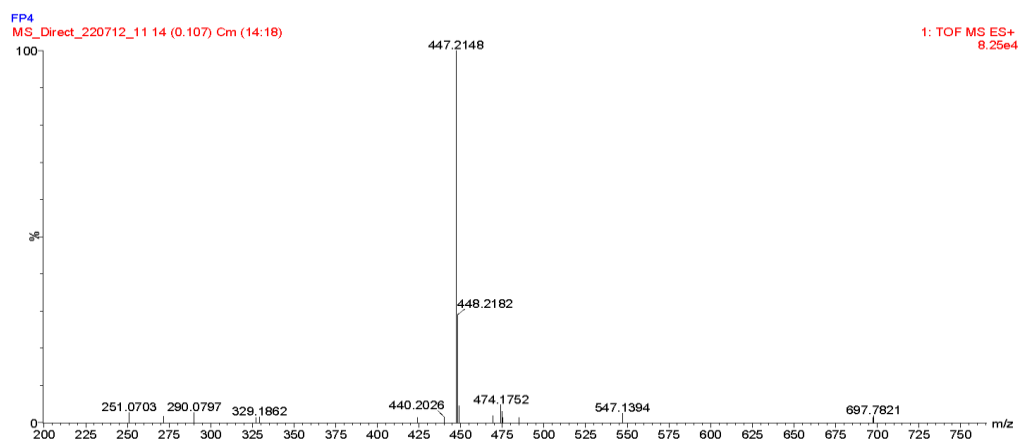

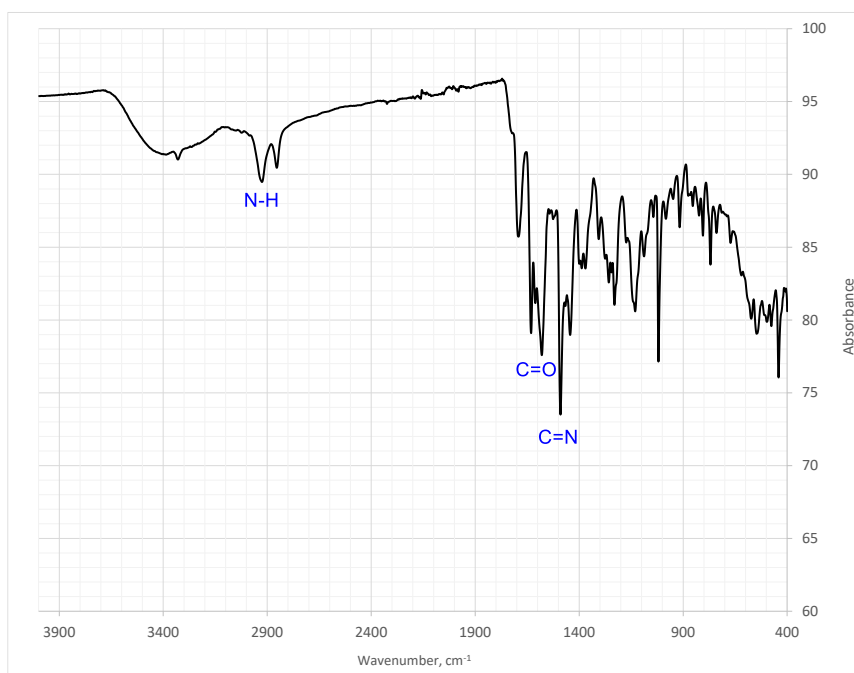**Figure 3.14**: HRMS spectrum of quinolone pyrazine hydrazone derivative **3.8e**.

Figure 3.15: FT-IR illustration of final compound **3.8e.**

3.4 Conclusions

In summary, the quinolone pyrazinamide hybrid molecules linked through hydrazone bond were successfully synthesised through a stepwise process involving a Schiff base condensation reaction. The synthesised compounds were obtained in modest to good yields. The structural identity of each compound was confirmed by routine analytical spectroscopic techniques. Although some of the synthesised compounds showed poor solubility in almost all solvents.

3.5 References

(1)   dos Santos Fernandes, G. F.; De Souza, P. C.; Moreno-Viguri, E.; Santivañez-Veliz, M.; Paucar, R.; Pérez-Silanes, S.; Chegaev, K.; Guglielmo, S.; Lazzarato, L.; Fruttero, R. Design, Synthesis, and Characterization of N-Oxide-Containing Heterocycles with in Vivo Sterilizing Antitubercular Activity. *J. Med. Chem.* **2017**, *60* (20), 8647–8660.

(2)   Fernandes, G.F.d.S.; Man Chin, C.; Dos Santos, J.L. Advances in Drug Discovery of New Antitubercular Multidrug-Resistant Compounds. *Pharamceuticals,* **2017**, *10* (2), 51.

(3)   Dartois, V.A.; Rubin, E.J.; Anti-tuberculosis treatment strategies and drug development: challenges and priorities., *Nat Rev Microbiol,* **2022**, 20, 685 – 70

(4)   Organization, W. H. *Global Tuberculosis Report 2022*; World Health Organization, **2022**.

(5)   Patel, K.; Jhamb, S. S.; Singh, P. P. Models of Latent Tuberculosis: Their Salient Features, Limitations, and Development. *J. Lab. Physicians* **2011**, *3* (02), 75–79.

(6)   Lienhardt, C.; Vernon, A. A.; Cavaleri, M.; Nambiar, S.; Nahid, P. Development of New TB Regimens: Harmonizing Trial Design, Product Registration Requirements, and Public Health Guidance. *PLoS Med.* **2019**, *16* (9), e1002915.

(7)   Ginsberg, A. M.; Spigelman, M. Challenges in Tuberculosis Drug Research and Development. *Nat. Med.* **2007**, *13* (3), 290–294.

(8)   Felipe dos Santos Fernandes, G.; Hartmann Jornada, P.; de Souza, C.; Man Chin, C.; Rogerio Pavan, F.; Leandro dos Santos, J. Current Advances in Antitubercular Drug Discovery: Potent Prototypes and New Targets. *Curr. Med. Chem.* **2015**, *22* (27), 3133–3161.

(9)   Wallis, R. S.; Maeurer, M.; Mwaba, P.; Chakaya, J.; Rustomjee, R.; Migliori, G. B.; Marais, B.; Schito, M.; Churchyard, G.; Swaminathan, S. Tuberculosis—Advances in Development of New Drugs, Treatment Regimens, Host-Directed Therapies, and Biomarkers. *Lancet Infect. Dis.* **2016**, *16* (4), e34–e46.

(10)   Beteck, R. M.; Seldon, R.; Jordaan, A.; Warner, D. F.; Hoppe, H. C.; Laming, D.; Legoabe, L. J.; Khanye, S. D. Quinolone-Isoniazid Hybrids: Synthesis and Preliminary in Vitro Cytotoxicity and Anti-Tuberculosis Evaluation. *Medchemcomm* **2019**, *10* (2), 326–331.

(11)   Neelarapu, R.; Maignan, J. R.; Lichorowic, C. L.; Monastyrskyi, A.; Mutka, T. S.; LaCrue, A. N.; Blake, L. D.; Casandra, D.; Mashkouri, S.; Burrows, J. N. Design and Synthesis of Orally Bioavailable Piperazine Substituted 4 (1 h)-Quinolones with Potent Antimalarial Activity: Structure–Activity and Structure–Property Relationship Studies. *J. Med. Chem.* **2018**, *61* (4), 1450–1473.

(12)   Larrivee-Aboussafy, C.; Jones, B. P.; Price, K. E.; Hardink, M. A.; McLaughlin, R. W.; Lillie, B. M.; Hawkins, J. M.; Vaidyanathan, R. DBU Catalysis of N, N′-Carbonyldiimidazole-Mediated Amidations. *Org. Lett.* **2010**, *12* (2), 324–327.

(13)   da Silva, Y. K. C.; Augusto, C. V.; de Castro Barbosa, M. L.; de Albuquerque Melo, G. M.; de Queiroz, A. C.; Dias, T. de L. M. F.; Júnior, W. B.; Barreiro, E. J.; Lima, L. M.; Alexandre-Moreira, M. S. Synthesis and Pharmacological Evaluation of Pyrazine N-Acylhydrazone Derivatives Designed as Novel Analgesic and Anti-Inflammatory Drug Candidates. *Bioorg. Med. Chem.* **2010**, *18* (14), 5007–5015.

(14)   Shenyang Pharmaceutical Univeristy. Preparation Method for 4-Aminoacetophenone. CN102924306A, **2012.**

(15)   Horta, P.; Henriques, M. S. C.; Brás, E. M.; Murtinheira, F.; Nogueira, F.; O'Neill, P. M.; Paixão, J. A.; Fausto, R.; Cristiano, M. L. S. On the Ordeal of Quinolone Preparation via Cyclisation of Aryl-Enamines; Synthesis and Structure of Ethyl 6-Methyl-7-Iodo-4-(3-Iodo-4-Methylphenoxy)-Quinoline-3-Carboxylate. *Pure Appl. Chem.* **2017**, *89* (6), 765–780.

(16)   Gould, R. G.; Jacobs, W. A. The Synthesis of Certain Substituted Quinolines and 5, 6-Benzoquinolines. *J. Am. Chem. Soc.* **1939**, *61* (10), 2890–2895.

(17)   Mishra, S.; Salahuddin, R. K.; Majumder, A.; Kumar, A.; Singh, C.; Tiglani, D. Updates on Synthesis and Biological Activities of Quinoline Derivatives: A

Review. *Int. J. Pharm. Res.* **2021**, *13* (1), 3941 – 3960.

(18) Renau, T. E.; Sanchez, J. P.; Gage, J. W.; Dever, J. A.; Shapiro, M. A.; Gracheck, S. J.; Domagala, J. M. Structure− Activity Relationships of the Quinolone Antibacterials against Mycobacteria: Effect of Structural Changes at N-1 and C-7. *J. Med. Chem.* **1996**, *39* (3), 729–735.

(19) Silva, P. J. New Insights into the Mechanism of Schiff Base Synthesis from Aromatic Amines in the Absence of Acid Catalyst or Polar Solvents. *J. Org. Chem.* **2020**, *2*, e4.

(20) Santerre, G. M.; Hansrote Jr, C. J.; Crowell, T. I. The Reaction of Aromatic Aldehydes with N-Butylamine. Acid Catalysis and Substituent Effects. *J. Am. Chem. Soc.* **1958**, *80* (5), 1254–1257.

Chapter Four

In vitro biological evaluation and *in silico* ADMET profiling of quinolone pyrazinamide hybrid molecules

4.1   Introduction

As mentioned previously, TB is chronic bacterial infectious disease driven by an airborne pathogen Mycobacterium tuberculosis. It has score of people fell sick and claimed over 2 million lives including 0.4 million cases of co-infected with HIV individuals[1]. This research involved the synthesis and study of pyrazinamide-quinolone hybrid molecules as potential antitubercular agents. Quinolones and pyrazinamide are proven anti-TB molecular frameworks with their large variety of biological activities. This together with intend to contribute to a global pandemic affecting millions of lives prompted us to pursue this project. The current chapter provides a collection of pharmacological data and *in silico* ADMET (Absorption, distribution, metabolism, excretion, and toxicity) parameters to probe the biological activity and the usefulness of the proposed compounds as anti-TB drugs. More importantly, poor ADMET parameters have been flagged as one of the causes of significant failure for the potential clinical drug candidates in trials.
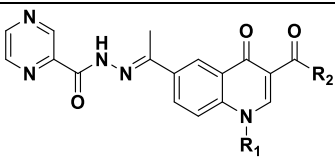
Potential drug agents should be effective and safe upon administration to patients. Hence, there is a need to investigate the toxicology profiles of the drug compounds[3]. The synthesised compounds were screened for anti-TB activity in broth microdilution assay against *Mtb* susceptible strain $H_{37}RvMA$. Moxifloxacin and isoniazid were included as standard reference drugs to measure the antitubercular activity of the compounds and the viability of the assays. The antitubercular activity of each compound is recorded as an MIC_{90}, which is the minimum concentration required to inhibit tubercular growth by 90%[4]. The biological screening assays were outsourced to the Drug Discovery and Development Centre (H3D).

4.2   Biological results and discussion

4.2.1 *In vitro* antitubercular activity of quinolone pyrazinamide hybrid molecules

The media in which the MIC was measured is believed to influence the behaviour of test compounds, hence the screening protocols involved the testing of each compound in 3 media compositions to monitor if the supplements have an impact on the recording of the MIC[5]. Compounds **3.8a-f** were screened *in vitro* for their potential antimycobacterial activity against the drug-sensitive *Mtb* H$_{37}$RvMA strain. Isoniazid (INH) and moxifloxacin (MOF) were included as reference drugs for all *in vitro* evaluations, and the results are displayed in **Table 4.1**.

Table 4.1 *In vitro* anti-*Mtb* H$_{37}$RvMA activity of quinolone-pyrazinamide hybrids.

Comp	R$_1$	R$_2$	MIC$_{90}$(µM)[a]		WlogP[b]
			Calc	Visual	
3.8a	H	EtO	54.5	>52.1	1.65
3.8b	Et	EtO	62.5	>62.5	2.14
3.8c	Bn	EtO	62.5	>62.5	2.94
3.8d	4-BrBn	EtO	62.5	>62.5	3.93
3.8e	Et	Piperidine	57.3	>62.5	2.21
3.8f	Bn	Bn	62.5	>62.5	3.77
MOF	-	-	0.102	0.09	-
INH	-	-	1.57	1.56	-

[a]Medium contained 7H9 CAS GLU Tx, 7H9 ADC GLU Tw and 7H9 ADC GLU Tx; [b]WlogP3, calculated lipophilicity

In three different media compositions[2], none of the synthesised compounds exhibited desirable growth inhibition of *Mtb* with MIC$_{90}$ values >50.2 µM. The observed lack of activity could be attributed to the poor solubility of these compounds in the aqueous

media. During the screening bioassay a high degree of compound precipitation was observed at the highest concentrations. Moxifloxacin and isoniazid performed as expected.

4.3   *In silico* physicochemical and drug-like parameters

Technological advancement has made the screening of novel compounds easier and more accessible. *In silico* ADMET compound profiling modelling tools have also received considerable attention due to their low cost and high throughput nature[6-7]. The open-access[5] website provides necessary information such as physicochemical properties (**Table 4.2**), which are used to filter unsuitable compounds that are non-aligned with the Lipinski rule of five.

Table 4.2: Physicochemical and ADME properties of quinolone-pyrazinamide compounds.

Comp	Log S		WLogP3	Mw g/mol	RO5 violations	PAINS	NRB	TPS (Å)
	(ESOL)	Ali						
3.8a	-2.98	-3.56	1.65	379.37	0	0	7	126.4
3.8b	-4.47	-5.03	3.17	469.49	0	0	9	115.5
3.8c	-5.39	-5.75	3.93	548.39	1	0	9	115.5
3.8d	-3.70	-3.82	2.21	446.50	0	0	7	109.6
3.8e	-3.38	-3.87	2.14	407.42	0	0	8	115.5
3.8f	-5.54	-6.24	3.77	530.58	1	0	10	118.3

All ADME parameters were obtained by using the open-access web tool, SwissADME. Abbreviations; ADME, absorption, distribution, metabolism, and excretion; Log S, calculated solubility; Ali, topological method of predicting aqueous solubility adapted from Ali et al; MW, molecular weight; PAIN, pan-assay interference compounds; RO5, Lipinski's rule of five; WlogP3, calculated lipophilicity; NRB, number of rotatable bonds; TPSA, topological polar surface area[8].

In silico DMPK and ADMET studies have been heavily utilised in modern medicinal chemistry to profile biological active compounds in the early phase of drug discovery[6]. More importantly, there is a high attrition rate of drug molecules in clinical trials due to poor pharmacokinetic (PK) properties and the requirements for orally administered antitubercular drugs. In our case, the web-based tools SwissADME

(http://www.swissadme.ch)[6] and pkCSM[9] were applied to determine the key physicochemical and ADME parameters of compounds **3.8a-f**. As can be seen in **Table 4.2**, despite the lack of *in vitro* antimycobacterial activity, the synthesised compounds **3.8a-f** displayed parameters that are within acceptable ranges of the Lipinski rule of five[10]. From the series, compound **3.8c** violated only one rule of five parameters with molecular weight (Mw) above the 500 g/mol threshold. Assessment of druggability of achieved compounds was done by applying PAINS (Pan-assay interference compounds) filter which suggested that the series showed no likelihood of acting as PAINS. All the compounds displayed acceptable topological polar surface area (TPSA) values in the range 126 – 109 Å^2 accompanied by high gastrointestinal absorption (**Table 4.3** and **Figure 4.1**).

Table 4.3: Pharmacokinetic data of compounds **3.8a-f** obtained using SwissADME.

Comp	GI Abs.	BBB	P-gp sub.	CYP				
				1A2	**2C19**	**2C9**	**2D6**	**3A4**
3.8a	High	No	No	No	Yes	Yes	No	Yes
3.8b	High	No	No	No	Yes	Yes	No	Yes
3.8c	High	No	No	No	Yes	Yes	No	Yes
3.8d	High	No	Yes	No	Yes	Yes	No	Yes
3.8e	High	No	No	No	No	Yes	No	Yes
3.8f	High	No	No	No	Yes	Yes	No	Yes

In terms of molecular flexibility, the synthesised compounds are predicted to exhibit a high probability of good oral bioavailability as measured by the number of rotatable bond values in the range of 7 – 10. None of these compounds showed blood-brain barrier (BBB) penetration (**Table 4.3** and **Figure 4.1**). The lack of BBB penetration suggests that these compounds are large (> 400-500 Da) and will likely form more than 8 hydrogen bonds[11]. These compounds have a lower risk of potentially causing CNS toxicity due to their limited to no access across the BBB[12].
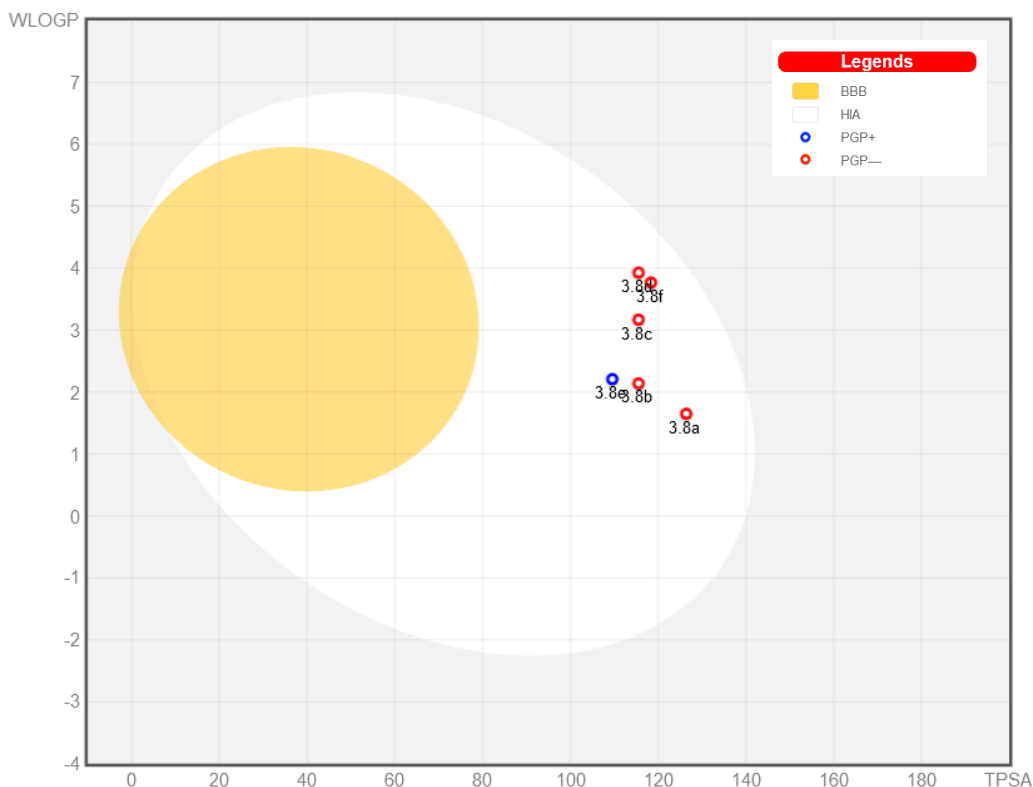
Figure 4.1: BOILED-Egg diagram of synthesised compounds **3.8a-f**. Yellow depicts BBB permeation and white represents gastrointestinal permeation. The blue dot indicates P-glycoprotein (+), i.e., a substrate of Pgp, and the red dot represents P-glycoprotein (-), i.e., a non-substrate of Pgp.

Some of the major drawbacks in TB treatment are linked to the transportation of antituberculosis compounds or drugs across host and mycobacterial membranes[13]. Upon administration, the antitubercular compounds encounter a multitude of human and mycobacterial cell transporters including P-glycoproteins (P-gp), also known as multi-drug resistance protein 1 (MDR1), which have a direct influence on the pharmacological outcome of these compounds[13]. Transporters such as P-gp can impede drug absorption. P-gp is an energy-dependent efflux transporter that aids in the efflux of molecules back into the intestinal lumen[14]. Compound **3.8e** is the only compound that showed affinity for the P-gp transporter. The rest of the other compounds are predicted as non-substrate of P-gp (**Figure 4.1**) suggesting that they could be considered for further exploration as antimycobacterial agents following appropriate optimisation[15].

TB is a disease that requires a prolonged period of multidrug treatment. More importantly, HIV infection and TB combination are fatal and contribute to the loss of life each year[16]. Therefore, most first-line TB drugs are susceptible to clinical drug-drug interactions[17]. Briefly, the drug-drug interaction is defined as the likelihood that one drug (perpetrator) may alter the pharmacological effects of another drug (victim) when administered concurrently[18]. Thus, we predicted using the SwissADME the likelihood of synthesised compounds to inhibit the microsomal enzymes, i.e., cytochrome P450 isoenzymes. Cytochrome P450 (CYP450) enzymes are important in xenobiotic metabolism, and they are found in almost all tissue. The induction and or inhibition of these enzymes will result in unwanted drug-drug interactions[19]. Except for CYP1A2 and CYP2D6, all the synthesised compounds were predicted to be potential inhibitors of isoenzymes CYP2C9, CYP2C19 and CYP3A4 (**Table 4.3**). This suggests that these compounds are unlikely to serve as suitable antimycobacterial agents.

4.4   Conclusions

In conclusion, compounds **3.8a-f** were tested for their potential antimycobacterial activity against the *Mtb* H$_{37}$RvMA strain. None of the compounds showed activity against susceptible *Mtb* H$_{37}$RvMA strain (MIC ≥ 57.3 µM). The lack of activity could be attributed to poor aqueous solubility. Despite the poor antimycobacterial activity, *in silico* studies predicted that the achieved compounds showed required drug-likeness profiles. The druggability of the compounds was assessed using PAINS, and none of the compounds showed any likelihood of acting as PAINS. The critical aspect that emerged in this study is that the synthesised compounds are unlikely to serve as ideal antimycobacterial agents as they are substrates of CYP isoenzymes.

4.5   References

(1)   World Health Organization. *Global Tuberculosis Report 2022*; Geneva, 2022.

(2)   Beteck, R. M.; Seldon, R.; Jordaan, A.; Warner, D. F.; Hoppe, H. C.; Laming, D.; Legoabe, L. J.; Khanye, S. D. Quinolone-Isoniazid Hybrids: Synthesis and Preliminary in Vitro Cytotoxicity and Anti-Tuberculosis Evaluation. *Medchemcomm* **2019**, *10* (2), 326–331.

(3)   Demirgan, R.; Karagöz, A.; Pekmez, M.; Önay-Uçar, E.; Artun, F. T.; Gürer, Ç.;

Mat, A. In Vitro Anticancer Activity and Cytotoxicity of Some Papaver Alkaloids on Cancer and Normal Cell Lines. *African J. Tradit. Complement. Altern. Med.* **2016**, *13* (3), 22–26.

(4)   Yamazhan, T.; Aydemir, Ş.; Tünger, A.; Serter, D.; Gökengin, D. In Vitro Activities of Various Antimicrobials against Brucella Melitensis Strains in the Aegean Region in Turkey. *Med. Princ. Pract.* **2005**, *14* (6), 413–416.

(5)   Franzblau, S. G.; Witzig, R. S.; McLaughlin, J. C.; Torres, P.; Madico, G.; Hernandez, A.; Degnan, M. T.; Cook, M. B.; Quenzer, V. K.; Ferguson, R. M. Rapid, Low-Technology MIC Determination with Clinical Mycobacterium Tuberculosis Isolates by Using the Microplate Alamar Blue Assay. *J. Clin. Microbiol.* **1998**, *36* (2), 362–366.

(6)   Daina, A.; Michielin, O.; Zoete, V. SwissADME: A Free Web Tool to Evaluate Pharmacokinetics, Drug-Likeness and Medicinal Chemistry Friendliness of Small Molecules. *Sci. Rep.* **2017**, *7* (1), 1–13.

(7)   Wang, Y.; Xing, J.; Xu, Y.; Zhou, N.; Peng, J.; Xiong, Z.; Liu, X.; Luo, X.; Luo, C.; Chen, K. In Silico ADME/T Modelling for Rational Drug Design. *Q. Rev. Biophys.* **2015**, *48* (4), 488–515.

(8)   Oderinlo, O. O.; Jordaan, A.; Seldon, R.; Isaacs, M.; Hoppe, H. C.; Warner, D. F.; Tukulula, M.; Khanye, S. D. Hydrazone-Tethered 5-(Pyridin-4-yl)-4H-1, 2, 4-triazole-3-thiol Hybrids: Synthesis, Characterisation, in Silico ADME Studies, and in Vitro Antimycobacterial Evaluation and Cytotoxicity. *ChemMedChem* **2023**, e202200572.

(9)   Pires, D. E. V; Blundell, T. L.; Ascher, D. B. PkCSM: Predicting Small-Molecule Pharmacokinetic and Toxicity Properties Using Graph-Based Signatures. *J. Med. Chem.* **2015**, *58* (9), 4066–4072.

(10) Lipinski, C. A.; Lombardo, F.; Dominy, B. W.; Feeney, P. J. Experimental and Computational Approaches to Estimate Solubility and Permeability in Drug Discovery and Development Settings. *Adv. Drug Deliv. Rev.* **1997**, *23* (1–3), 3–25.

(11) Pardridge, W. M. Drug Transport across the Blood–Brain Barrier. *J. Cereb. Blood. Flow. Metab.* **2012**, *32* (11), 1959–1972.

(12) Wager, T. T.; Liras, J. L.; Mente, S.; Trapa, P. Strategies to Minimize CNS

Toxicity: In Vitro High-Throughput Assays and Computational Modeling. *Expert Opin. Drug Metab. Toxicol.* **2012**, *8* (5), 531–542.

(13) Te Brake, L. H. M.; de Knegt, G. J.; de Steenwinkel, J. E.; Van Dam, T. J. P.; Burger, D. M.; Russel, F. G. M.; van Crevel, R.; Koenderink, J. B.; Aarnoutse, R. E. The Role of Efflux Pumps in Tuberculosis Treatment and Their Promise as a Target in Drug Development: Unraveling the Black Box. *Annu. Rev. Pharmacol. Toxicol.* **2018**, *58*, 271–291.

(14) Alagga, A. A.; Gupta, V. Drug Absorption. In *StatPearls [Internet]*; StatPearls Publishing, **2021.**

(15) Prachayasittikul, V.; Prachayasittikul, V. P-Glycoprotein Transporter in Drug Development. *EXCLI J.* **2016**, *15*, 113.

(16) Pooranagangadevi, N.; Padmapriyadarsini, C. Treatment of Tuberculosis and the Drug Interactions Associated With HIV-TB Co-Infection Treatment. *Front. Trop. Dis.* **2022**, *3*, 834013.

(17) Riccardi, N.; Canetti, D.; Rodari, P.; Besozzi, G.; Saderi, L.; Dettori, M.; Codecasa, L. R.; Sotgiu, G. Tuberculosis and Pharmacological Interactions: A Narrative Review. *Curr. Res. Pharmacol. Drug Discov.* **2021**, *2*, 100007.

(18) Yew, W. W. Clinically Significant Interactions with Drugs Used in the Treatment of Tuberculosis. *Drug Saf.* **2002**, *25*, 111–113.

(19) O Nettleton, D.; J Einolf, H. Assessment of Cytochrome P450 Enzyme Inhibition and Inactivation in Drug Discovery and Development. *Curr. Top. Med. Chem.* **2011**, *11* (4), 382–403.

Chapter Five

Experimental procedure and methods

5.1   General methods

All the chemicals and solvents used in this study were purchased from either Sigma-Aldrich or Merck KGaA. Some of the solvents were purchased from SPELLBOUND laboratory solutions. Unless stated otherwise, all chemicals were used without further purification. Reactions were monitored by thin layer chromatography (TLC) using Merck F254 aluminium-backed plates (originally supplied as 200 mm × 200 mm) precoated with silica gel (60 F_{254}) from Merck KGaA. Ultraviolet (UV 254 or 366 nm) light was used to visualize the TLC plates. Silica gel column chromatography was used for purification using silica gel 60 Å, 230-400 mesh ASTM (0.040-0.063 mm) from Merck KGaA. For smaller quantities of crude compounds, preparative thin-layer chromatography was used. Silica gel 60 PF_{254} supplied by Merck KGaA.

All compounds were characterized by ^{1}H and ^{13}C NMR, infrared spectroscopy, and mass spectrometry. The ^{1}H and ^{13}C NMR spectra were recorded in deuterated solvents on Bruker Biospin 300, Avance II 400 or Avance II 600 MHz spectrometers and internally referenced to the solvent peaks (CDCl$_3$-d with chemical shifts of 7.26 ppm for ^{1}H NMR and 77.2 ppm for ^{13}C NMR; DMSO-d_6 whose chemical shifts are 2.5 ppm for ^{1}H NMR and 39.5 ppm for ^{13}C NMR). Spectra were processed using MestReNova version 6.0.2-5475 software. The chemical shifts were recorded in parts per million (ppm) and J-coupling constants are in Hertz (Hz). The abbreviations used to denote signal multiplicities are depicted as s = singlet, bs = broad singlet, d = doublet, dd = doublet of doublets, ddd = doublet of doublet of doublets, t = triplet, td = triplet of doublets and m = multiplet. The high-resolution electrospray ionization accurate mass measurements (HRMS-ESI) were recorded in positive or negative mode using Waters Synapt G2 (Central Analytical Facility, Stellenbosch University). Melting points were determined using a Stuart melting point apparatus model: SMP30. IR spectra were recorded on a Perkin-Elmer FT-IR spectrum 100 spectrometers.

5.2 Synthesis of ethyl pyrazine-2-carboxylate, 3.5a[1]
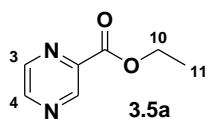
A 50 mL round bottom flask was charged with pyrazine carboxylic acid (2.482 g, 20.0mmol), EtOH (20 mL) and concentrated H_2SO_4 (1 mL). The reaction mixture was allowed to stir at room temperature for 10 mins and then heated to reflux for 10 h. TLC confirmed the completion of the reaction. Thereafter, the resultant reaction product was allowed to cool to ambient temperature. The product was washed with $NaHCO_3$ solution to neutralize the solution. The organic phase was obtained through liquid extraction using DCM. The organic phase was dried using Na_2SO_4 and filtered. The solvent was removed under reduced pressure and the solid product was obtained as a yellow-brown crystalline solid. Yield = 36%; M.p: 49-51 °C (Lit. 48-49°C)[2]; ^{1}H NMR (400 MHz, $CDCl_3$) δ_H = 9.30 (s, 1H, H-5), 8.74 (t, J = 4.0 Hz, 1H, H-3), 8.71 (s, 1H, H-4), 4.49 (q, J = 7.1 Hz, 2H, H-10), 1.44 (t, J = 7.1 Hz, 3H, CH_3). ^{13}C NMR (101 MHz, $CDCl_3$) δ_C = 164.03, 147.73, 146.38, 144.50, 143.62, 62.52, 14.36.

5.3 Synthesis of pyrazine-2-carbohydrazide, 3.7[1]
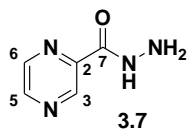
A 50 ml round bottom flask was charged with a dry ester, ethyl-2-carboxylate (1.920 g, 12.6 mmol) and ethanol (15 mL). The reaction mixture was allowed to stir to uniformity. Hydrazine hydrate (2.89 mL, 126 mmol) was gradually added to the reaction mixture and stirring continued for an additional 2 h. The precipitate was filtered. Thereafter, the solid product was dried under a vacuum to give compound **3.22** as a white-yellow solid. Yield = 65.6%, M.p. = 159-160 °C (Lit.[3] 158 °C) ^{1}H NMR (400 MHz, DMSO) δ_H =10.14 (s, 1H, NH), 9.12 (s, 1H, H-3), 8.83 (s, 1H, H-5), 8.69 (s, 1H, H-6), 4.65 (s, 2H, NH_2). ^{13}C NMR (101 MHz, DMSO) δ_C = 161.96, 147.72, 145.34, 143.94, 143.68.

5.4 Synthesis of quinolone

5.4.1 Synthesis of 4-aminoacetophenone, 3.3
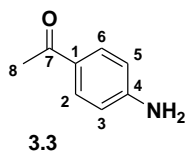
3.3 A 250 mL round bottom flask was charged with EtOH (70 mL) and 4-nitro acetophenone (3.30 g or mL, 20 mmol). The resultant reaction mixture was allowed to stir for 15 minutes at room temperature. Iron powder (4.15 mg, 75.0 mmol) was added to the reaction mixture. The reaction mixture was heated to 60 °C and 15 mL of concentrated hydrochloric acid was added dropwise over a period of 30 min. The reaction was refluxed for an hour until the iron powder was mostly dissolved. After cooling, the reaction contents were poured into 100 mL of cold water and neutralised using sodium hydroxide solution to give a sludge. The sludge was washed with ethyl acetate (150 mL) and stirred for 15 mins. The reaction product was extracted with ethyl acetate (3 × 50mL). The organic phases were combined, and solvents evaporated *in vacuo* to give the product a white solid. Yield = 70.3%; M.p.: 102 – 104 °C; FT-IR v_{max}/cm^{-1}: 3200 (N-H), 1650 (C=O). ^{1}H NMR (400 MHz, DMSO) δ_H =7.67 (t, J = 9.4 Hz, 2H, H-2, H-6), 6.56 (d, J = 8.6 Hz, 2H, H-3, H-5), 6.02 (s, 2H, NH$_2$), 2.38 (s, 3H, CH$_3$-8). 13C NMR (101 MHz, DMSO) δ 195.42, 154.08, 131.03, 125.32, 112.93, 26.30.

5.4.2 Synthesis of diethyl 2-(((4-acetylphenyl)amino)methyl)malonate, 3.4
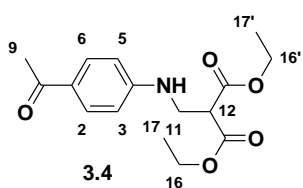
3.4 A 100 mL round bottom flask was charged with 4-aminoacetophenone (1.9 g, 14.1 mmol), diethyl ethyoxymethylenne malonate (3.04 g, 14.1 mmol) and acetonitrile (25 mL). The contents were allowed to stir and heated to reflux overnight. TLC confirmed the progression of the reaction to completion. Thereafter, the solvent was evaporated to give a yellow-white solid. M.p. = 88-93.3 °C. ^{1}H NMR (400 MHz, CDCl$_3$) δ_H = 8.54 (d, J = 13.4 Hz, 1H, NH), 7.98 (d, J = 8.4 Hz, 2H, H-2, H-6), 7.18 (d, J = 8.4 Hz, 2H, H-3, H-5), 4.35 – 4.23 (m, 4H, 2H-16, 2H-16'), 4.18 (m, J = 9.2, 6.5 Hz, 2H, H-11) 3.66 (bs, 1H, H-12), 2.58 (s, 3H, CH$_3$-9), 1.67 (s, 2H, H-

12), 1.27 – 1.45 (m, 6H, H-17, H-17') . ^{13}C NMR (101 MHz, CDCl$_3$) δ$_C$ = 196.50, 168.77, 143.05, 133.30, 130.56, 116.32, 72.36, 60.85, 60.46, 26.48, 15.27, 14.27.

5.4.3 Synthesis of diethyl 2-(((4-acetylphenyl) amino) methyl) malonate, 3.6a
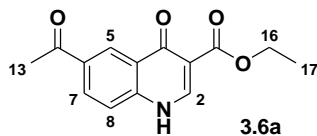

A 100 mL round bottom flask was charged with diphenyl ether, and it was allowed to heat up while monitoring the temperature. The malonate ester was added to the round bottom flask. The mixture was allowed to heat up to 245 °C where the timer started for the next 1 h. The reaction was not permitted to heat up above 260 °C. Thereafter, the reaction contents were poured into cold hexane. A solid precipitate formed, and the solvent was filtered away using gravitational filtration. The crude product was purified by silica gel column chromatography (9:1; ethyl acetate: hexane). Yellow solid. Yield = 69.9%, M.p. = 270-294 °C, ^{1}H NMR (400 MHz, DMSO) δ$_H$ = 14.87 (bs, 1H, NH-1), 9.10 (s, 1H, H-2), 8.86 (s, 1H, H-5), 8.39 (d, J = 8.3 Hz, 1H, H-8), 8.14 (d, J = 8.5 Hz, 1H, H-7), 4.62 (q, J = 6.4 Hz, 2H, H-16), 2.71 (s, 3H, CH$_3$-13), 1.42 (t, J = 6.3 Hz, 3H, H-17). ^{13}C NMR (101 MHz, DMSO) δ$_C$ = 197.14, 178.37, 166.09, 150.79, 142.08, 134.11, 133.02, 127.24, 125.71, 119.23, 108.69, 49.72, 27.29, 14.95.

### 5.4.4 General procedure for the synthesis of *N*-alkylated quinolone[3]

A 50 mL round bottom flask was charged with quinolone 3.1 (10 mmol) and K$_2$CO$_3$ (20 mmol) in DMF (10-15 mL) or a solvent mixture of chloroform and tetrahydrofuran. (2:1). The reaction mixture was initially stirred for 10 minutes at room temperature. Thereafter, an alkyl halogen (100 mmol) was added, and the resultant reaction mixture was heated to reflux temperature and refluxed for 10 h. The TLC showed the reaction progression to completion. Thereafter, the solvents were evaporated *in vacuo* and the final crude product was purified using silica gel column chromatography (100% ethyl acetate). *N-alkyl* substituted products were obtained with yields in the range of 20-40%.

## Ethyl 6-acetyl-1-ethyl-1,4-dihydro-4-oxoquinoline-3-carboxylate, 3.6b$_2$
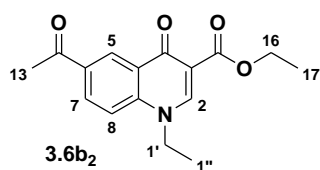
White solid. Yield = 67%, M.p. = 220 – 240 °C, ^{1}H NMR (400 MHz, CDCl3) δ_H = 11.08 (s, 1H, H-2), 7.98 (d, J = 8.3 Hz, 1H, H-7), 7.58 (s, 1H, H-5), 7.17 (d, J = 8.3 Hz, 1H, H-8), 4.35 – 4.14 (m, 4H, CH$_2$-1', CH$_2$-17), 2.57 (s, 3H, CH$_3$- 13), 1.41 – 1.24 (m, 6H, CH$_3$-1'', CH$_3$-18). ^{13}C NMR (101 MHz, CDCl$_3$) δ_C = 196.41, 168.7, 165.40, 163.64, 150.45, 143.06, 133.33, 130.54, 116.31, 106.29, 95.78, 60.76, 60.42, 26.44, 15.25, 14.26.

Ethyl 6-acetyl-1-benzyl-1,4-dihydro-4-oxoquinoline-3-carboxylate, 3.6b$_3$
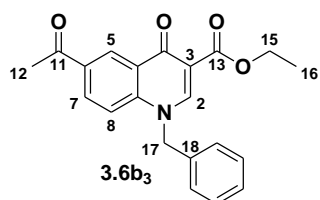
White solid. Yield = 70%, ^{1}H NMR (400 MHz, CDCl3) δ_H = 9.05 (s, 1H, H-2), 8.62 (s, 1H, H-5), 8.16 (d, J = 8.8 Hz, 1H, H-7), 7.43 – 7.31 (m, 5H, H-18), 7.16 (d, J = 6.7 Hz, 1H, H-8), 5.43 (s, 2H, H-17), 4.41 (q, J = 7.0 Hz, 2H, H-15), 2.67 (s, 3H, CH$_3$-12), 1.42 (t, J = 7.1 Hz, 3H, H-16). ^{13}C NMR (101 MHz, CDCl$_3$) δ_C = 195.8, 173.1, 164.2, 149.2, 141.0, 132.7, 132.4, 130.4, 128.5 (2C), 128.2, 127.8, 127.6, 125.0 (2C), 116.2, 111.4, 60.2, 56.6, 25.6, 13.4.

## Ethyl 1-(4-bromobenzyl)-6-acetyl-1,4-dihydro-4-oxoquinoline-3-carboxylate, 3.6b$_4$
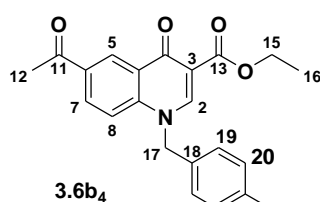
White solid. Yield = 64%, ^{1}H NMR (400 MHz, CDCl3) δ_H = 9.04 (d, J = 1.7 Hz, 1H, H-5), 8.59 (s, 1H, H-2), 8.17 (dd, J = 8.9, 1.8 Hz, 1H, H-7), 7.41 - 7.45 (m, J = 7.3 Hz, 2H, H-19, H-20), 7.33 (d, J = 8.9 Hz, 1H, H-8), 7.04 (d, J = 8.2 Hz, 2H, H-19', H-20'), 5.37 (s, 2H, H-17), 4.42 (q, J = 7.1 Hz, 2H, H-15), 2.68 (s, 3H, CH$_3$-12), 1.43 (t, J = 7.1 Hz, 3H, H-16). ^{13}C NMR (101 MHz, CDCl$_3$) δ_C = 196.9, 174.1, 165.3,

150.2, 142.0, 133.7, 132.8 (2C), 131.9, 131.7, 130.1, 129.4, 127.8 (2C), 123.0, 117.1, 112.8, 61.4, 57.1, 26.7, 14.5.

5.4.5 General procedure for the amidation of the ester[3]

A 50 mL round bottom flask was charged with the quinolone ester **3.14** (0.72 mmol), amine (3.584 mmol) and chloroform as a solvent. The mixture was stirred for 5 mins. After the addition of DBU, the resultant reaction mixture was heated to reflux overnight. The TLC showed the reaction progression to completion. The reaction contents were evaporated *in vacuo* to obtain a crude product. The crude mixture was purified using column chromatography using a solvent system of ethyl acetate with hexane (90-100%: 0-10%).

**6-Acetyl-1-ethyl-3-(piperidine-1-carbonyl)quinolin-4(1H)-one 3.6c$_1$**
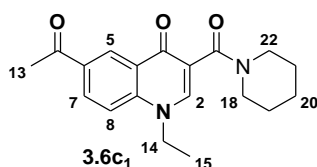
White-yellow solid. Yield = 35%[4], M.p. > 228 °C, ^{1}H NMR (400 MHz, CDCl$_3$) δ$_H$ = 8.99 (d, J = 1.5 Hz, 1H, H-5), 8.35 – 8.25 (m, 1H, H-7), 7.99 (s, 1H, H-5), 7.52 (d, J = 9.0 Hz, 1H, H-8), 4.20 – 4.56 (m, 2H, H-14), 3.72 (s, 2H, H-18), 3.35 (s, 2H, H-22), 2.67 (s, 3H, CH$_3$-13), 1.65 -1.83 (m, 6H, H-19-21), 1.54 (t, J = 7.1 Hz, 3H, H-15). ^{13}C NMR (101 MHz, CDCl$_3$) δ$_C$ = 197.12, 173.31, 164.99, 145.14, 141.79, 132.65, 131.15, 129.39, 126.92, 120.47, 116.02, 48.80, 43.43, 26.67 (2C), 25.64, 24.51 (2C), 14.48.

5.5   General procedure for the synthesis of quinolone pyrazinamide hybrids

A 50 mL round bottom flask was charged with a quinolone **3.8a – f** (233.5 mg, 0.7 mmol)**,** pyrazinamide **3.7** (100 mg, 0.7 mmol) and ethanol (15-25 mL) as a solvent. The contents of the flask were heated to reflux for approximately 10 mins. Glacial acetic acid (4-5 drops) was added to the reaction as a catalyst. The reaction was run for 24 h. A solid precipitate formed in the reaction. The reaction was cooled to room temperature and the solid was collected via gravitational filtration and allowed to dry in the open air. The resulting solids were dried and collected. The product was collected at a good yield (30-60%).

Ethyl-1,4-dihydro-4-oxo-6-((*E*)-1-(pyrazine-2-carboylimino)ethyl)quinoline-3-carboxylate, 3.8a
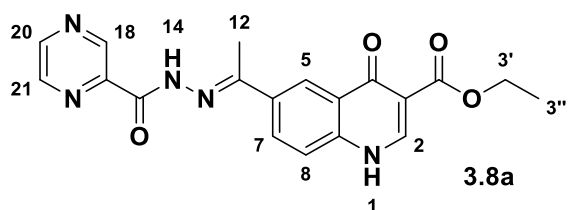
White solid, Yield = 53%, M.p. = 190 – 200 °C, FT-IR V_{max}/ cm^{-1}: 3335 (N-H), 3241 (N-H), 1697 (C=O), 1021 (C-O) ^{1}H NMR (400 MHz, DMSO) δ_H = 11.13 (s, 1H, NH-1), 9.29 (s, 1H, NH-14), 8.96 (s, 1H, H-18), 8.83 (s, 1H, H-2), 8.71 (s, 1H, H-5), 8.58 (ud, *J* =, 1H, H-20), 8.28 (d, *J* = 8.9 Hz, 1H, H-21), 8.20 (d, *J* = 8.7 Hz, 1H, H-7), 7.69 (d, *J* = 8.6 Hz, 1H, H-8), 4.23 (q, *J* = 7.1 Hz, 2H, H-3'), 2.66 (s, 3H, CH$_3$-12), 1.29 (t, *J* = 7.0 Hz, 3H, H-3''). HRMS (ESI) *m/z*: calcd for C$_{19}$H$_{17}$N$_5$O$_4$ [M+H]$^+$: 380.13594 found 380.1374.

Ethyl (*E*)-1-ethyl-4-oxo-6-(1-(2-(pyrazine-2-carbonyl)hydrazono)ethyl)-1,4-dihydroquinoline-3-carboxylate, 3.8b
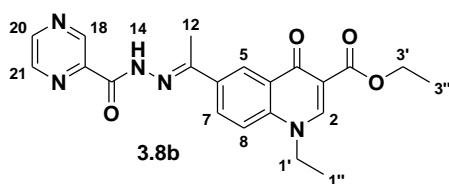
Yellow solid, Yield = 40%, M.p. = 160 – 165 °C, FT-IR V_{max}/cm^{-1}: 3300 (N-H), 1697 (C=O), 1647 (C=N), ^{1}H NMR (400 MHz, CDCl$_3$) δ_H = 11.08 (d, *J* = 13.5 Hz, 1H, NH-14), 10.70 (s, 1H, H-18), 9.51 (s, 1H, H-2), 8.82 (d, *J* = 8.0 Hz, 1H, H-20), 8.56 (d, *J* = 6.8 Hz, 1H, H-21), 8.52 (s, 1H, H-5), 7.93 (d, *J* = 8.6 Hz, 1H, H-7), 7.15 (d, *J* = 8.5 Hz, 1H, H-8), 4.17 – 4.28 (m, 7.1 Hz, 4H, H-1', H-3'), 2.40 (s, 3H, CH$_3$-12), 1.26 – 1.34 (m, 6H, H-1'', H-3''). ^{13}C NMR (101 MHz, CDCl$_3$) δ_C = 168.95, 165.64, 158.58, 152.88, 151.03, 147.93, 144.91, 144.04, 142.54, 140.46, 133.80, 130.56, 128.51, 116.68, 116.32, 94.46, 60.62, 60.33, 14.37, 13.25; HRMS (ESI) *m/z*: calcd for C$_{21}$H$_{21}$N$_5$O$_4$ [M+H]$^+$: 408.16724 found 408.16724.

## Ethyl (E)-1-benzyl-4-oxo-6-(1-(2-(pyrazine-2-carbonyl)hydrazono)ethyl)-1,4-dihydroquinoline-3-carboxylate 3.8c
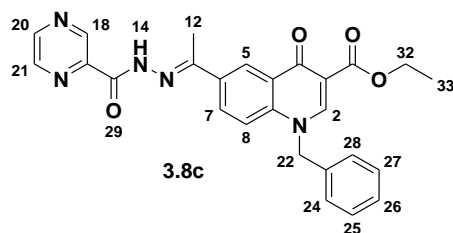
White solid, Yield = 50 %, M.p. = 190 – 200 °C, FT-IR Vmax/cm-1: 3344 (N-H), 1979 (C=N), 1697 (C=O). 1H NMR (400 MHz, CDCl$_3$) δ 10.76 (s, 1H, H-18), 9.48 (s, 1H, H-2), 9.04 (d, J = 8.0 Hz, 1H, H-20), 8.82 (d, J = 8.0 Hz, 1H, H-21), 8.71 (s, 1H, H-5), 8.63 – 8.55 (m, 2H, H-1, H-7), 8.48 (d, J = 7.3 Hz, 1H, H-8), 7.42 – 7.31 (m, 3H, H-28, H-24, H-26), 7.16 – 7.18 (m, 2H, H-27, H-25), 5.42 (s, 2H, CH$_2$-22), 4.41 (m, 6H, H-32), 2.49 (s, 3H, CH$_3$-12), 1.42 (t, J = 7.1 Hz, 3H, CH3-33), 4.26 (q, J = 8.0, 2H, H-32), 1.99 (s, 3H, CH$_3$-12) 1.21 (s, 3H, CH$_3$-33); HRMS (ESI) m/z: calcd for C$_{26}$H$_{23}$N$_5$O$_4$ [M+H]+: 470.18284 found 470.1829.

Ethyl-1-(4-bromobenzyl)-1,4-dihydro-4-oxo-6-((*E*)-1-(pyrazine-2-carboylimino)ethyl)quinoline-3-carboxylate, 3.8d
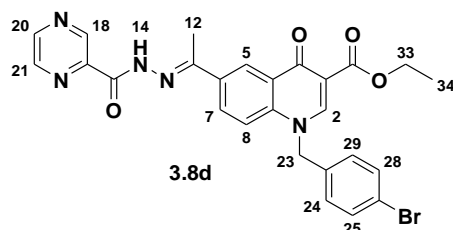

White solid. Yield = 61.7%, M.p. = 260-280°C; FT-IR Vmax /cm-1: 3535 (N-H), 1705 (C=N), 1493 (C=O). ^{1}H NMR (400 MHz, CDCl$_3$) δH = 10.77 (s, 1H, H-18), 9.49 (s, 1H, H-2), 8.81 (d, J = 8.0, 1H, H-20), 8.71 (s, 1H, H-5), 8.59 (d, J = 7.2 Hz, 1H, H-21), 8.17 (d, J = 7.9 Hz, 1H, H-7), 7.50 (d, J = 7.6 Hz, 2H, H-24, H-29), 7.33 (d, J = 8.6 Hz, 1H, H-8), 7.04 (d, J = 7.8 Hz, 2H, H-28, H-25), 5.38 (s, 2H, CH$_2$-23), 4.41 (t, J = 6.8 Hz, 2H, CH$_2$-33), 2.17 (s, 3H, CH$_3$-12), 1.40 – 1.44 (m, 3H, CH$_3$-34). HRMS (ESI) m/z: calcd for C$_{26}$H$_{22}$BrN$_5$O$_4$ [M+H] +: 548.09334 found 548.0917.

(*E*)-N'-(1-(1-ethyl-4-oxo-3-(piperidine-1-carbonyl)-1,4-dihydroquinolin-6-yl)ethylidene)pyrazine-2-carbohydrazide, 3.8e
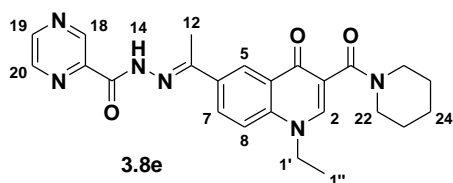
Yellow brown solid, Yield = 30%, M.p = 180 – 200 °C, FT-IR V_{max}/cm^{-1}: 2924 (N-H), 1692 (C=N), 1630 (C=O). ^{1}H NMR (400 MHz, CDCl$_3$) δ_H = 10.79 (s, 1H, H-18), 9.45 (s, 1H, H-2), 8.81 (d, J = 8.0 Hz, 1H, H-19), 8.68 – 8.60 (m, 1H, H-20), 8.54 (d, *J* = 8.0 Hz, 1H, H-7), 8.02 (s, 1H, H-5), 7.50 (d, *J* = 8 Hz, 1H, H-8), 4.23 – 4.29 (m, 2H, CH$_2$-1'), 3.72 (s, 2H, H-22) 3.36 (s, 2H, H-26), 3, 2.52 (s, 3H, CH$_3$-12), 1.40 – 1.67 (m, 6H, H-23, H-24, H-25), 1.53 (t, *J* = 7.2 Hz, 3H, CH$_3$-1''). ^{13}C NMR (101 MHz, CDCl$_3$) δ_C = 173.19, 165.46, 158.72, 152.71, 147.98, 144.83, 143.94, 142.62, 139.90, 133.37, 130.89, 127.04, 125.88, 119.58, 116.04, 48.74, 43.46, 26.69, 25.65, 24.52, 14.58, 13.03; HRMS (ESI) *m/z*: calcd for C$_{24}$H$_{26}$N$_6$O$_3$ [M+H]$^+$: 447.21444 found 447.2148.

(*E*)-N,1-dibenzyl-4-oxo-6-(1-(2-(pyrazine-2-carbonyl)hydrazono)ethyl)-1,4-dihydroquinoline-3-carboxamide, 3.8f
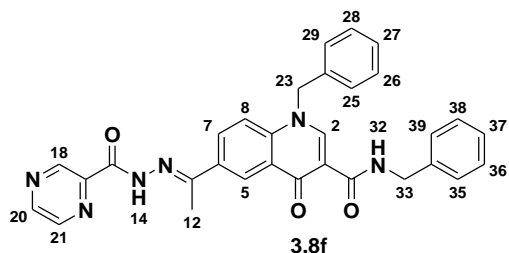
White solid, Yield = 37.0 % M.p = 216 – 222.9°C ^{1}H NMR (400 MHz, CDCl$_3$) δ_H = 10.75 (s, 1H, NH-14), 9.50 (s, 1H, H-2), 8.82 (ud, *J* = 2.2 Hz, 1H, H-20), 8.71 (bs, 1H, H-21), 8.59 (ud, *J* = 12, 1H, H-5), 8.48 (dd, *J* = 9.1, 2.0 Hz, 1H, H-7), 7.50 – 7.30 (m, 10H, H:35-39;25-29), 7.17 (d, *J* = 6.7 Hz, 1H, H-8), 5.41 (s, 2H, CH$_2$-23), 4.69 (s, 2H, CH$_2$-33), 2.50 (s, CH$_3$-12). HRMS (ESI) *m/z*: calcd forC$_{31}$H$_{26}$N$_6$O$_3$ [M+H] $^+$: 530.2066 found 531.2135.

5.6 Experimental procedure for the *in vitro* studies performed on the quinolone pyrazinamide hybrid for anti-TB activity.

The test samples were prepared in 100 % DMSO (Sigma Aldrich) at a stock concentration of 10 mM. Further 2-fold serial dilutions were prepared in growth medium in 96-well round bottom plates on the day of the experiment. A concentration range of 62.5 – 0.122 µM was tested for each sample. Isoniazid (INH) and Moxifloxacin (MOXI) were included as the reference drugs in all experiments at concentration ranges of 62.5 – 0.122 µM and 6.25 – 0.012 µM, respectively. A maximum inhibition control (Rif at 0.15 µM) and a minimum inhibition control (0.625 % DMSO) were included on each test plate. A culture of *Mtb* H37RvMA5, in 7H9_ADC_GLU_TW, was grown to an optical density (OD600) of 0.5 - 0.7 and diluted down to OD600 of 0.001 in each medium. A volume of 50 µL of the diluted culture (~1 × 104 bacilli) was added to each well of each test plate, for a final volume of 100 µl per well. Each compound was tested in duplicate. The assay plates were incubated at 37 °C with 5 % CO_2 and humidification. The assay was scored visually on day 7, and the Visual MIC was recorded as the lowest concentration at which no bacterial pellet was observed. One-tenth of the assay volume of resazurin (0.2 mg/ml prepared in PBS) was then added to each well of the assay plate and re-incubated for 24 h. The relative fluorescence units (RFU) (excitation 540 nm; emission 590 nm) of each well was measured using a SpecraMax i3x Plate reader on day 8 (Serial no. 363703271, Molecular Devices Corporation 1311 Orleans Drive Sunnyvale, California). Data analysis was performed using Dotmatics software (https://www.dotmatics.com/solutions/dataintelligence-lab-software). Briefly, raw RFU data was normalized to the minimum and maximum inhibition controls to generate a dose-response curve (% inhibition), using the Levenberg-Marquardt damped least squares method, from which the MIC is calculated using the 4-parameter curve fit protocol. The lowest concentration of drug that inhibits 90 % of the growth of the bacterial population is the Calculated MI Growth of bacteria was observed and measured both qualitatively and quantitatively.

5.7 References

(1)   da Silva, Y. K. C.; Augusto, C. V.; de Castro Barbosa, M. L.; de Albuquerque

Melo, G. M.; de Queiroz, A. C.; Dias, T. de L. M. F.; Júnior, W. B.; Barreiro, E. J.; Lima, L. M.; Alexandre-Moreira, M. S. Synthesis and Pharmacological Evaluation of Pyrazine N-Acylhydrazone Derivatives Designed as Novel Analgesic and Anti-Inflammatory Drug Candidates. *Bioorg. Med. Chem.* **2010**, *18* (14), 5007–5015.

(2)   Yoshino, T.; Imori, S.; Togo, H. Efficient Esterification of Carboxylic Acids and Phosphonic Acids with Trialkyl Orthoacetate in Ionic Liquid. *Tetrahedron* **2006**, *62* (6), 1309–1317.

(3)   Vergara, F. M. F.; Lima, C. H. da S.; Maria das Graças, M. de O.; Candéa, A. L. P.; Lourenço, M. C. S.; Ferreira, M. de L.; Kaiser, C. R.; de Souza, M. V. N. Synthesis and Antimycobacterial Activity of N′-[(E)-(Monosubstituted-Benzylidene)]-2-Pyrazinecarbohydrazide Derivatives. *Eur. J. Med. Chem.* **2009**, *44* (12), 4954–4959.

(4)   Zulu, A. I. Synthesis, Characterization and Antiparasitic Evaluation of Chalcone Hybrids, MSc Thesis, Rhodes University, South Africa, **2021**.